TECHNISCHE UNIVERSITÄT MÜNCHEN

Institut für Klinische Chemie und Pathobiochemie

der Technischen Universität München

und

Institut für Klinische Chemie

der Medizinischen Hochschule Hannover

Mechanisms of monocyte activation and differentiation

Judith D. Kandemir

Vollständiger Abdruck der von der Fakultät für Chemie

der Technischen Universität München zur Erlangung des akademischen Grades eines

Doktors der Naturwissenschaften

genehmigten Dissertation.

Vorsitzender: Univ.-Prof. Dr. Chr. F. W. Becker

Prüfer der Dissertation:

1. Univ.-Prof. Dr. J. Buchner
2. Univ.-Prof. Dr. K. Brand,
   Medizinische Hochschule Hannover

Die Dissertation wurde am 24.08.2010 bei der Technischen Universität München eingereicht und durch die Fakultät für Chemie am 21.10.2010 angenommen.

Table of contents

Abstract

Monocytes are an integral part of the immune system, linking immunity's innate and adaptive branches. As professional antigen-presenting cells they are capable of activating cells of the lymphocytic lineages, which represent the adaptive compartment of the immune system. Upon activation (e.g., by pathogenic components, or by cytokines such as tumor necrosis factor [TNF; TNF-α]) monocytes produce a variety of cytokines and chemokines, including interleukin-8 (IL-8), which recruit and activate immune cells. Monocytes also differentiate towards tissue macrophages, and albeit it is known that transcription factors of the C/EBP and ETS families play an important role during the differentiation process, their exact role remains unknown. The aim of this work was to analyze the TNF tolerance phenomenon in primary human monocytes and to analyze the role of C/EBPβ during monocytic differentiation.

TNF tolerance is characterized by a significant suppression of the otherwise readily inducible expression of important cellular factors like IL-8 after prolonged stimulation with low doses of TNF. Since in previous publications TNF tolerance was assessed mainly in cell lines, one aim of this study was to investigate this condition in primary human monocytes isolated from whole blood drawn from healthy blood donors and to identify novel differentially regulated genes by gene expression analysis. To ensure high purity of isolated monocytes, flow cytometric analyses confirmed the presence of at least 95% CD45$^+$ CD14$^+$ double positive cells (i.e., monocytes) after isolation and ruled out a possible contamination with lymphocyte subpopulations. Further experiments aimed at gaining a better understanding of the cell material examined confirmed that, upon stimulation with TNF, the primary human monocytes could be readily induced to secrete IL-8 in a time- and dose-dependent manner, as measured by ELISA. However, in these cells a TNF tolerant phenotype, which has been described for the premonocytic cell line THP-1, could not be stably induced at the level of IL-8 protein expression. This heterogeneity of monocytes exposed to the conditions of TNF tolerance was also observed by gene expression analysis and confirmed at the mRNA level by real-time quantitative (RT-q) PCR. By further assessing the data from the microarray analysis it could be confirmed, however, that a large number of genes involved in signal transduction, transcription, the regulation of apoptosis and of immunological processes, as well as mediating other important cellular functions, were stably induced by TNF stimulation in human monocytes. The instability of TNF tolerance in these primary cells possibly indicates

that the genotype plays an important role in their ability to undergo TNF-induced deactivation.

The upregulation of C/EBPβ during monocytic differentiation has been known for a long time, yet its implications remained unclear. Premonocytic THP-1 cells stimulated with PMA, which have widely been used to study monocytic differentiation, were chosen as a model for this work. Morphological analysis by light microscopy confirmed that PMA induced dramatic changes in this cell line, which consists of basally round, non-adherend cells and became flattened, amoeboid, and polygonal by this treatment. Western blot analysis detecting nuclear C/EBPβ corroborated previous reports that this transcription factor is dramatically induced during monocytic differentiation. When assessing the differential upregulation of its three isoforms LAP* ("liver activating protein"), LAP, and LIP ("liver inhibitory protein") in detail it became evident that the LAP/LIP ratio changes notably during PMA-induced monocytic differentiation of premonocytic THP-1 cells, skewing the ratio towards the transcriptionally active isoforms of C/EBPβ. Concurrently, nuclear expression of the large C/EBPα isoform p42 remained constant while the inhibitory small isoform p30 was slightly induced, suggesting an attenuation of C/EBPα functionality while that of C/EBPβ was augmented. Both C/EBPα and C/EBPβ were only weakly expressed in the cytoplasm of differentiating THP-1. The use of a proliferation assay confirmed that THP-1 treated with PMA became significantly growth inhibited. Remarkably, the observed inhibition of proliferation coincided temporally with the induction of the LAP/LIP ratio, suggesting a causal link between these two events. Overexpression of C/EBPβ LAP* in the human epithelial cell line HeLa directly showed the growth inhibitory effect of this transcription factor in additional proliferation assays. As a second model, C/EBPβ wt and ko macrophage-like cell lines were subsequently used to further understand the influence of C/EBPβ on differentiation. By morphological analysis, a striking difference regarding the morphologies of these cell lines was detected. While C/EBPβ wt macrophage-like cells appeared like normal macrophages, C/EBPβ ko cells remained strictly round despite being adherend. Remarkably, the proliferation rates of C/EBPβ wt cells, as detected by both direct cell counting and proliferation assays, were significantly reduced compared to C/EBPβ ko cells. Additionally, cell cycle analyses confirmed that after serum withdrawal, which is a prototypic tool to synchronize a cell population, the latter started cycling more readily than C/EBPβ wt cells. Calculation of the cycling indices [$(S+G_2M)/G_0G_1$] of both cell lines at different time points revealed that after synchronization, the C/EBPβ ko cell line indeed started progressing through the cell cycle earlier than the C/EBPβ wt cells. In order to gain insight into the

mechanisms by which C/EBPβ influences cell cycle progression, expression of retinoblastoma protein (Rb), which is a strong repressor of cell cycle progression, and its phosphorylation were analyzed by western blotting in PMA-treated THP-1. The results showed that cellular Rb levels and, to a greater extent, phosphorylation of Rb were reduced by treatment with PMA. Remarkably, the level of Rb, regardless of PMA stimulation, was significantly lower in THP-1 transfected with C/EBPβ-specific siRNA, indicating that the presence of C/EBPβ during monocytic differentiation attenuates the PMA-induced reduction of Rb and serves to stabilize the level of hypophosphorylated Rb within the cell. An attempt to confirm the proliferation data from the C/EBPβ ko macrophage-like cells using THP-1 transfected with C/EBPβ siRNA provided contradictory results as cells treated this way proliferated at lower rates than control cells. Interestingly, a direct comparison of the dominating isoform expression patterns in native THP-1 and C/EBPβ wt macrophage-like cells revealed that the former express mainly LIP, while in the latter, LAP predominates over the other isoforms. Taking this observation into account, these experiments provided further evidence for differential roles of LAP*/LAP and LIP during cell cycle progression. In a next step, a possible link between the observed differences regarding proliferation rates and morphologies of the C/EBPβ wt and ko cell lines was examined by subjecting the cells to serum withdrawal. Surprisingly, serum-starved C/EBPβ ko cells acquired a macrophage morphology, indicating that in these cell lines, the discrepancy between their proliferation rates indeed determines their distinct cellular appearances. C/EBPα, despite being slightly upregulated in C/EBPβ ko macrophage-like cells, thus appeared not to be able to compensate for the loss of C/EBPβ. Since the ETS family transcription factor PU.1 was found to be strongly induced by PMA treatment in the THP-1 cell line, its expression level was subsequently assessed in C/EBPβ ko cells. Interestingly, PU.1 remained expressed in C/EBPβ ko cells, albeit at lower levels than in C/EBPβ wt cells, thereby probably determining their macrophage fate. Overexpression experiments in THP-1 cells confirmed that C/EBPβ directly induces PU.1 expression, explaining the lower levels of this protein in C/EBPβ ko cells. Finally the question was addressed whether PMA remained capable of inducing morphological changes in C/EBPβ ko macrophage-like cells or in THP-1 transfected with C/EBPβ siRNA. In both cases, morphological analysis revealed that PMA treatment shifted the appearance of these cells notably towards a macrophage-like phenotype despite the absence, or attenuation, respectively, of C/EBPβ. Furthermore it could be shown by use of siRNA that, other than C/EBPβ, PU.1 is absolutely required for PMA-induced morphological changes in THP-1. Thus, the experiments presented herein indicate that two major roles of

C/EBPβ during monocytic differentiation are (i) the inhibition of cell cycle progression to which Rb may contribute and (ii) the enhancement of PU.1 activity by directly augmenting its expression. These results thus help to further understand the role of C/EBPβ during monocytic differentiation while confirming the crucial role of PU.1 during this process.

Overall, the results presented in this study extend current knowledge about monocytes. While their activation by cytokines like TNF was readily observable, attenuation of cytokine-induced signaling, as exemplified by the TNF tolerance phenomenon in this study, appeared to be dependent on various other factors that are possibly determined by the genetic background of the cells. If such factors proved to be important, the development of TNF tolerance could be linked to critical illnesses such as immunosuppression during late stages of sepsis. Additionally, the experiments presented herein further elucidate the role of C/EBPβ during monocytic differentiation, which appeared to be mainly restricted to an inhibition of proliferation and the induction of PU.1 expression. Combined, the results presented in this work extend our molecular knowledge of the regulation of crucial monocytic functions, which may be important for a better understanding of inflammatory and malignant processes.

Abbreviations

List includes standard abbreviations not defined in the text.

AP-1	Activator protein 1
APC	Antigen-presenting cell *or*
APC	Allophycocyanin
aPKC	Atypical protein kinase C
ATRA	*All-trans* retinoic acid
BD	Basic domain
BSA	Bovine serum albumin
bZIP	Basic leucine zipper domain
CD	Cluster of differentiation
C/EBP	CCAAT/enhancer binding protein
CEF	Chicken embryonic fibroblast
c-FLIP	Cellular FLICE-inhibitory protein
CFU (-GM)	(Granulocyte-monocyte) colony-forming unit
CHIT1	Chitinase 1
c_i	Cycling index
cIAP1	Cellular inhibitor of apoptosis 1
CMP	Common myeloid progenitor
CUGBP1	CUG repeat binding protein 1
DC	Dendritic cell
DMSO	Dimethyl sulfoxide
DNA	Deoxyribonucleic acid
DSMZ	Deutsche Sammlung von Mikroorganismen und Zellkulturen
DTT	Dithiothreitol
EDTA	Ethylenediaminetetraacetic acid
Egr-1	Early growth response 1
eIF2α	Eukaryotic translation initiation factor 2α
ER	Endoplasmic reticulum
ERK	Extracellular signal-regulated kinase
ETS	E-twenty six
FACS	Fluorescence-activated cell sorting
FCS	Fetal calf serum
FITC	Fluorescein isothiocyanate

FL	Full-length
FN	Fibronectin
FSC	Forward scatter
G-CSFR	Granulocyte colony-stimulating factor receptor
GFP	Green fluorescent protein
GMP	Granulocyte-monocyte progenitor
GRCh37	Genome Reference Consortium Human Build 37
HLA-DR	Human leukocyte antigen DR
HSC	Hematopoietic stem cell
IκB	Inhibitor of κB
IKK	IκB kinase
IL	Interleukin
IVT	*in vitro* transcription
JNK	c-Jun N-terminal kinase
ko	Knock-out
LAL	Limulus amoebocyte lysate
LAP	Liver activating protein
LIP	Liver inhibitory protein
LPS	Lipopolysaccharide
LZ	Leucine zipper
MafB	v-*maf* musculoaponeurotic fibrosarcoma oncogene homolog B
MAP3K	Mitogen-activated protein kinase kinase kinase
M-CSF(R)	Macrophage colony-stimulating factor (receptor)
MD-2	Myeloid differentiation factor-2
MEF	Mouse embryonic fibroblast
MEKK	MAPK/ERK kinase kinase
METS	Mitogenic ETS transcriptional repressor
MHC	Major histocompatibility complex
mTOR	Mammalian target of rapamycin
NDRG1	n-Myc downstream regulated gene 1
NE	Neutrophil elastase
NF-IL6	Nuclear factor IL-6
NF-κB	Nuclear factor κB
NK cell	Natural killer cell

ns	Not significant
PBMC	Peripheral blood mononuclear cells
PBS	Phosphate-buffered saline
PCNA	Proliferating cell nuclear antigen
PCR	Polymerase chain reaction
PE	Phycoerythrin
PFA	Paraformaldehyde
PI3K	Phosphoinositide 3-kinase
PKB/PKC	Protein kinase B/C
PMA	Phorbol 12-myristate 13-actetate
PMN	Polymorphonuclear leukocytes
PRR	Pattern-recognition receptor
PU.1	Purine rich box-1
Pyk2	Proline-rich tyrosine kinase 2
RA	Retinoic acid
Rb	Retinoblastoma protein
RD	Regulatory domain
re	Re-transfected
RHD	Rel homology domain
RLU	Relative light unit
RNA	Ribonucleic acid
ROS	Reactive oxygen species
RSK	p90 ribosomal S6 kinase
RT-qPCR	Real-time quantitative PCR
SDS	Sodium dodecyl sulfate
SFFV	Spleen focus forming virus
Sfpi1	SFFV proviral integration 1
SMase	Sphingomyelinase
SOCS1	Silencer of cytokine signaling 1
SPI1	SFFV proviral integration oncogene spi1
STAT	Signal transducer and activator of transcription
TAD	Transactivation domain
TBP	TATA box binding protein
TBS	Tris-buffered saline

TLR	Toll-like receptor
TNF	Tumor necrosis factor
TNFR1/2	TNF receptor 1/2
TRAF2	TNF receptor associated factor 2
TRAF3IP2	TRAF3 interacting protein 2
uORF	Upper open reading frame
UPL	Universal probe library
UTR	Untranslated region
wt	Wild-type
XIAP	X-chromosome-linked inhibitor of apoptosis

1. Introduction

Monocytes are a cell type present in the blood of humans and all vertebrates. They represent a class of cells responsible for coordinating innate and adaptive immunity *via* the production of cytokines and other effector molecules upon activation. The differentiation of monocytes from immature hematopoietic precursor cells occurs along the myeloid lineage. Mature monocytes are able to further differentiate towards macrophages (1).

1.1 Monocytes as a component of the immune system

As mononuclear phagocytic cells, monocytes can be found in the bloodstream of all vertebrates (1). Together with dendritic cells (DCs), granulocytes, natural killer (NK) cells, and mast cells they constitute the cellular component of the innate immune system (2). As such, they are crucial in the immediate immune response to pathogenic microorganisms.

Monocytes fulfill three main functions. As part of the mononuclear phagocyte system they ingest and destroy pathogens and other substances that might be harmful for the organism. Second, upon stimulation they produce a large number of effector molecules necessary for the induction and orchestration of the adaptive arm of the immune system. Finally, they are the origin of all tissue macrophages and, chiefly under inflammatory conditions, are also able to differentiate towards DCs (1).

About 5-10% of all leukocytes located in the peripheral blood are monocytes (1,3). In humans, their morphology is heterogeneous in terms of size and shape as well as in the expression of cell surface molecules (1,3). The presence of CD14 and HLA-DR antigens in the plasma membrane is a characteristic feature of all monocytes (3,4). CD14 is a co-receptor necessary for the function of toll-like receptor 4 (TLR4), which is a pattern-recognition receptor (PRR) essential for the detection of lipopolysaccharide (LPS) by cells of the innate immune system (5). HLA-DR is a major histocompatibility complex (MHC) class II molecule present on professional antigen-presenting cells (APCs). Monocytes/ macrophages, DCs, and B cells belong to this class of cells. APCs actively phagocytize pathogens, digest foreign proteins, and embed these peptides in their MHC class II receptors for presentation to T cells, which are a component of the adaptive immune system (6). On the other hand, CD16 and chemokine receptors, CCR2 in particular, are differentially expressed by monocytes (1,3,4). A large number of scavenger receptors are present on the monocytic cell surface, enabling these cells to remove toxic components or apoptotic cell debris from the system (1).

The monocyte subset expressing high levels of CD14 but no detectable CD16 (CD14^{hi} CD16$^-$) is the classical monocyte as initially identified and is the main subset present under physiological conditions (1,3,4). They can be further characterized by the expression of the chemokine receptor CCR2 and the absence of CX$_3$CR1 (7). Accordingly, they are mainly attracted by CCL2 in migration assays (8). In addition, they tend to produce anti-inflammatory cytokines, e.g., interleukin 10 (IL-10), upon activation (1,4).

In contrast, monocytes characterized by low expression of CD14 and the presence of CD16 (CD14$^+$ CD16$^+$) are induced in large numbers during infection and inflammation (9,10). They have been termed "proinflammatory monocytes" as they are the main producers of IL-1 and tumor necrosis factor (TNF; TNF-α) upon activation by LPS (1). Contrary to classical monocytes, the expression of CX$_3$CR1 is high in these cells, while only low levels of CCL2 are detected, making them targets for fractalkine-induced chemotaxis (7,8).

On average, mature monocytes remain in the bloodstream for only 3 days before extravasation and further differentiation and specialization (11). Apart from differentiating towards normal tissue macrophages and DCs, monocyte maturation contributes to the regeneration of osteoclasts responsible for the turnover of bone material, and the generation of tissue-specific macrophages, e.g., alveolar macrophages in the lung, Kupffer cells in the liver, or Langerhans cells in the epidermis (3,4).

1.2 Monocyte activation

Monocytes can be activated by a large number of molecules including pathogenic components and endogenous cytokines. One of the most important factors in monocyte activation is TNF, which can be produced by monocytes and most other cells of an organism upon activation. TNF in turn is able to activate monocytes and induces them to produce a wide range of effector molecules (1,12).

1.2.1 Cellular effects mediated by TNF

The cytokine TNF, which can be produced by a variety of different cell types including monocytes/macrophages, is regarded as a mediator of inflammatory and immunological processes (12). It was first discovered and described due to its cytotoxicity towards certain tumor cells (13). Its functions, however, were soon discovered to be far more complex. The TNF-induced production of chemokines and adhesion molecules, for example, plays an important role during chemotaxis, the adhesion events involved in this process, and the recruitment of leukocytes (14). Due to its influence on diverse cell types of the immune system, TNF is able to modulate processes of both innate and adaptive immunity (15). For

instance, TNF augments the activity of phagocytic cells, thus enhancing their capacity to remove pathogens (15,16). It is further able to stimulate antigen presentation in monocytes, thereby modulating the activation of lymphocytes (17). In addition, TNF-induced signaling mediates crucial functions during fundamental cellular processes such as proliferation, differentiation, and apoptosis (12). An elevated systematic production of TNF can be detected during sepsis and septic shock (18). The dysregulation of signal transduction or gene regulation mediated by TNF is also of critical importance in the pathogenesis of chronically inflammatory diseases and malignant processes (19,20).

1.2.2   Signal transduction and gene regulation induced by TNF

TNF exerts its effects by binding to two different receptors (TNFR1, TNFR2), leading to trimerization of the receptors, the association of several specific proteins, and the formation of multi-protein signaling complexes (12). TNF receptor associated factor 2 (TRAF2) plays a central role in the initial processes of TNF-induced signal transduction, resulting in an activation of the inhibitor of κB (IκB) kinase (IKK) complex, the proteolysis of IκB, and the activation of the transcription factor nuclear factor κB (NF-κB) (12,21). On the other hand, TRAF2 can also activate mitogen-activated protein kinase kinase kinases (also referred to as MAPK/ERK kinase kinases [MAP3Ks/MEKKs]) such as c-Jun N-terminal kinase (JNK) or p38, leading to the activation of the transcription factor activator protein 1 (AP-1) (12,21). NF-κB, as well as AP-1, then regulate the expression of genes involved in inflammatory and immunological processes (12,21). Moreover, the signal transduction pathways described are not rigidly separated but may also interact with one another. For instance, MEKK-3 is involved in the phosphorylation of the IKK complex, and TRAF3 interacting protein 2 (TRAF3IP2) might be the direct link between these two pathways (22,23). Additional molecules, including the kinases phosphoinositide 3-kinase (PI3K) and Akt/PKB (protein kinase B) as well as signal transducer and activator of transcription (STAT) transcription factors, also play a role during the signal transduction induced by TNF (24,25). It has further been suggested that sphingomyelinases (SMases) and atypical protein kinase C (aPKC) participate in TNF-induced signaling cascades (26,27). In addition, TNF mediates programmed cell death *via* different signaling pathways, e.g., through caspase-8/caspase-3 (12,21). Conversely, under certain conditions TNF causes an inhibition of apoptotic processes by activating NF-κB, which regulates the expression of anti-apoptotic proteins including cellular inhibitor of apoptosis 1 (cIAP1), X-chromosome-linked inhibitor of apoptosis (XIAP), and cellular FLICE-inhibitory protein (c-FLIP) (21,28). The signaling pathways described here are summarized in Figure 1.

Figure 1 *Cellular signaling induced by TNF.* Trimeric TNF binds to TNFR1 or TNFR2, inducing its trimerization. TRAF2 mediates signaling to the IKK complex *via* multiple signal transduction proteins, resulting in the activation of NF-κB. MEKKs are also activated by TRAF2 as well as through SMase signaling involving ceramides, leading to the induction of AP-1. Jak2 associates to the TNFR complex and activates STAT. The alternative pathway leads to the activation of caspases from their inactive pro-caspase form. Gene expression induced by the activated transcription factors leads to the production of proinflammatory genes, while NF-κB also induces the expression of proteins inhibiting the pro-apoptotic pathway [modified according to (12)].

1.2.3 Definition of tolerance

The tolerance phenomenon is an important mechanism for a multitude of immunological processes and is defined by the loss of sensitivity of a cell or a system towards repeated stimulation with the same substance (29). On one hand, under certain conditions tolerance

can be regarded as a protective concept for the cell when it repeatedly comes into contact with a certain stimulus (5,18). To exemplify this, tolerance processes play an important role during acute inflammatory diseases such as sepsis by reducing the detrimental effects resulting from a permanent stimulation with cytokines (18). On the other hand, tolerance may be a risk factor for the development of cellular anergy accompanied by paralysis of immunologically relevant cells (18,29,30). Phenomena similar to tolerance probably also play important roles during different chronic inflammatory or vascular processes (29,31,32). For example, sepsis is a systemic disease caused by microorganisms and/or their toxic products that can be accompanied by severe organic dysfunction (33). It is one of the most common complications found in patients treated in intensive care units and can be described as a severe over-activation of the immune system resulting in hyperinflammation, followed by immune paralysis (18,33). Almost a third of all patients suffering from severe sepsis die in the course of the disease (34). LPS tolerance, also commonly called endotoxin tolerance, is a classical example of immunological tolerance. It is mainly mediated by monocytes/macrophages *in vivo* and negatively affects the inducibility of receptors, signaling molecules, and negative regulators (35). As the expression profiles of LPS tolerant monocytes resemble those of immune cells recovered from septic patients, this form of tolerance has been suggested to play an important role in the immunoparalysis occurring during sepsis (29,35).

1.2.4   TNF-induced tolerance

Remarkably, there is evidence from *in vivo* studies indicating that repeated contact with TNF leads to the development of tolerance. Research in different animal species reveals that distinct effects mediated by TNF, like fever or gastrointestinal toxicity, are affected by this type of tolerance (36,37). Tumor-bearing mice also develop tolerance against an otherwise lethal dose of TNF by appropriate pre-treatment with this cytokine (38). It was further suggested that TNF tolerance *in vivo* is mediated by TNFR1, while an alteration of the bioavailability of TNF as well as its neutralization by antibodies was regarded as being unlikely (39,40). On the other hand, cyclooxygenase inhibitors such as indometacin are able to disrupt the development of tolerance when applied repeatedly (41). Moreover, several forms of cross-tolerance between TNF and LPS have been described (42). Accordingly, a pre-treatment with TNF protects against LPS-induced fever, which is not the case in the opposite direction (36,43). Since the development of TNF tolerance proceeds more slowly than that of LPS tolerance in animal models, different mechanisms seem to be responsible for the two phenomena (43).

Only a few results from cell culture studies characterizing the molecular basis of TNF tolerance exist thus far (44). A study performed with SW480 tumor cells demonstrates that a long-term pre-incubation (72 h) with a low dose of TNF can induce TNF as well as LPS tolerance. This treatment results in a reduced activity of the transcription factor NF-κB, compared to the non pre-incubated control (45). An 18 h pre-incubation of monocytic THP-1 cells with TNF, IL-1β, or LPS induces tolerance against stimulation with the same agonist as well as several forms of cross-tolerance, accompanied by reduced degradation of the NF-κB inhibitor protein IκB-α as well as attenuated phosphorylation of both JNK and extracellular signal-regulated kinase (ERK) (46). Furthermore, a short-term pre-treatment of FS4 fibroblasts with TNF leads to a selective tolerance against renewed stimulation with this cytokine, but not against IL-1β. This effect involves persistent activation of the TNF signal transduction pathway which negatively affects re-synthesis of IκB-α. (47). It could be shown in primary hepatocytes that the development of tolerance involves increased production of silencer of cytokine signaling 1 (SOCS1) 12 h after induction (48). In monocytic cells, the transcription factor CCAAT/enhancer binding protein β (C/EBPβ), through interaction with the NF-κB subunit p65, inhibits phosphorylation of this subunit and thereby expression of NF-κB dependent target genes (49,50). However, the hitherto available studies show that the basic mechanisms and functional consequences of TNF tolerance have not yet been satisfactorily elucidated.

1.3   Monocyte differentiation

Like all other cells of the hematopoietic system, monocytes are derived from hematopoietic stem cells that differentiate along the myeloid lineage. Mature monocytes are further able to differentiate towards macrophages found in various tissues of the body. Differentiation processes are closely regulated by a number of transcription factors, although their exact role is still elusive (1).

1.3.1   The C/EBP family of transcription factors

C/EBP proteins are transcription factors that recognize the common CCAAT box motif present in the promoters of genes involved in inflammation, differentiation, and proliferation (51,52). The six family members C/EBPα, β, γ, δ, ε, and ζ have been named chronologically according to the order of their discovery and display differing expression patterns in the tissues assessed (see 1.3.2 below). Several alternative names exist for all C/EBP proteins, for example nuclear factor IL-6 (NF-IL6) in the case of C/EBPβ.

All C/EBP proteins contain a conserved C-terminal basic leucine zipper (bZIP) domain consisting of the basic domain (BD) mediating DNA binding and a leucine zipper (LZ) motif responsible for protein-protein interactions (52). Through the LZ, C/EBP proteins can form homo- or heterodimers with family members and other transcription factors containing an LZ motif, thus modulating their DNA binding specificities. In this context, the interactions between different C/EBP proteins (*via* the composition of dimers) or the association of the C/EBPβ bZIP domain with the Rel homology domain (RHD) of the NF-κB subunits are examples for important regulatory protein-protein interplay (53,54). By interaction with their bZIP domains, the AP-1 family members Fos and Jun are additionally able to heterodimerize with C/EBPβ, inhibiting its transactivation potential (55). At the N terminus, C/EBP type transcription factors can contain one or several transactivation domains (TADs) and negative regulatory domains (RDs). The low conservation of their N termini determines their differential regulation by a variety of different factors (52). C/EBPα, β, and ε are expressed as at least two different-sized isoforms by alternative codon usage or differential splicing (see 1.3.4 below), further fine-tuning the target gene specificities of these proteins. As the shorter isoforms are N-terminally truncated, they often lack the TADs and are thus repressors of C/EBP function (56) (Figure 2). Of all C/EBP proteins, the functions of C/EBPα and β have been studied most excessively. Both the *CEBPA* and *CEBPB* genes can give rise to one or two large isoforms capable of initiating transcription of target genes, i.e., C/EBPα p42 and the two large C/EBPβ isoforms LAP* and LAP ("liver activating protein") (52). On the other hand, they code for the small, N-terminally truncated isoforms
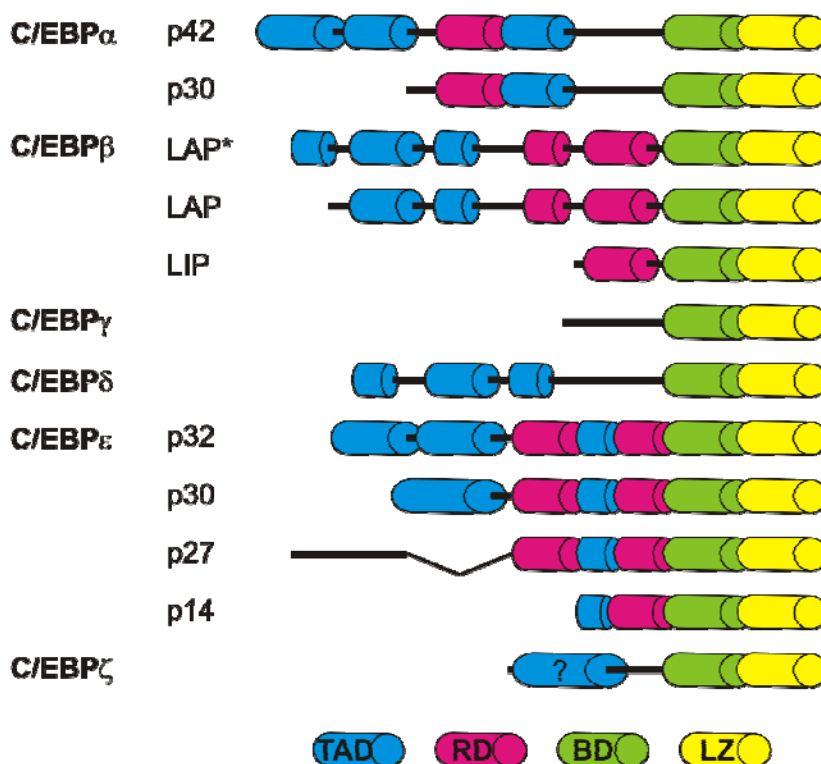

Figure 2 *Schematic representation of C/EBP protein structures.* Domains are shown as cylindrical structures, lines represent stretches connecting functional domains. The N terminus of C/EBPε p27 is spliced to the first functional domain [modified according to (52)].

C/EBPα p30 and C/EBPβ LIP ("liver inhibitory protein"). These may act as dominant negative inhibitors by hetero-dimerization with other C/EBP family members and/or isoforms, thereby blocking their transactivation potential (52).

The activity of C/EBP transcription factors is regulated both at the transcriptional and post-translational level. At the transcriptional level, the amount of protein produced as well as the isoform expressed determines the extent of C/EBP activity. Agents such as TNF, IL-1, or LPS are able to induce C/EBPβ expression, for example (52). At the post-translational level, the balance of translocation to the nucleus as well as the modulation of DNA binding capacity and of the transactivation potential play crucial roles in the regulation of the C/EBP system (57). The activity of C/EBPs is further modulated by phosphorylation of specific serine and threonine residues present in the TADs of the proteins (52).

1.3.2   C/EBP expression patterns

The expression patterns of CEBP family members vary widely and they can be detected in various tissues. Only C/EBPγ and ζ are expressed in most tissues, although the detected mRNA levels vary several-fold (58,59). While C/EBPα and β are present in numerous distinct tissues (52), C/EBPε appears to be restricted mainly to the myeloid and lymphoid lineages (60).

C/EBPα can be detected in the liver, skeletal muscle, intestine, lung, pancreas, adrenal gland, placenta, in adipose tissue as well as peripheral-blood leukocytes (61-63). At the sites of its most prominent expression, i.e., the liver and adipose tissue, C/EBPα is maximally expressed only in terminally differentiated cells (61,63). C/EBPδ expression is restricted mostly to the lung, kidney, spleen, intestine, and adipose tissue (63,64), with one report additionally showing high expression rates in the nervous system (65).

High levels of C/EBPβ can be found in the liver, lung, spleen, kidney, ovaries, testes, the adipose tissue, and in myelomonocytic cells (66,67). Consistently, its expression can be readily detected in monocytes, macrophages, and mature B cells (68). The level of C/EBPβ is increased during differentiation as well as by inflammatory stimuli like LPS (68-70). Monocytic differentiation in particular has long been associated with an upregulation of both C/EBPβ mRNA and protein (71,72). More recently it was shown that C/EBPβ activity during PMA-induced differentiation of monocytes is critically regulated through phosphorylation of Thr^{235} (73).

The varying expression patterns of C/EBP family members suggest that the functions of the individual proteins may be quite distinct.

1.3.3 Phenotypes of C/EBP knock-out mice

The most prominent functions of C/EBP proteins have been studied by the generation of gene-specific knock-out (ko) mice. Their phenotypes differ widely depending on the targeted C/EBP family member.

The most prominent feature of C/EBPα ko mice is their failure to properly store hepatic glycogen, resulting in impaired energy homeostasis and an early death (74). As a result of improper proliferation, the lung and liver architecture of these mice is abnormal as well (75). Another work demonstrates that granulopoiesis requires the presence of C/EBPα, as mice with a deletion of this gene fail to produce granulocytes, but not monocytes, due to a lack of granulocyte colony-stimulating factor receptor (G-CSFR) expression (76).

C/EBPβ ko mice exhibit a deregulated proliferative potential in the hematopoietic compartment (77). The mice develop lymphadenopathy and splenomegaly and are more susceptible to pathogenic infections, which also appears to lead to the development of skin lesions (77). While IL-6 is readily detectable, IL-12 expression is completely abolished in these animals. In addition, macrophage function is dramatically impaired due to their failure to release NO_2^- in response to infection with *Candida albicans* (77), *Salmonella typhimurium*, or *Listeria monocytogenes* (78). Furthermore, C/EBPβ is essential for the proper differentiation of mammary gland epithelium, and C/EBPβ ko mice fail to produce necessary milk proteins (79,80). Due to the lack of corpora lutea in their ovaries, female C/EBPβ ko mice are sterile (81).

Mice with a targeted disruption of C/EBPε succumb to infection early after birth due to a functional failure of neutrophils (82). In addition, tissue damage occurs as a result of uncontrolled neutrophil proliferation (83). Macrophage differentiation and function has also been reported to be impaired in C/EBPε ko mice (84).

Defects in C/EBPδ ko mice are mainly limited to the central nervous system, resulting in abnormal behavioral responses (65) and to the mammary gland in females, exhibiting augmented cellular growth (85). C/EBPβ and δ double-ko mice display a severe failure to accumulate lipid in adipose tissue, suggesting a maturation defect of adipocytes (86). This effect is less pronounced in single (i.e., C/EBPβ or δ) ko mice, indicating a synergy of both factors during adipogenesis (86).

C/EBPγ ko mice die within hours after birth, possibly due to lung defects (87). To circumvent this problem, bone marrow chimeras were established by transferring spleen cells of newborn C/EBPγ ko mice into lethally irradiated C/EBPγ wild-type (wt) mice. NK cells from these chimeras exhibit reduced activity and interferon-γ production (87).

Finally, studies using ko mice revealed the critical importance of C/EBPζ in signaling pathways mediating ER stress-induced apoptosis (52).

1.3.4 Regulation of isoform expression

Of the six C/EBP family members, three of their genes (i.e., *CEBPA*, *CEBPB*, and *CEBPE*) give rise to two or more different sized polypeptides, all of which contain the bZIP domain necessary for DNA binding and association with other proteins.

In the case of C/EBPα and C/EBPβ, all isoforms are translated from the same mRNA strand encoded by their respective intronless genes. *CEBPA* gives rise to the two isoforms p42 and p30, while *CEBPB* can be expressed as LAP*, LAP, and LIP (52). A leaky ribosome scanning mechanism has clearly been demonstrated to be of crucial importance in the case of C/EBPβ, where changing the proximity of the LAP AUG to a perfect Kozak sequence abrogated translation initiation at the LIP AUG (88). Expression of the truncated isoforms lacking the TAD is further dependent on transcription of a short out of frame upper open reading frame (uORF) present in both the *CEBPA* and *CEBPB* genes (56). uORF transcription reinforces the leaky scanning mechanism in which the ribosomes fail to recognize and initiate at the AUG of the full-length (FL) isoform due to its presence in a non-perfect Kozak consensus sequence, resulting in the generation of the short isoforms (56,88). The eukaryotic translation initiation factor 2α (eIF2α) has also been suggested to facilitate re-initiation at the LIP start codon in mammary epithelial cells (89).

In contrast, generation of the C/EBPε isoforms is mediated by a different mechanism. The gene contains two promoters, and the mRNAs are further spliced after transcription (52,90). Consequently, *CEBPE* can be expressed as either p32, p30, p27, and/or p14. No truncated isoforms of C/EBPγ, δ, and ζ exist as each is expressed solely as one full-length protein (52) (compare Figure 2).

1.3.5 Generation of LIP and implications of ratio alterations

Generation of LIP is mediated by CUG repeat binding protein 1 (CUGBP1). Its expression can be induced by C/EBPβ (91), and CUGBP1 binding to the uORF located between the translation start sites for LAP* and LAP is necessary for LIP expression (92). Translation of the short peptide encoded by the uORF prevents re-initiation at the AUG site for LAP located in close proximity, thereby skewing the LAP/LIP ratio (56). The critical importance of functional transcription of the uORF was recently demonstrated by Wethmar *et al.* In their study they find reduced LIP, but not full-length C/EBPβ levels in mice harboring a point mutation in the start codon of the *Cebpb* uORF, abolishing its expression (93). How

expression of the uORF is regulated is not completely understood. Evidence exists that signaling through the mammalian target of rapamycin (mTOR) pathway can directly affect differential expression of full-length and truncated isoforms (56). Modulation of the LAP/LIP ratio has also been implicated in the maturation of B cells (68). Studies investigating the potential of LIP to inhibit the activity of the longer C/EBPβ isoforms have demonstrated that the amount of LIP that needs to be present relative to LAP* and LAP can range from a molar excess in B cells (68) to substoichiometric levels in hepatocytes (88), possibly indicating altered susceptibilities to the action of LIP in different cell types. The inhibitory function of LIP can be attributed to its ability to form heterodimers with the large isoforms of C/EBP proteins, thereby rendering them inactive, and by its higher affinity to the C/EBP consensus sequence (88).

1.3.6   Effects of C/EBPβ proteins on proliferation

A number of studies suggest that C/EBPβ plays an important role in the regulation of cell cycle progression and proliferation (51,94). C/EBPβ ko mice display impaired differentiation of mammary gland epithelium, which could be demonstrated to be cell-intrinsic (79,80). Several lines of evidence indicate that LIP is upregulated in mouse (89) as well as human (95) mammary carcinomas and may therefore be a factor facilitating tumor formation by promoting proliferation rather than differentiation. In fact, this has been confirmed in the mouse model (96). A different mechanism of the influence of C/EBPβ on proliferation and tumorigenesis has been proposed by Lamb *et al.* (97). In their work they provide evidence that C/EBPβ represses expression of cyclin D1 target genes necessary for cell cycle progression. The association of cyclin D1 with C/EBPβ attenuates this repression in a large number of different tumors (97), possibly through modulation of its interactions with a mediator complex critical for transcriptional activity (98). Furthermore, expression of C/EBPβ is inhibited in BCR/ABL-transformed leukemia cells, and forced expression of this protein induces differentiation while inhibiting proliferation in this model (91). B cells reprogrammed towards a macrophage-like phenotype by overexpression of C/EBPβ were found to increase in number, while the same cells reprogrammed by the introduction of C/EBPα fail to proliferate (99). The growth factor-induced proliferation of hepatocytes has additionally been linked to phosphorylation of a critical residue (Thr^{217} in mouse and Ser^{105} in rat) of C/EBPβ, which is mediated by interaction with the p90 ribosomal S6 kinase (RSK) (100).

However, the studies cited above did not investigate the (potentially) differential effects of the three C/EBPβ isoforms on cellular proliferation, although several publications pay attention to

the effects that a change in the isoform ratio might exert. In 3T3-L1 preadipocytes, for example, LIP expression inhibits differentiation and promotes proliferation (56), and the same effect is also observed in primary chicken embryonic fibroblasts (CEF) (101). In the latter study, C/EBPβ ko CEFs also had a proliferative advantage over their C/EBPβ wt counterparts demonstrating that in this cell type, C/EBPβ primarily acts as a cell cycle inhibitor (101). Moreover, the activity of AP-1 is regulated by LIP in CEFs, leading to an elevation of cyclin D1 levels (101). LIP is also present in a complex containing E2F in epithelial cells (102). On the other hand, LAP attenuates the expression of cyclin D1, D2, and E and induces the cell cycle inhibitor p27^{Kip1} in the same study, resulting in reduced proliferation rates (102). In mouse embryonic fibroblasts (MEFs), C/EBPβ expression reduces the levels of cell cycle progression proteins such as cyclin A2, c-Myc, or proliferating cell nuclear antigen (PCNA) (103). The exact role of C/EBPβ on cyclin D1 expression is not yet clear, as conflicting data exist showing that LAP, but not LAP* or LIP, activate transcription from this promoter in mammary epithelial cells (104). In addition, the absence of C/EBPβ in mammary gland epithelial cells results in impaired, not increased, proliferation during pregnancy (79), and a similar effect was observed in hepatic stellate cells (105). This discrepancy may be due to the lack of full-length C/EBPβ in these systems. Further evidence for this notion is provided in a study showing that LIP itself has no effect on proliferation of hepatoma cells, but it is able to counteract the LAP-induced block of G_1-S phase transition (106). For its ability to inhibit proliferation in this model, the DNA-binding BD of LAP is dispensable while its LZ dimerization domain is of critical importance (106). In a recent mouse model demonstrating the importance of the uORF for LIP expression, MEFs from uORF ko mice exhibit slower expansion rates in culture compared to control MEFs (93). This study further shows that the reduction of LIP levels in uORF ko mice reduces the regeneration potential of the liver after partial hepatectomy, coinciding with delayed S phase entry of hepatocytes (93).

A study by Sebastian *et al.* demonstrates that C/EBPβ ko MEFs fail to undergo Ras^{V12}-induced cell cycle arrest (103). They show that in this model, a cooperative association between C/EBPβ and the retinoblastoma protein (Rb):E2F complex is necessary to induce oncogene-induced senescence (103). Hypophosphorylated Rb is able to bind C/EBPβ and transactivate its transcriptional function in differentiating adipocytes (107) and monocytic cells (108). In contrast, Rb phosphorylation, which is necessary for the G_1-S transition of the cell cycle, is elevated in cells expressing LIP (101). Since all three isoforms have been demonstrated to interact with Rb, association of these two proteins has to be mediated by the C-terminal region of C/EBPβ comprising the LZ and BD (108). An additional study shows

that Rb expression is induced concomitantly with C/EBPβ during deltanoid-induced differentiation in HL-60 cells, further hinting towards a functional cooperation between both proteins (109).

C/EBPβ has also been implicated in the regulation of apoptosis. In murine hepatic stellate cells, phosphorylation of Thr^{217} creates an interaction surface for procaspases-1 and -8, thereby inhibiting their self-activation capacity (105). This observation might help explain why C/EBPβ ko macrophages transformed by *v-myc* and *v-raf* cannot be established as a viable cell line (110). Additionally, C/EBPβ appears to be crucial for skin tumorigenesis induced by Ras signaling as C/EBPβ ko mice are completely resistant to tumor induction, presumably due to increased apoptosis of transformed cells (111).

1.3.7 The transcription factor PU.1

Purine rich box-1 (PU.1), encoded by the spleen focus forming virus (SFFV) proviral integration oncogene spi1 (*SPI1*) gene in humans and the SFFV proviral integration 1 (*Sfpi1*) gene in mice, is a transcription factor belonging to the E-twenty six (ETS) family of proteins that is essential for monocyte and macrophage differentiation. Mice lacking the *Sfpi1* gene are completely devoid of these two cell types and die shortly after birth. PU.1 expression is mainly restricted to the hematopoietic system and most pronounced in macrophages. High levels of PU.1 are also found in monocytes and granulocytes. The ETS domain consisting of a winged helix-loop-helix motif is responsible for DNA binding and involved in protein-protein interactions of PU.1 with members of the ETS family or other transcription factors, including C/EBPs. PU.1 activity can be regulated *via* phosphorylation induced by various cellular stimuli (112).

1.3.8 Mechanisms of differentiation

Hematopoietic stem cells (HSCs) in the fetal liver or the adult bone marrow are pluripotent and the progenitors of all cell types found in the blood (113). These cells give rise to the common myeloid progenitor (CMP) capable of generating all cells of the myeloid, but not the lymphoid lineage. The transcription factor PU.1 is required for the formation of the CMP stage (114,115). By antagonizing the action of GATA transcription factors, PU.1 further directs differentiation of CMPs towards the granulocyte-monocyte progenitor (GMP) stage (1,116,117). GMPs are also commonly called granulocyte-monocyte colony forming units (CFU-GM) capable of differentiating towards granulocytes and monocytes but not erythrocytes or mast cells (113). Commitment decisions leading to the generation of either

granulocytes or monocytes are mainly controlled by PU.1 and C/EBP transcription factors (see 1.3.9 below).

For research purposes, cells of the myeloid lineage can be differentiated towards monocytes/macrophages by stimuli such as phorbol esters (e.g., phorbol myristate acetate [PMA]), deltanoids (e.g., vitamin D_3), or lineage-specific cytokines (e.g., macrophage colony stimulating factor [M-CSF]). The premonocytic cell line THP-1 has proved to be a particularly good tool for the study of monocytic differentiation (118), yet other cell lines are also widely used. It was shown, for example, that secretion of fibronectin (FN) mediated by a pathway involving PKC-β is required for PMA-induced monocytic differentiation of HL-60 cells (119). FN in turn appears to activate signaling through interactions with integrins, as seen by the subsequent activation of the integrin-signaling nonreceptor tyrosine kinase p72^{Syk} (119). However, many important mechanisms occurring during monocytic differentiation are not yet well understood.

1.3.9   Transcriptional regulation

Genome-wide analyses of the transcriptome have revealed that the expression of a large number of genes, including those coding for several transcription factors, are differentially expressed during monocyte maturation (120-122).

Transcription factors of the C/EBP family, and C/EBPβ in particular, have long been implicated in the regulation of monocytic differentiation (71,72). C/EBPα appears to be more important for the maturation of granulocytes as there is evidence of its down-regulation in mature monocytes (72). One report shows that at the GMP stage, C/EBPα inhibits the activity of PU.1, resulting in the maturation towards granulocytes while inhibiting monocytic differentiation (123). Conversely, there is evidence that under certain conditions, C/EBPβ is also able to induce granulocytic differentiation (124-126), while C/EBPα or ε can induce monocytic differentiation in myelomonocytic cells including THP-1 (127). Additionally, expression of C/EBPβ from the *Cebpa* locus restores granulopoiesis in C/EBPα ko mice which are normally unable to produce granulocytes (128). Together, these results imply a partial redundancy in C/EBP family functions during blood cell differentiation.

Several important macrophage-associated genes are regulated by C/EBPβ, including the proline-rich tyrosine kinase 2 (Pyk2) which is associated with PMA-induced macrophage spreading and motility (129). Additionally, C/EBPβ is indispensable in deltanoid-induced differentiation of HL-60 cells (109). In a recent report, Chen *et al.* show that C/EBPβ as well as PU.1 can be induced by treatment with *all-trans* retinoic acid (ATRA) in a n-Myc downstream regulated gene 1 (NDRG1)-dependent manner (130). C/EBPε has also been

implicated in macrophage differentiation as mice deficient for this transcription factor contain only immature macrophages, and their biological activity is reduced (84).

The generation of PU.1 ko mice harboring a null mutation in the *Sfpi1* gene by two independent groups has demonstrated and confirmed an absolute requirement of this transcription factor for the generation of myeloid cells in general and the monocyte-macrophage lineage in particular (131,132). Progenitor cells from PU.1 ko mice do not respond to M-CSF due to the lack of proper M-CSF receptor (M-CSFR) expression, indicating that cytokine signaling is impaired (133). This is further confirmed by a study showing that transfection of cDNA encoding M-CSFR into PU.1 ko myeloid progenitor cells restores their ability to form macrophage colonies, as do controls re-transfected with PU.1 (134). Of note, PU.1 is actively induced by C/EBPα and C/EBPβ (124,135,136). High levels of PU.1 at the GMP stage antagonize the (inhibitory) function of C/EBPα, resulting in the generation of monocytes at the expense of granulocytes (114,123). Conversely, upregulation by C/EBPβ may help promote PU.1 activity at the same stage, thus enforcing the development of the monocytic phenotype.

There is no absolute requirement for C/EBPβ in the establishment of the myeloid lineage and the differentiation of monocytes and macrophages *in vivo* (77,137). However, several reports indicate that C/EBP family members are necessary for full activation of PU.1 transcriptional potential. C/EBPα, for example, has been shown to regulate the M-CSF and neutrophil elastase (NE) promoters in synergy with PU.1 and other factors (138,139). At the IL-1β promoter, C/EBPβ and PU.1 directly interact *via* their ETS and bZIP domains, and this interaction potently augments PU.1 activity (140-142). Although both the C/EBP and ETS binding sites are necessary for full promoter activation, the TAD of PU.1 is dispensable, in contrast to the C/EBPβ TAD (142). In addition, functional cooperativity between C/EBPβ and PU.1 has recently been reported at the promoter for myeloid differentiation factor-2 (MD-2) in IL-6-stimulated hepatocytes (143) and putatively also occurs at the chitinase 1 (*CHIT1*) promoter in differentiating THP-1 cells (73). Similar interactions have been demonstrated to occur between PU.1 and C/EBPδ (144). A direct protein-protein interaction with c-Jun further enhances the transcriptional activity of PU.1 (140), and activation of AP-1 has been implicated in PMA-induced monocytic differentiation (145). It has been reported that C/EBPβ is sufficient for the reprogramming of committed cells of different lineages, i.e., T or B lymphocytes, towards a monocyte/macrophage phenotype (99,146). In contrast, fibroblasts can be differentiated towards the same lineage only when C/EBPβ is co-expressed with PU.1 (147).

Several other transcription factors have been implicated in monocytic differentiation as well. In overexpression experiments v-*maf* musculoaponeurotic fibrosarcoma oncogene homolog B (MafB), which is also a member of the bZIP transcription factor family, directs the differentiation of the human bipotent myeloid progenitor cells U937 and HL-60 towards this fate (148). MafB is highly expressed in mature monocytes and macrophages (149), yet the fine-tuning of its level is highly critical, especially at the progenitor stage. A recent study by Sarrazin *et al.* demonstrates that low MafB expression in HSCs enhances their sensitivity to M-CSF, resulting in the generation of PU.1^{+} daughter cells capable of specifically repopulating the myelomonocytic lineage *in vivo* (150). Early growth response 1 (Egr-1), a zinc finger transcription factor, has been implicated in the determination of a monocytic fate as well (1,151). While its expression can be detected in both mature macrophages and neutrophils, in *in vitro* experiments it is necessary for the induction of monocytic differentiation while preventing the generation of granulocytes (152,153). However, studies with ko mice show that both MafB and Egr-1 are dispensable for full macrophage differentiation and function (154,155).

In summary, the stepwise differentiation of HSCs towards mature monocytes and macrophages requires the tight regulation of a number of transcription factors, which modulate cell fate through their mutual interactions. In particular, the exact role of the different C/EBP proteins in this process is not yet well understood.

1.3.10 Cell cycle modulation

A genome-wide analysis of expression patterns has revealed an overrepresentation of genes associated with the cell cycle during monocyte to macrophage differentiation (122). Differentiation usually coincides with an inhibition of proliferation (1), yet halting of the cell cycle is not absolutely necessary for monocytic maturation (156). Rb, which has been extensively implicated in differentiation processes, is an important negative regulator of cell cycle progression. Its hypophosphorylated form binds the transcription factor E2F1 and thereby inhibits expression of E2F target genes necessary for progression from G_1 to S phase. Phosphorylation of Rb leads to dissociation of this complex enabling E2F1 to activate cell cycle-specific genes [reviewed in (157)]. The knock-down of Rb expression inhibits deltanoid-induced differentiation of HL-60 (109). In cells induced to undergo monocytic differentiation, total Rb increases while its phosphorylation level decreases noticeably, coinciding with cell cycle arrest at the G_1-S transition (158,159). Another group confirmed an increase of total Rb levels, which remain hypophosphorylated, during monocytic differentiation of human myeloid progenitors (160). When Rb expression is ablated, these
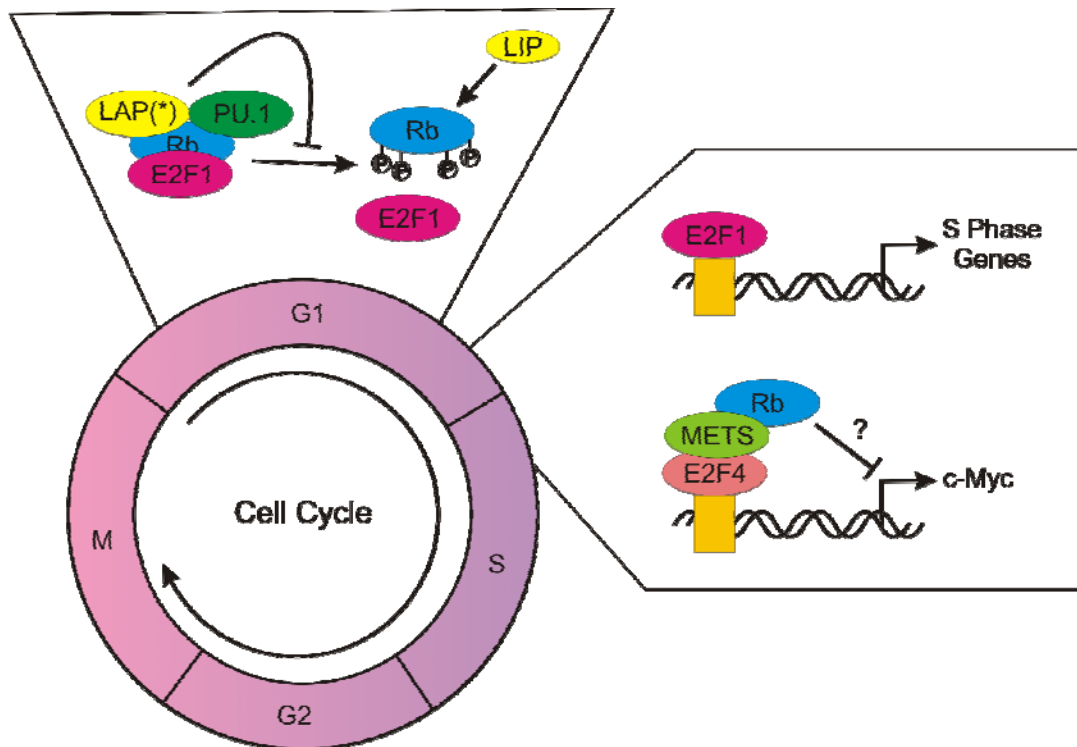
Figure 3 *Cell cycle control by Rb.* During the G_1 phase of the cell cycle, unphosphorylated Rb binds E2F1. Upon phosphorylation of at least 4 different serines, E2F1 is freed to bind to promoters of S phase genes, inducing cell cycle progression. The large isoforms of C/EBPβ (LAP$^{(*)}$) and PU.1 are able to bind unphosphorylated Rb, preventing its phosphorylation and thus preventing release of E2F1. C/EBPβ LIP appears to stabilize phosphorylated Rb. Rb is necessary for METS-induced repression of *c-Myc* expression which is necessary during the S phase of the cell cycle [modified according to (94)].

cells differentiate along the granulocytic lineage (160). Interestingly, the TAD of PU.1 has been demonstrated to bind Rb (161). Therefore, it is conceivable that Rb might play an important role in enabling interactions between C/EBPβ and PU.1 by bringing these factors into close proximity.

Rb has also been reported to exert functions apart from direct modulation of the cell cycle. For example, it appears to be essential for the function of mitogenic ETS transcriptional suppressor (METS) which is maximally expressed in terminally differentiated macrophages and inhibits promoters of cell cycle associated genes like *c-Myc* (162). In summary, Rb plays an important role during differentiation-induced cell cycle arrest, and several lines of evidence point towards an important role of C/EBPβ and/or PU.1 in this process (Figure 3).

2.   Materials and methods

2.1   Buffers and media

Concentrations of chemicals in buffers are given as working concentrations unless indicated otherwise.

Buffer A

10 mM HEPES (Sigma-Aldrich, Munich, Germany), 10 mM KCl (Carl Roth, Karlsruhe, Germany), 300 mM Sucrose (Roth), 1.5 mM $MgCl_2$ (Merck, Darmstadt, Germany), 0.01% (v/v) Nonidet-P40 (AppliChem, Darmstadt, Germany) in H_2O supplemented with 3x Complete EDTA-free Protease Inhibitor Cocktail (Roche Pharma, Grenzach-Wyhlen, Germany).

Buffer B

20 mM HEPES, 100 mM KCl, 100 mM NaCl (Mallinckrodt Baker, Griesheim, Germany), 20% (v/v) Glycerol (Merck) in H_2O supplemented with 3x Complete EDTA-free Protease Inhibitor Cocktail.

Buffer C

150 mM NaCl, 25 mM $MgCl_2$, 50 mM Tris-HCl pH 7.4 (AppliChem), 10% Glycerol, 1% Nonidet-P40 in H_2O supplemented with 3x Complete EDTA-free Protease Inhibitor Cocktail.

Erythrocyte Lysis Buffer

153.7 mM NH_4Cl (Merck), 11.9 mM $NaHCO_3$ (Merck), 890 nM EDTA (Sigma-Aldrich), pH 7.3 in H_2O.

FACS Buffer

5% (w/v) BSA (Roche), 0.02% (w/v) NaN_3 (Merck) in PBS.

PBS

137 mM NaCl, 2.65 mM KCl, 65 mM Na_2HPO_4 (Mallinckrodt Baker), 1.47 mM KH_2PO_4 (Merck), pH 7.4 in H_2O.

SDS Buffer (Tris-Glycine)

50 mM Tris (AppliChem), 383.6 mM Glycine (AppliChem), 1.6 mM EDTA, 0.1% (w/v) SDS (AppliChem), pH 8.5-8.7 in H_2O.

SDS Loading Buffer (4x)

250 mM Tris-HCl, 8% (w/v) SDS, 40% Glycerol, 200 mM DTT (AppliChem), 0.04% (w/v) bromophenol blue (AppliChem), pH 6.8 in H_2O.

TBS-T

137 mM NaCl, 20 mM Tris, 0.1% (v/v) Tween® 20 (Sigma-Aldrich), pH 7.6 in H_2O.

Transfer Buffer

25 mM Tris, 191.8 mM Glycine, 20% (v/v) Ethanol (Th. Geyer, Renningen, Germany), pH 8.3 in H_2O.

Western Blot Staining Solution

260 nM Ponceau S (Sigma-Aldrich), 18.4 mM Trichloroacetic acid (Merck) in H_2O.

2.2 Antibodies and reagents

PMA, recombinant human TNF, and the antibody directed against actin were purchased from Sigma-Aldrich. The antibody against C/EBPβ (H-7) was from Santa Cruz Biotechnology (Heidelberg, Germany), antibodies raised against C/EBPα, Rb P-Ser[608], Rb P-Ser[795], total Rb, and PU.1 were obtained from Cell Signaling Technology (Danvers, MA, USA). The antibody detecting C/EBPε was from Acris Antibodies (Herford, Germany), TATA box binding protein (TBP) from Abcam (Cambridge, UK). Horseradish peroxidase-coupled secondary antibodies raised against rabbit or mouse IgG were from Vector Laboratories (Peterborough, UK). The following antibodies were used for flow cytometric analyses: CD3-APC, CD8-PE, CD16-PE, CD19-PE, and HLA-DR-APC (BD Biosciences, Heidelberg, Germany), CD4-FITC, CD14-FITC, CD45-AlexaFluor®405 and CD56-FITC (Caltag™ Laboratories, Invitrogen) as well as the respective isotype control antibodies.

2.3 Cell culture

Human acute monocytic leukemia THP-1 and human epithelial HeLa cells were purchased from Deutsche Sammlung von Mikroorganismen und Zellkulturen (DSMZ, Braunschweig, Germany). Mouse C/EBPβ wt, ko as well as re-transfected with C/EBPβ (re) macrophage-like cells were kindly provided by Valeria Poli (137). The cells were cultivated in RPMI (Biochrom, Berlin, Germany) supplemented with 7.5% FCS (Biochrom), 100 U/ml penicillin, and 100 µg/ml streptomycin (Biochrom) at 37°C in a humidified atmosphere containing 5% CO_2. THP-1 were split before reaching a density of $1 \cdot 10^6$ cells/ml, HeLa as well as C/EBPβ wt, ko, and re macrophage-like cells upon reaching approximately 70-80% confluency using a Trypsin-EDTA solution (Sigma-Aldrich). All cell culture media and reagents were routinely tested for endotoxin content using the Limulus Amoebocyte Lysate (LAL) assay (Lonza, Cologne, Germany). Absorbances were measured in 96 well plates using an ELx808 Absorbance Microplate Reader (BioTek Instruments, Bad Friedrichshall, Germany). Cell culture supernatants of all cell lines were tested for contamination with mycoplasma every 4-8 weeks utilizing the MycoAlert® Mycoplasma Detection Kit (Lonza) according to

manufacturer's instructions. Luminescence was measured in white-walled 96 well plates in an ORION L Luminometer (Berthold Detection Systems, Pforzheim, Germany).

2.4 Isolation of primary human monocytes

Whole blood samples from healthy blood donors were kindly provided by the Gesundheitsamt München and the Institute for Transfusion Medicine (MHH). Buffy coat was prepared by density centrifugation on Ficoll® (Biochrom) using LeucoSep® tubes (Greiner Bio-One, Frickenhausen, Germany) to avoid contamination with polymorphonuclear leukocytes (PMN). The separated peripheral blood mononuclear cells (PBMCs) were washed in RPMI supplemented with 2% FCS and quantified in a hematology analyzer (Sysmex Deutschland, Norderstedt, Germany). Subsequently, monocytes were negatively isolated using the human Monocyte Isolation Kit II (Miltenyi Biotec, Bergisch Gladbach, Germany) according to manufacturer's instructions. Ice-cold sterile PBS (Biochrom) supplemented with 5% FCS and 2 mM EDTA was used as stain and wash buffer during the procedure. Purified monocytes were seeded into 12 well plates at a density of $4 \cdot 10^6$ cells per well in a total of 2 ml of RPMI supplemented with 8% FCS, 100 U/ml penicillin, 100 µg/ml streptomycin, OPI Media Supplement (Sigma-Aldrich), and non-essential amino acids (Gibco® Invitrogen, Karlsruhe, Germany) and were allowed to adhere for 1 h at 37°C in a humidified atmosphere containing 5% CO_2. Non-adherend cells were subsequently removed by washing with monocyte culture medium. The purity of isolated monocytes was routinely tested by FACS® analysis (see 2.7 below).

2.5 Plasmids and siRNA

pTracer-FL was designed to contain the full-length *CEBPB* sequence capable of producing all three C/EBPβ isoforms under the control of a CMV promoter from a pTracer vector background. It was constructed and kindly provided by Romina Gutsch (Institute of Clinical Chemistry, MHH). The construct was transformed into OneShot® Top Ten Chemically Competent *E. coli* (Invitrogen) according to the protocol. Positive clones were subsequently selected for ampicillin resistance, and the presence of insert was verified by PCR and/or sequence analysis. Plasmids were isolated using the NucleoBond® Xtra Maxi EF kit according to manufacturer's instructions (MACHEREY-NAGEL, Düren, Germany).

3'-AlexaFluor®488-labeled siRNA oligonucleotides were purchased from QIAGEN (Hilden, Germany). The siRNA targeting C/EBPβ mRNA had the sense sequence 5'-gcccugaguaaucgcuuaa. Both strands contained a 3'-dTdT overhang. AllStars Negative

Control siRNA (QIAGEN) was used for control experiments. The siRNA oligonucleotides were resuspended in siRNA Resuspension Buffer (QIAGEN) and annealed by boiling at 90°C for 1 min and subsequent incubation at 37 h for 1 h.

Unlabeled PU.1-specific siRNA was purchased from Santa Cruz and resuspended in water provided by the manufacturer.

The resulting stock concentrations of the siRNAs applied were 40 μM for AllStars and C/EBPβ and 10 μM for PU.1.

2.6   Transfections

Transfection of THP-1 with the plasmids described was achieved using Nucleofector® technology (Lonza). In detail, $1.5 \cdot 10^6$ THP-1 were transfected using the Cell Line Nucleofector® Kit V and the indicated amount of plasmid with program T-008. Cells were then seeded in 12 well plates in a total volume of 1.6 ml. RPMI medium used was supplemented with 10% FCS, the standard amount of penicillin and streptomycin (see Chapter 2.3), and 0.05 mM 2-mercaptoethanol (AppliChem). Assessment of transfection efficiency was performed at least 5 h after transfection by visualizing green fluorescent protein (GFP) expression using an Axiovert 35 fluorescence microscope (Carl Zeiss, Oberkochen, Germany).

The siRNA transfection of THP-1 was performed using the Cell Line Nucleofector® Kit V with 100 or 400 pmol siRNA, $1 \cdot 10^6$ cells, and program A-030. Cells were transferred to 12 well plates and cultivated in a total of 1.6 ml using the medium described above. Prior to analysis to determine transfection efficiency using a fluorescence microscope, cells transfected with AllStars siRNA were washed once to remove fluorescent siRNA that had not been internalized by the cells. Cells were incubated for at least 24 h at 37°C before stimulation or harvest.

2.7   FACS® analysis

Freshly isolated peripheral human monocytes (see 2.4 above) and the cell fraction that was retained in the magnetic isolation column during the isolation procedure were used for analysis. Control cells were subjected to erythrocyte lysis using Erythrocyte Lysis Buffer prior to the staining reaction. Lysis was stopped by addition of FCS after incubation for 7 min at RT. In each case $5 \cdot 10^5$ cells were labeled with fluorophore-tagged antibodies per staining reaction. Cells were transferred to V-bottom 96 well plates and centrifuged prior to resuspension in FACS buffer. The following antibody combinations were used in one

staining reaction (dilutions indicated in brackets): CD45 (1:100), CD3 (1:5), CD4 (1:50), and CD8 (1:5); CD45, CD14 (1:50), CD16 (1:5), and HLA-DR (1:5); CD45, CD3, CD19 (1:5), and CD56 (1:20); as well as the isotype controls AlexaFluor®405 (1:100), PE (1:5), FITC (1:20), and APC (1:5). Cells were incubated in the dark in antibody mixture for 30 min on ice and subsequently washed thrice in FACS buffer. In the end, cells were fixed in 1% PFA (Sigma-Aldrich) and stored at 4°C until detection using the LSR II flow cytometer (BD Biosciences). Graphic representations were generated using FACSDiVa™ Software (BD Biosciences).

2.8   Stimulation and differentiation of cells

For induction of TNF tolerance, primary human monocytes were incubated with a low dose of TNF as indicated for 72 h and re-stimulated with a high TNF dose (see labeling) for 2.5 h prior to sample preparation. For dose-response experiments, cells were left untreated for 72 h and stimulated with the indicated amount of TNF for 5 h.

Human monocytic THP-1 cells and mouse C/EBPβ wt, re, or ko macrophage-like cells were stimulated for 6-72 h with 1, 10, or 100 nM PMA prior to morphologic analysis using a Zeiss Axiovert 35 light microscope or protein preparation as described below (see 2.10). All cells were seeded at least 17 h before the start of stimulation. For protein extraction, $1.5 \cdot 10^7$ THP-1 were seeded in 30 ml in large (T75) tissue culture flasks, while $1.8 \cdot 10^6$ C/EBPβ wt or ko cells were seeded in 3 ml in 6 well plates. C/EBPβ macrophage-like cells were seeded at a density of $3 \cdot 10^5$ cells in 3 ml in 6 well plates for microscopy. THP-1 that had been transfected with siRNA (see 2.6 above) were counted 24 h after nucleofection. $4 \cdot 10^5$ cells were then seeded in 3 ml in 6 well plates and immediately stimulated with PMA. Morphology was assessed after 24 h of PMA-induced differentiation.

2.9   ELISA

Cells were stimulated with the indicated amount of TNF for the time specified. Supernatants were cleared of all cells by centrifugation and subsequently analyzed using the Quantikine® Human CXCL8/IL-8 Immunoassay (R&D Systems, Wiesbaden, Germany) according to manufacturer's instructions. All samples and standards were measured in duplicate. Plates were read using the ELx808 Absorbance Microplate Reader.

2.10 Preparation of protein extracts

Whole cell extracts were prepared by disruption of the plasma membrane in Buffer C. Cell pellets in Buffer C were kept on ice for 5 min, ultrasonicated for 10 sec, and placed on ice for another 5 min. Insoluble portions were separated from the extract by centrifugation ($17000 \times g$, 10 min, 4°C).

Separation of nuclear from cytoplasmic protein fractions was achieved by disrupting the plasma membrane with Buffer A on ice for 5 min. Nuclei were separated from the resulting cytoplasmic extract by spinning at maximum speed for 30 sec and, after an additional wash step in Buffer A, disrupted by the addition of Buffer B. After ultrasonication, nuclear extracts were obtained by spinning down insoluble parts at maximum speed for 30 sec.

Protein concentrations were determined by the Bradford method using the Bio-Rad assay (Bio-Rad Laboratories, Munich, Germany) in a 96 well format according to manufacturer's instructions. Measurement was performed in triplicate for each sample using the ELx808 Absorbance Microplate Reader. Protein extracts were stored at -80°C until further use.

2.11 Real-time quantitative (RT-q) PCR

Cells were harvested and RNA isolated using the RNeasy Mini Kit (QIAGEN) according to manufacturer's instructions. RNA was eluted in 50 µl RNase-free H_2O and concentrations were determined using the NanoDrop ND-1000 photometer (peqlab, Erlangen, Germany). Unless indicated otherwise, 1 µg of total RNA was reverse transcribed using the SuperScript™ II Reverse Transcriptase kit (Invitrogen) as described in the manual. RT-qPCR was performed using the LightCycler® 480 system (Roche) in a 96 well format. *IL8* and *CEBPB* were measured using Universal Probe Library Probes (UPL) 72 and 70, respectively, as well as the following primers: 5'-agacagcagagcacacaagc and 5'-atggttccttccggtggt (*IL8*); 5'-tgggacccagcatgtctc and 5'-tccgcctcgtagtagaagttg (*CEBPB*). LightCycler® 480 Probes Master (Roche) was used for the reaction and measurement was performed according to manufacturer's instructions.

GAPDH was measured using the primers 5'-tgctgagtatgtcgtggagtc and 5'-ggatgcagggatgatgt-tct as well as the hybridization probes 5'-Cy5-ccatgccatcactgccacccagaagact and 5'-gacaactttggtatcgtggaaggactcatgaccaca-3'-FITC. The reaction mix contained 50% LightCycler® 480 Probes Master (Roche), 5% DMSO (Sigma-Aldrich), 25% cDNA, 0.1 pmol/µl of each primer, and 0.2 pmol/µl of both hybridization probes in a total volume of 20 µl. Measurement was performed using the following program (see next page):

Temperature	Duration	Ramp Rate	Number of Cycles
95°C	5:01 min	4.4°C/s	1
95°C	10 s	4.4°C/s	
59°C	30 s	2.2°C/s	45
72°C	30 s	4.4°C/s	
37°C	30 s	2.2°C/s	1

2.12 Microarray analysis

Total cellular RNA was isolated and its concentration measured as described above (Chapter 2.11). 1 µg of RNA was reverse transcribed using the GeneChip® One-Cycle cDNA Synthesis Kit and Sample Cleanup Module according to manufacturer's instructions (Affymetrix, High Wycombe, UK). The resulting cDNA template was transcribed to yield biotinylated cRNA using the GeneChip® Expression 3'-Amplification Reagents for *in vitro* transcription (IVT) Labeling, provided in a kit by Affymetrix. cRNA was subsequently hybridized to the HG-U133 Plus 2.0 microarray (Affymetrix) containing probes for over 47,000 human transcripts, stained, and scanned using a GeneChip® Scanner 3000 7G (Affymetrix).

Reverse transcription, labeling, hybridization, and measurement was performed by the Roland Lang lab in the context of a cooperation with the Institute of Medical Microbiology, Immunology, and Hygiene (Klinikum rechts der Isar der TU München, Munich, Germany).

IL8 is represented by the two probe sets 202859_x_at and 211506_s_at on the HG-U133 Plus 2.0 chip used. As the values obtained by both probe sets resembled each other in regard to the pattern and magnitude of stimulus-dependent induction, only the former probe set was used for the analysis of cellular activation.

2.13 Western blots

Protein extracts were prepared for SDS-PAGE by dilution with SDS Loading Buffer and boiling for 10 min at 95°C. Depending on the molecular mass of the protein analyzed, samples were separated on 10%, 12%, or 16% precast SDS gels (biostep, Jahnsdorf, Germany) at 125 V in minigel chambers (peqlab). Proteins were then transferred to 0.45 µm nitrocellulose membranes (Bio-Rad) by blotting in a tank blotter (peqlab) at 400 mA for 100 Vh. Prior to blocking, membranes were stained for 5 min in Western Blot Staining Solution to verify equal protein transfer across the area of the membrane. Blocking was done for 1 h at room temperature in 5% skim milk powder (Merck) dissolved in PBS-T or TBS-T, depending on the antibody used. Antibody dilutions and buffers used are summarized in

Antibody	Company	Dilution	Dilution Buffer
Rabbit anti-Actin	Sigma-Aldrich	1:1000	5% BSA/PBS-T
Rabbit anti-C/EBPα	Cell Signaling	1:500	5% MMP/TBS-T
Mouse anti-C/EBPβ	Santa Cruz	1:200	5% BSA/TBS-T
Rabbit anti-C/EBPε	Acris	1:500	5% BSA/PBS-T
Rabbit anti-PU.1	Cell Signaling	1:1000	5% BSA/TBS-T
Mouse anti-Rb	Cell Signaling	1:2000	5% MMP/TBS-T
Rabbit anti-Rb (P-Ser^{608})	Cell Signaling	1:1000	5% BSA/TBS-T
Rabbit anti-Rb (P-Ser^{795})	Cell Signaling	1:1000	5% BSA/TBS-T
Mouse anti-TBP	Abcam	1:2000	1% MMP/PBS-T (0.05%)

Table 1 *List of antibodies used for western blotting.* Dilutions were prepared in the dilution buffer indicated. Tween$^{®}$ 20 was used at a concentration of 0.1% unless indicated otherwise.

Table 1. Membranes were incubated with the primary antibody over night at 4°C to allow for binding to immobilized antigen. After washing with the respective buffer, membranes were shaken in the corresponding secondary antibody for 1 h at RT. The dilutions of secondary antibodies were 1:5000 for anti-mouse and 1:10000 for anti-rabbit in the same buffer system used for the respective primary antibody. Chemiluminescence was detected with SuperSignal West Femto Maximum Sensitivity Substrate (Thermo Fisher Scientific, Bonn, Germany) using the MF-ChemiBIS 3.2 imaging system (biostep). Band intensities were analyzed using the TotalLab TL100 software (Nonlinear Dynamics, Newcastle Upon Tyne, UK) and depicted using GraphPad Prism5 (GraphPad Software, La Jolla, CA, USA). Where indicated, membranes were stripped in between detections by shaking in 0.2 M NaOH for 30 min. Membranes were washed for 5 min in H_2O before and after the stripping procedure and subsequently blocked again with skim milk solution.

2.14 Proliferation assay

Cells were seeded in 100 µl of culture medium in white-walled 96 well plates. A total of 10,000 (transfected) THP-1 or 5000 C/EBPβ (wt or ko) macrophage-like cells were used per well. HeLa were seeded at 5000 cells per well and transfected with 25 ng plasmid DNA using SuperFect$^{®}$ Transfection Reagent (QIAGEN) according to the protocol provided. One plate was prepared for each time point analyzed. After incubation at 37°C for the time indicated, cells were lysed with 50 µl of Cell Lysis Reagent (ViaLight$^{®}$ Plus Kit, Lonza) and frozen at -80°C until measurement. The analysis was then carried out according to manufacturer's instructions using an ORION L Luminometer (Berthold Detection Systems). Measurements were performed in triplicate. The proliferation assay using HeLa was measured in duplicate by Romina Gutsch.

2.15 Cell cycle analysis

Cell cycle analysis was performed using the CycleTest™ PLUS DNA Reagent Kit (BD Biosciences). Where indicated, macrophage-like cells (C/EBPβ wt and ko) were synchronized to ensure population homogeneity either by serum withdrawal at least over night or by allowing them to grow to a high density. The latter was achieved by seeding $3 \cdot 10^6$ macrophages in a large (T75) tissue culture flask and incubation for 4 days at 37°C. Medium was renewed after 3 days to avoid starvation of the cells in the process. Synchronized cells were then seeded in new tissue culture flasks (T25) using 0.2 M EDTA in PBS for disruption of adherence. They were subsequently incubated at 37°C and harvested at the times indicated by trypsinization followed by centrifugation. Washing was performed with the Buffer Solution provided and cell suspensions were subsequently stored at -80°C. All samples were then thawed together and stained for 10 min at RT in CycleTest Buffer A. CycleTest Buffer B was added for additional 10 min at RT. CycleTest Buffer C containing propidium iodide was then added to the cells and incubated in the dark at 4°C for 10 min. Cells were centrifuged through a 35 μm cell strainer with nylon mesh (BD Biosciences) and kept on ice until measurement. Analysis was performed using either a FACSCalibur™ or a LSR II flow cytometer (both from BD Biosciences). Cell duplexes were excluded from analysis by a forward scatter-W (FSC-W) *vs.* FSC-H dotplot. Graphic representations were generated using FACSDiVa™ Software and GraphPad Prism 5. Cycling index (c_i) was calculated by adding the percentages of cells in S and G_2M phases and dividing them by the percentage in G_0G_1 [$c_i = (S+G_2M)/G_0G_1$].

2.16 Computational sequence analysis

The free software TFSEARCH ver. 1.3 by E. Wingender, R. Knueppel, P. Dietze, and H. Karas (GBF-Braunschweig), which is available online at http://www.cbrc.jp/research/db/ TFSEARCH.html, was used to identify potential transcription factor binding sites in the human *RB1* and *E2F1* promoter regions. Sequences used for the analyses were from the Genome Reference Consortium Human Build 37 (GRCh37).

RB1 is located on chromosome 13, of which the region comprising base pairs 48,876,316 – 48,878,048, representing sequences up to 1568 bp upstream of the *RB1* start codon, was analyzed. This region also included the complete 5'-UTR of the corresponding mRNA. The sequence was retrieved from NCBI PubMed (NCBI Reference Sequence NC_000013.10).

E2F1 is located on chromosome 20, of which the region comprising base pairs 32,274,071 – 32,275,666 was analyzed, representing sequences up to 1457 bp upstream of the *E2F1* start

codon, also containing the complete 5'-UTR. The sequence was retrieved from NCBI PubMed (NCBI Reference Sequence NC_000020.10).

2.17 Statistical analyses

Statistical analysis by student's t test or Mann-Whitney U test was performed using the statistics tool provided with GraphPad Prism 5 where indicated.

3.   Results

3.1   Mechanisms of monocyte activation

3.1.1   Assessment of monocyte purity

TNF tolerance is a phenomenon rendering cells unresponsive to repeated stimulation with the cytokine TNF.   Parts of the underlying mechanisms have been studied in the human monocytic cell line THP-1 (49,50).   For this study, primary human monocytes were investigated to confirm TNF tolerance in these cells and to further elucidate the mechanisms involved.   In order to ensure the purity of the monocyte fraction isolated from human peripheral blood, the cells were analyzed by flow cytometry.   As shown in Figure 4B (*Monocyte*), 95.0% of the cells that became (transiently) adherend after the isolation procedure are double-positive for both HLA-DR and CD14 (green color), both of which are suitable monocyte markers in humans (1).   The dot plot of the FSC (Figure 4A) clearly shows that the cell population detectable in the buffy coat at the bottom left (see *Isotype* as well as *Input*), which corresponds to the lymphocyte subset, is depleted in the monocyte sample, while the monocyte/macrophage fraction located in the central area is highly enriched. Although most cells in the buffy coat (86.1%) expectedly stain positive for CD45, which is a marker of hematopoietic cells (163), that fraction is further increased to 99.7% of all gated cells after the monocyte isolation procedure (Figure 4C, *Input* and *Monocyte*, respectively). An additional cell population observed to the lower left of the main monocyte population was gated as a new population P2 (shown in yellow; Figure 4A).   It represents monocytes with a different morphology presumably due to scraping the cells from the cell culture dish.   Gate P2 contains 8.5% of all cells gated and is double-positive for HLA-DR and CD14 as shown in Figure 4B, thus eliminating the possibility of contamination by a different cell fraction.   In addition, this population is not visible in either the isotype or input dot-plots in Figure 4A, also supporting the notion that these cells are not a population that is normally present in buffy coat but are rather a result of the experimental procedures applied.

In a next step, it was attempted to directly detect possibly contaminating cell populations in the isolated monocytes.   Potential contaminants would likely be lymphocytes, as granulocytic and erythrocyte fractions are removed by density centrifugation during the isolation procedure (see 2.4) and confirmed to be present at very low levels by measurement in a hematology analyzer (data not shown).   However, both lymphocytes and monocytes are mononuclear cells and are therefore present in the buffy coat used to isolate the monocytic fraction.   Therefore antibodies against CD3 (to detect T cells), CD19 (to detect B cells), and CD56 (to detect NK
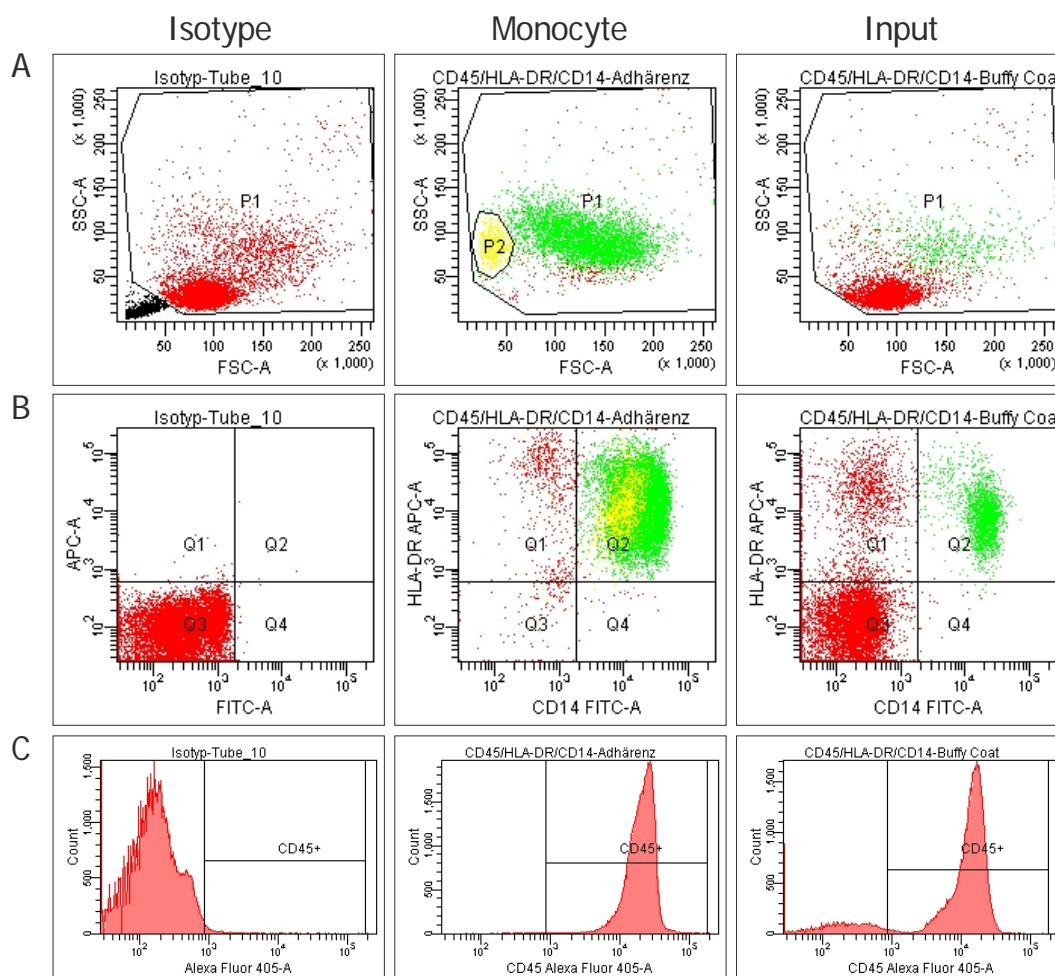
Figure 4 *Monocytes are highly enriched in isolated cell fraction.* Cells were stained with CD45-Alexa-Fluor®405, CD14-FITC, and HLA-DR-APC (Monocyte; Input) or the proper negative control antibodies (Isotype) to ensure specificity of antibody binding. All cells presented in B were gated for P1 (A) and subsequently CD45^{+} (C). Cell fractions used: buffy coat for panels Isotype and Input; cells obtained at the end of the isolation procedure for panel Monocyte.

cells) were used. Figure 5A shows FSCs of the corresponding cell fractions with the colors marking the populations gated below. In contrast to the buffy coat, where 56.4% of all cells are positive for the T cell marker CD3 (Figure 5B, *Input*), only 0.014% of all cells in the monocytic fraction express CD3 (*Monocyte*). However, it is apparent that the staining with antibody to CD56 cannot be used to distinguish monocytes from NK cells (Figure 5B). This antibody is found to bind to 10.1% of all cells present in the buffy coat but to 90.8% of cells after the monocyte isolation protocol. It is known that macrophages are able to bind FITC unspecifically (S. Willenzon, Institute of Immunology, MHH; personal communication). When comparing these numbers to those in Figure 4B, where 11.5% of the cells in the buffy coat qualify as monocytes by HLA-DR and CD14 co-staining and that percentage is increased to 95.0% after the isolation procedure, it is evident that in the sample taken after monocyte isolation the CD56 antibody must be mostly bound by monocytes. Finally, only 0.006% of all

cells are positive for CD19 after monocyte isolation, while in the buffy coat 4.1% of all cells are characterized as B cells by use of this antibody (Figure 5C). 88.0% of all cells in the buffy coat fraction stain positive for CD45, while that number is increased to 99.7% in the monocyte fraction (Figure 5D).

To further rule out a contamination with T cells, a differential staining for CD4$^+$ and CD8$^+$ T
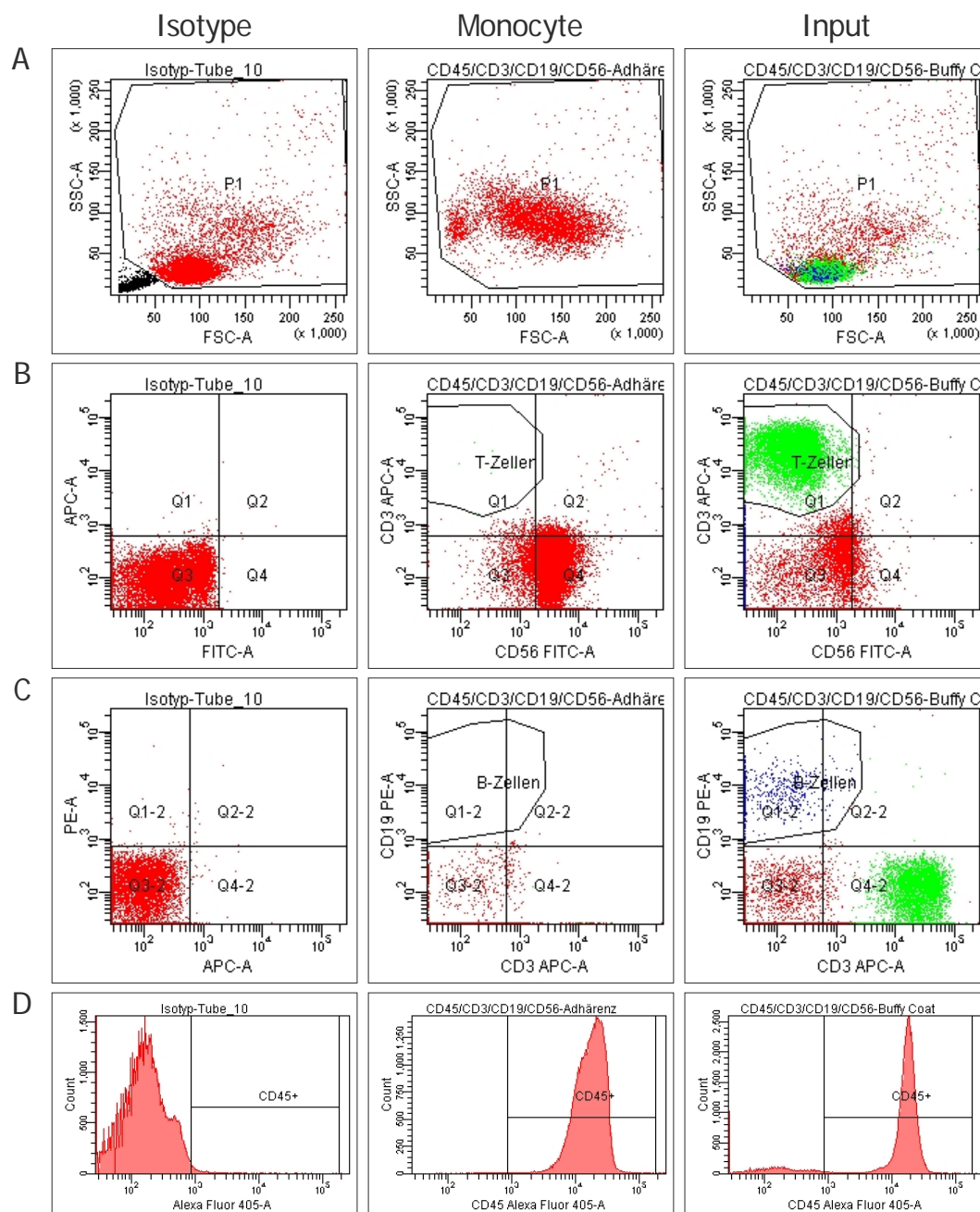

Figure 5 *Lymphocytes are depleted in purified human monocyte fractions.* Cells were stained with CD45-AlexaFluor®405, CD3-APC, CD19-PE, and CD56-FITC (Monocyte; Input) or the proper negative control antibodies (Isotype) to ensure specificity of antibody binding. All cells presented in B and C were gated for P1 (A) and subsequently CD45$^+$ (D). PE fluorescence was corrected for unspecific signals emanating from FITC using suitable singly stained samples (not shown). Cell fractions used were: buffy coat for panels Isotype and Input, and cells obtained at the end of the isolation procedure for panel Monocyte.

cells was performed. Figure 6A shows the FSC dot plots corresponding to those samples. As seen in Figure 6B, 44.6% of all cells in the buffy coat are CD4$^+$ T cells (*Input*), while that number is reduced to 0.1% in isolated monocytes (*Monocyte*). However, a large number (83.7%) of CD4$^+$ CD3$^-$ cells is visible in the monocyte fraction. This can be explained by two factors: 1) monocytes express low levels of CD4 (164); and 2) macrophages unspecifically
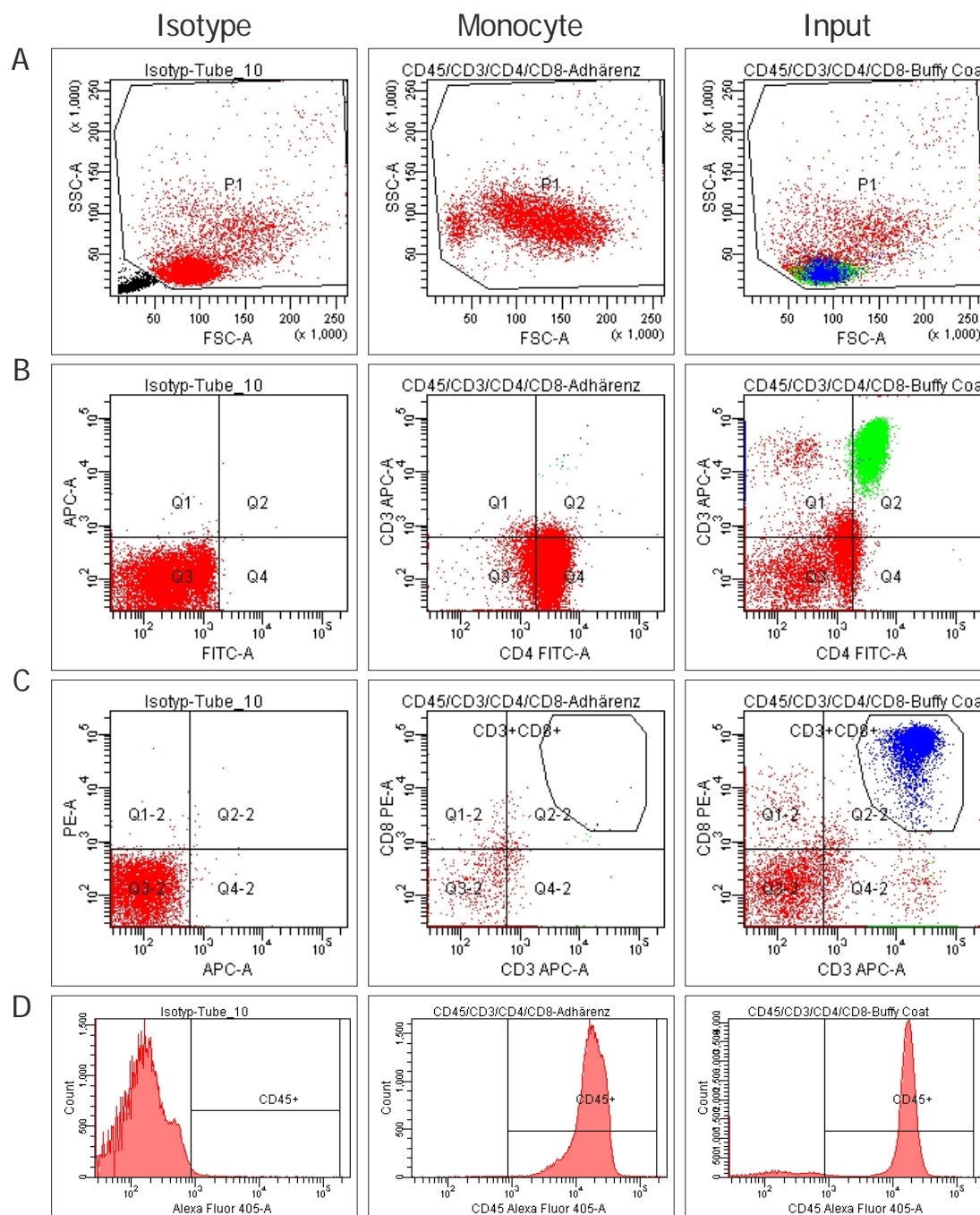

Figure 6 *T lymphocytes are depleted in purified human monocyte fractions.* Cells were stained with CD45-AlexaFluor®405, CD3-APC, CD4-FITC, and CD8-PE (Monocyte; Input) or the proper negative control antibodies (Isotype) to ensure specificity of antibody binding. All cells presented in B and C were gated for P1 (A) and subsequently CD45$^+$ (D). PE fluorescence was corrected for unspecific signals emanating from FITC using suitable singly stained samples (not shown). Cell fractions used were: buffy coat for panels Isotype and Input, and cells obtained at the end of the isolation procedure for panel Monocyte.

bind FITC, which was conjugated to the antibody. Most likely, the considerable increase observed in Figure 6B is due to a combination of both factors. However, as those cells do not stain positive for CD3, these are not T cells. Finally only 0.028% of all cells present in the monocyte preparation stain positive for both CD8 and CD3 (Figure 6C, *Monocyte*). In contrast, CD8$^+$ T cells make up 14.8% of the buffy coat (*Input*). Together, the CD4$^+$ and CD8$^+$ T cells in the buffy coat that were detected in Figure 6 roughly reach the same proportion as the 56.4% T cells detected in Figure 5. Staining for CD45 is again increased in the monocyte fraction compared to the buffy coat input (Figure 6D).

Overall, a highly pure monocyte population is obtained by use of the isolation protocol described. The cells stain positive for CD14-FITC as the shift observed with this antibody (Figure 4B) is far stronger than the shifts seen with CD56-FITC (Figure 5B) and CD4-FITC (Figure 6B). In conclusion, monocytes are enriched to at least 95% purity, but since no contaminant analyzed is close to accounting for 1% of all cells, a purity of over 99% can be assumed.

3.1.2 Evaluation of the inducibility of primary monocytes by TNF

In a next step, the inducibility of isolated human monocytes by TNF was tested in order to determine the optimal dose for the following experiments. Extracellular IL-8 concentration was used as the readout parameter of choice as it has been shown previously that both *IL8* gene transcription and IL-8 protein production correlate well with the TNF-tolerant state in THP-1 cells (49,50).
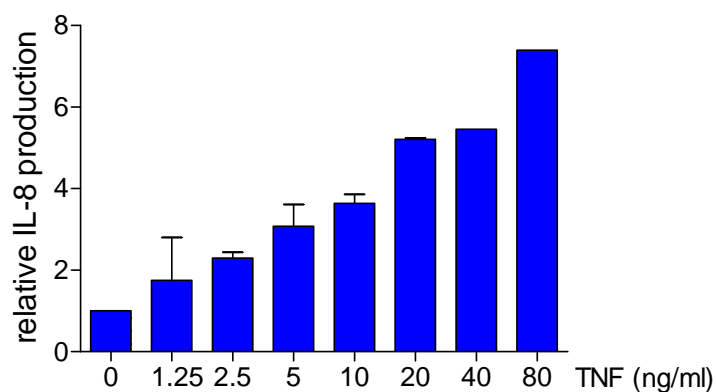
TNF given 72 h after isolation is able to induce IL-8 production in primary human monocytes in a dose-dependent manner (Figure 7). Relative IL-8 levels in the cell culture supernatants are slightly increased after a 5 h stimulation with 1.25 ng/ml of TNF. IL-8 production is induced up to 7.4-fold with 80 ng/ml, which was the highest concentration of TNF tested in these experiments. The TNF lot used for these experiments had an activity of

Figure 7 *TNF induces IL-8 secretion of monocytes in a dose-dependent manner.* Primary human monocytes were seeded at a density of approximately 4·10^6/well and incubated in normal culture medium for 72 h. Cells were then stimulated with the indicated concentration of TNF for 5 h prior to analysis of the cell culture supernatants by IL-8 ELISA. Measurement was performed in duplicate. Values are calculated relative to unstimulated controls and presented as mean ± SD of two independent (except 40 and 80 ng/ml) experiments.

20 U/ng, meaning that an increase of IL-8 production can be seen starting at 25 U/ml. 5-fold induction of IL-8 is observed with a TNF concentration of 400 U/ml.

In another experiment shown in Figure 8, the duration of TNF induced IL-8 production in primary monocytes was investigated. While the effect of 10 ng/ml of TNF (yellow bars) on IL-8 production is readily detectable in the supernatants even after 72 h of incubation, the lower concentration of 1 ng/ml (red bars) fails to induce a similar effect. This activity, corresponding to 20 U/ml, is too low to stimulate the monocyte preparation used for this experiment, while 25 U/ml is sufficient to slightly induce two others (see Fig. 7), indicating that TNF appears to start exerting its biological activity around this concentration. Its ability to stimulate IL-8 production at this low concentration is most likely dependent on the genotype and/or overall health status of the blood donor.

Figure 8 *TNF induces monocytic IL-8 production in a time-dependent manner.* Primary human monocytes were stimulated with 1 or 10 ng/ml of TNF or left untreated (Control). After incubation for the times indicated cells were harvested and supernatant analyzed for IL-8 by ELISA. All samples were measured in duplicate. IL-8 concentrations were calculated relative to the respective control cells at each time point.

The capacity of the higher dose of TNF to increase IL-8 production in human monocytes exhibits a pronounced time-dependence. IL-8 is induced strongest (15.7-fold) in monocytes treated for 24 h with TNF. After 72 h of stimulation, IL-8 induction is strongly reduced but still 2.1-fold higher than in non-stimulated control cells. Thus, TNF is able to induce IL-8 production in primary human monocytes even after 72 h of incubation without the need to replenish the stimulus in the course of the experiment.

3.1.3 TNF tolerance is a heterogenic phenomenon in primary human monocytes

In order to generate samples for a global gene expression analysis, monocytes derived from over 10 different whole blood samples were pre-incubated with a low dose of TNF (1 ng/ml) for 72 h followed by re-stimulation with a high dose of TNF (20 ng/ml) for an additional 2.5 h. Control samples incubated for the same times in normal medium without TNF were prepared as well. As in previous experiments IL-8 production was chosen as a parameter for cellular activation.
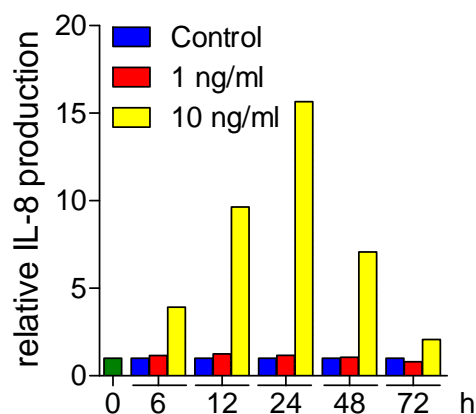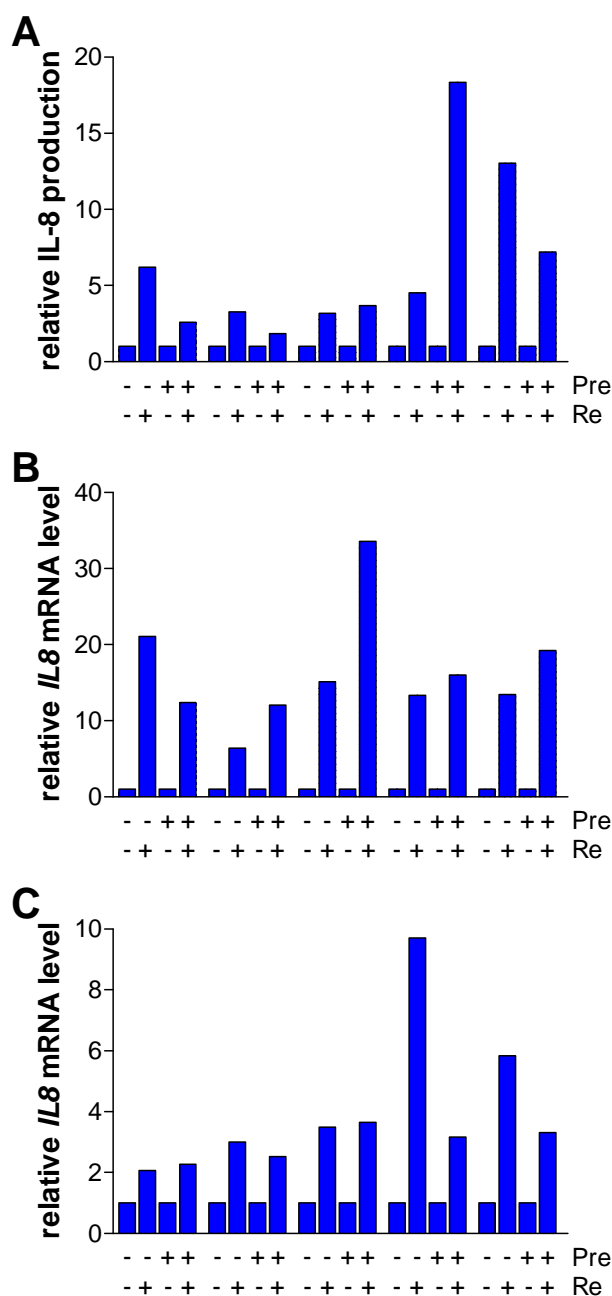
Figure 9 *TNF is unable to consistently induce tolerance in primary human monocytes.* (A) Primary human monocytes were stimulated with TNF (1 ng/ml) for 72 h or left untreated (Pre). Cells were subsequently stimulated with 20 ng/ml of TNF or left untreated (Re). The supernatant of each sample was analyzed by IL-8 ELISA. Induction of IL-8 production was calculated relative to the respective control samples (pre- and re-stimulated values were normalized to pre-stimulated samples, re-stimulation relative to non-treated controls). (B) Samples were analyzed by Affymetrix® microarray. Values of probe set 202859_x_at corresponding to the *IL8* gene are shown. Re-stimulated samples were normalized to controls as described in (A). (C) Monocytes were stimulated with 10 ng/ml (Pre) and 100 ng/ml (Re) of TNF and analyzed by RT-qPCR. Sample data were normalized to GAPDH and calculated relative to controls as described in (A).

As a first step, supernatants of monocyte samples subjected to the conditions inducing TNF tolerance were analyzed by ELISA. IL-8 production after treatment with a high dose of TNF was calculated as fold induction of the respective control cells, which were left untreated or stimulated with a low dose of TNF for 72 h. A graphical representation of five different experiments is shown in Figure 9A. Importantly, re-stimulation of monocytes not pre-stimulated with TNF results in an at least 3-fold induction of IL-8 production compared to non-stimulated cells, indicating that the monocytes in the experiments used are not pre-activated by the isolation procedure. Tolerance, i.e., reduced TNF-induced IL-8 production in cells pre-treated with TNF, could be achieved in three of the five monocyte preparations assessed. In the remaining two samples IL-8 was induced to a similar extent or even stronger after pre-incubation with TNF. Since the induction in the latter sample is higher than in the control re-stimulated sample, some form of superinduction can be assumed.

This effect is even more evident when assessing cellular *IL8* mRNA production in response to stimulation

with TNF. *IL8* expression was measured by gene expression analysis using Affymetrix® microarrays. Inductions of mRNA levels were calculated relative to controls as described above (Figure 9B). Strikingly, only one of the five preparations reveals an *IL8* expression pattern resembling a tolerance phenomenon. In all other four preparations *IL8* mRNA induction by a high dose of TNF is higher in cells that had been pre-stimulated with a low dose of TNF for 72 h.

Analysis of cellular *IL8* mRNA levels by RT-qPCR further confirms the heterogeneity of primary human monocytes to the induction of TNF tolerance. For these experiments, the monocytes were pre-incubated with 10 ng/ml of TNF and re-stimulated with a concentration of 100 ng/ml. Nevertheless, only two of five monocyte samples analyzed exhibit a marked inhibition of *IL8* expression after stimulation with TNF under conditions of TNF tolerance (Figure 9C). In the remaining three samples, however, *IL8* expression is induced to the same extent regardless of a pre-stimulation of the cells with TNF. A dramatic superinduction as observed in one sample each in Figures 9A and B above cannot be detected.

Overall, these results show that, in contrast to THP-1 monocytic cells, primary human monocytes do not exhibit marked features of tolerance upon repeated stimulation with TNF under the conditions described. TNF tolerance can occur in these cells as evident in Figure 9. However, this effect is not stable and varies greatly between different monocyte preparations and, thus, blood donors. It was therefore impossible to further characterize TNF tolerance in primary human monocytes as the observed effect is too heterogeneous. Larger patient or blood donor groups will be necessary for further studies of TNF tolerance in primary human monocytes.

3.1.4 Assessment of gene families induced by TNF stimulation of monocytes

To extract new information from the data generated by gene expression analysis, the TNF-mediated induction of different gene families was assessed. In order to achieve this, for each gene the values of the re-stimulated sample (20 ng/ml TNF for 2.5 h) were calculated relative to the values obtained in the respective control cells. Further analysis eliminated all genes in which the induction was not at least 2-fold in a minimum of five of eight monocyte preparations assessed. Genes remaining were subsequently sorted according to gene information tags assigned to each Affymetrix probe set.

As shown in Figure 10, TNF-induced genes can be divided into 11 gene families. Not surprisingly, 29% of the genes found by this algorithm belong to the group encoding proteins mediating cellular signal transduction. 15% belong to a group encoding proteins involved in inflammation and the immune response, while 12% are associated with the regulation of

apoptosis. In the latter fraction, most genes give rise to anti- as opposed to pro-apoptotic proteins and peptides, confirming that TNF mainly induces pro-survival signaling. Other genes induced by TNF include those involved in transcription (12%), the regulation of cell cycle progression and proliferation (11%), transport events (9%), cell motility and migration (10%), and adhesion mechanisms (6%). A substantial proportion of all genes identified additionally plays a role in metabolic processes (5%), catabolism in particular (3%), or is involved in the biosynthesis and folding of proteins (2%). 26% of all genes induced by TNF in primary human monocytes do not belong to any of the functional groups mentioned or are transcripts of unknown function.

TNF is thus able to induce a variety of genes involved in diverse cellular functions. The immediate purpose with which TNF is usually associated (i.e., signal transduction, immunity including chemotaxis, regulation of apoptosis, and proliferation) is represented by the most prominent groups. In addition, the data demonstrate that TNF induces changes in the cell's metabolic processes and thus has a profound impact on cellular functionality overall.
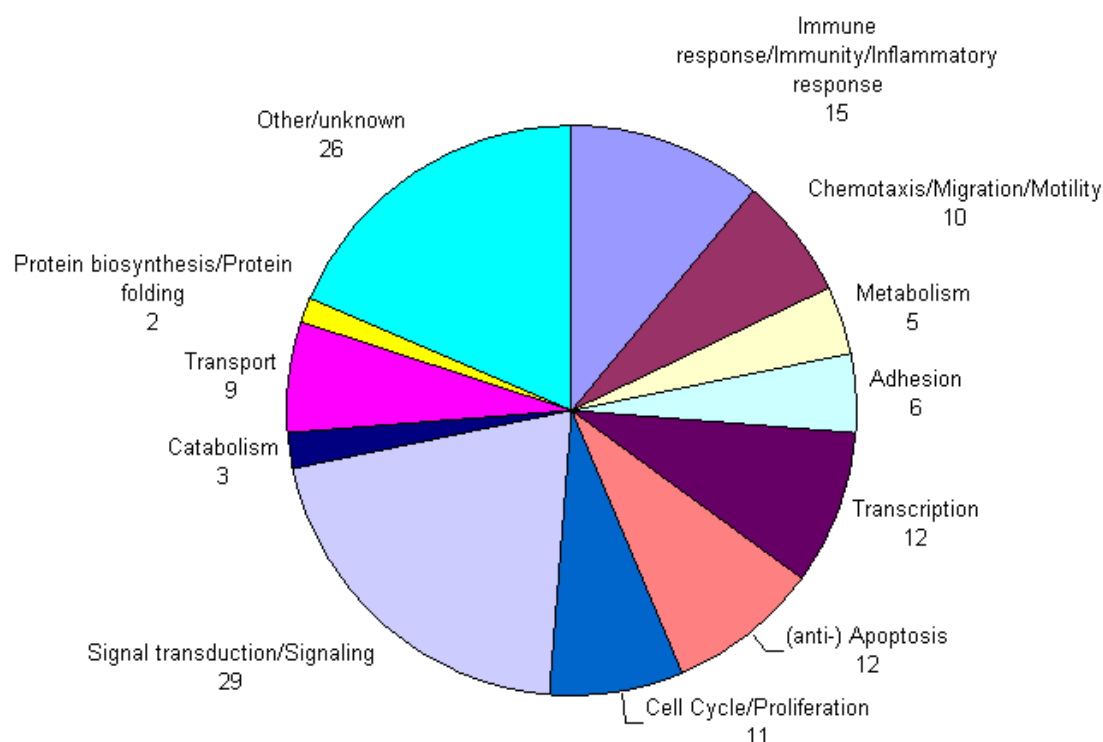

Figure 10 *Schematic representation of TNF-induced genes.* Primary human monocytes were incubated in normal growth medium for 72 h before stimulation with 20 ng/ml TNF for 2.5 h. A non-stimulated control sample was included in each monocyte preparation. Samples were then analyzed by Affymetrix® microarray. Fold inductions were calculated by normalization of stimulated data to the values obtained in the respective non-stimulated controls. All genes induced at least 2-fold in five or more of eight independent monocyte preparations (260) were analyzed for cellular function. Diagram shows relative distribution of all genes affected. Percentages are indicated for each group of genes.

3.2   Mechanisms of monocyte differentiation

3.2.1   Morphological changes during PMA-induced monocytic differentiation

Monocytes are a component of the mononuclear leukocyte subset of the innate arm of the immune system. They are essential for both the clearance of pathogens and the modulation of the adaptive immune response to infection (1). Their development from myeloid precursors as well as their maturation towards tissue macrophages are regulated by the activity of various transcription factors (113). Blood-borne human monocytes usually have a half-life of about 3 days before extravasation and further differentiation towards macrophages (1,11). For research purposes, THP-1 cells stimulated with PMA have been widely used as a tool to study the processes involved in monocytic differentiation (118).

In this study, THP-1 were incubated in the presence of increasing concentrations of PMA (1, 10, 100 nM) for 24 h. Changes in cellular morphology were then assessed by light microscopy. Figure 11 shows the result of one

Figure 11 *PMA induces morphological changes in THP-1.* Monocytic THP-1 cells were incubated in the absence (A) or presence (B) of 100 nM PMA for 24 h. Magnification, ×320.

representative experiment conducted with 100 nM PMA. THP-1 incubated in normal growth medium constitute a very homogenous population of round, non-adherend cells (Figure 11A). Upon stimulation with PMA, these cells lose their round morphology and strongly adhere to the surface of the cell culture plate (Figure 11B). Their shape is dramatically flattened and becomes amoeboid. Additionally, it becomes difficult to discern single cells as they increasingly attach to neighboring cells. By morphological analysis, 1 nM of PMA was sufficient to induce macrophage-like adherence and cytoplasmic extensions (data not shown). PMA thus induces a macrophage morphology in THP-1 cells within 24 h of incubation, indicating differentiation of these cells towards a macrophage-like phenotype.

3.2.2   Regulation of C/EBPβ during PMA-induced monocytic differentiation

Members of the C/EBP family of transcription factors are thought to play an important role during monocytic differentiation, although the ETS family transcription factor PU.1 seems to
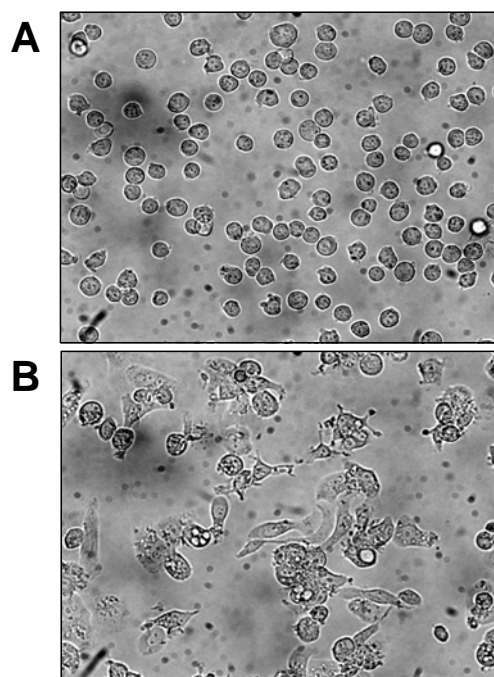
be of singular importance in this process (1,113,131,133,137). Interestingly, C/EBPβ has been reported to be strongly upregulated during monocytic differentiation, although its exact role remains elusive (71-73). To further address this issue, THP-1 were exposed to 100 nM PMA for up to 72 h to monitor C/EBPβ protein expression by western blotting.

The antibody used in these experiments has been generated against the protein's C-terminus and is thus capable of detecting all three C/EBPβ isoforms (LAP*, LAP, and LIP). Nuclear extract was prepared from THP-1 cells differentiated towards the macrophage-like phenotype by incubation with PMA for 6, 24, 48, and 72 h (Figure 12A). C/EBPβ levels in the nuclei (upper panel) are low in non-treated control cells taken directly after seeding (0 h) and are induced only slightly by longer incubation in normal cell culture medium. In PMA-treated THP-1, however, C/EBPβ increases remarkably starting at 24 h of stimulation. C/EBPβ is even more dramatically increased after 48 h but seems to reach a peak as levels do not increase much further after 72 h of stimulation. Of note, the three isoforms appear to behave differently during monocytic differentiation. While the longer and transcriptionally active isoforms LAP* and LAP increase dramatically upon incubation with PMA, the truncated, transcriptionally inactive isoform LIP is only induced to a lesser extent.

In order to quantify the changes of expression of the three C/EBPβ isoforms, the specific bands detected in the nucleic extracts were quantified. The obtained chemiluminescence values of each LAP*, LAP, and LIP were normalized to the loading control TBP and plotted relative to the respective isoform value of the control sample taken at 0 h (Figure 12B). As indicated by the western blot data, the expression of all three C/EBPβ isoforms is indeed enhanced in THP-1 incubated in normal medium for 48 and 72 h. While the induction of LIP (yellow bars) remains moderate (3.2±1.3-fold) after 48 h, LAP* (blue bars) and LAP (red bars) are expressed at 13.2±0.1- and 8.1±5.1-fold higher levels, respectively. This level of protein expression is maintained after 72 h of incubation. However, when compared to the inductions seen in PMA-treated cells, these changes appear small. Starting at 24 h after the addition of PMA to the cell culture vessel, LAP* and LAP are strongly induced (27.7±9.6- and 10.6±6.5-fold, respectively) as compared to non-treated controls prepared at the same time. After 48 h, all C/EBPβ isoforms are expressed at much higher levels than in controls, and this elevation is maintained until at least 72 h after the begin of stimulation with PMA. The inductions observed are 77.1±2.8-fold for LAP*, 30.0±10.3-fold for LAP, and 9.7±6.3-fold for LIP at this latest time point assessed.

Another attempt to visualize the dramatic changes in C/EBPβ expression seen in differentiating monocytic THP-1 cells is shown in Figure 12C. Here, the band intensities of
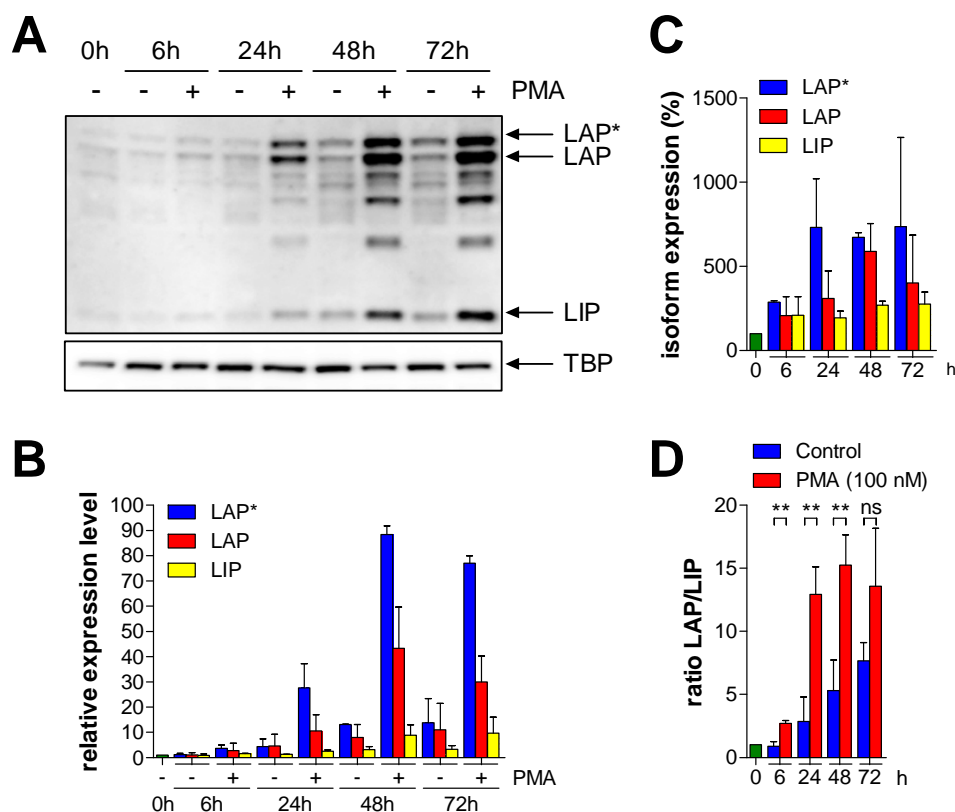
Figure 12 *Expression of C/EBPβ isoforms is differentially induced by PMA.* (A) THP-1 were cultivated ± 100 nM PMA. At the times indicated, nucleic extracts were prepared and analyzed for C/EBPβ expression by western blot (upper panel). The membrane was re-probed with TBP as loading control (lower panel). (B) Quantitative analysis of the time course of C/EBPβ isoform expression. Western blots of nucleic extracts as shown in (A) were quantified by densitometry and normalized to loading control. Expression of LAP*, LAP, and LIP were calculated relative to the respective values obtained at 0 h (green bar). (C) As in (B), but isoform expression was calculated relative to the value obtained at each respective time without PMA treatment. Green bar, value at 0 h (100%). (D) Ratios of LAP* and LAP to LIP in the same blots as in (B) were calculated for each time point analyzed. Green bar, value at 0 h. All data are given as mean ± SD of two (B, C) or three (D) independent experiments. ** $p \leq 0.01$ (student's t test); ns, not significant.

the three isoforms were calculated relative to the non-treated control cells taken at each respective time, which was set to 100% after normalization to TBP. Clearly, an induction of C/EBPβ expression can be seen as early as 6 h after the addition of PMA. A progressive increase of all three isoforms is observed until 48 h. At this time, LAP* (blue bars) is induced 672.8±29.3%, LAP (red bars) expression is 589.2±166.5% higher than in the control, and LIP (yellow bars) is augmented by 270.0±23.9%. These expression levels are maintained until 72 h after the start of PMA stimulation.

From these data, it is obvious that the ratio of LAP* and LAP to LIP, i.e., the proportion of transcriptionally active to transcriptionally inactive C/EBPβ isoforms, changes dramatically during PMA-induced monocytic differentiation of THP-1. Changes in the LAP/LIP ratio have been implicated in the regulation of proliferation and differentiation, for example in

hepatocytes (88,165). Therefore, the ratio of the long C/EBPβ isoforms, LAP* and LAP (for this purpose simply referred to as LAP) to the truncated isoform LIP was calculated (Figure 12D). Values determined at the various time points were calculated relative to the control sample (0 h, green bar). It is evident that the LAP/LIP ratio increases over time in both PMA-treated (red bars) and non-stimulated control cells (blue bars). However, the extent of this modulation is far more dramatic in differentiating THP-1, where a slight change (2.70±0.2-fold induction) can be observed already after 6 h. The ratio further increases until it reaches a maximum at 48 h of PMA treatment, when it is induced 15.2±2.4-fold. At 72 h, this ratio is mostly maintained. Non-treated control cells exhibit a progressive increase of the LAP/LIP ratio until 72 h, but the induction remains comparably weak (7.7±1.5-fold). A statistical analysis by student's t test confirms that the observed LAP/LIP ratios 6, 24, and 48 h after treatment with PMA are significantly different from those observed in control THP-1 taken at the same times ($p \leq 0.01$).

Taken together, these data demonstrate a strong increase in C/EBPβ expression during PMA-induced monocytic differentiation of THP-1 cells. Additionally, the LAP/LIP ratio is altered dramatically during differentiation. The observed increase of the isoform ratio occurs within 24 h and remains relatively stable at later time points, presumably in order to enforce the appearance and maintenance of the macrophage phenotype.

3.2.3 Regulation of C/EBPα during PMA-induced monocytic differentiation

Apart from C/EBPβ, the transcription factors C/EBPα and C/EBPε have also been implicated in the determination of cell fate in the hematopoietic system (72). The exact role of C/EBPα in the differentiation process is not yet clear. While there is evidence that expression of this protein is reduced during monocytic differentiation (72), other groups have shown that fibroblasts as well as T and B cells can be reprogrammed to macrophage-like cells by transfection of C/EBPα in combination with PU.1 (99,146,147). Therefore, C/EBPα expression was determined in the same protein extracts used for the detection of C/EBPβ (see 3.2.2 above).

C/EBPα is readily detected in the nuclear compartment by western blotting (Figure 13A, upper panel). In non-treated control cells p42, the transcriptionally active isoform of C/EBPα, is the predominant isoform. This remains unchanged until at 48 h an increase of p30 expression is evident. However, this is true regardless of PMA treatment and therefore, this appears to be a matter of incubation time. Nonetheless, at 72 h, which is the latest time point assessed in this series of experiments, p30 is increased visibly in cells incubated with PMA over the level observed in cells incubated in normal cell culture medium. On the other hand,

an induction of p42 can be seen in non-treated THP-1, whereas its levels, especially at early time points, appear to be slightly reduced with PMA treatment. Thus, in cells treated with PMA, the level of p42 is reduced compared to controls, while p30 is increased.

These findings are further illustrated in the bar diagram shown in Figure 13B. Band intensities of nuclear p42 and p30 were quantified, normalized to the loading control TBP, and calculated relative to the levels measured in non-treated controls at the time of seeding (0 h, green bar). Within the first 24 h of incubation, no changes in the expression levels of p42 (blue bars) and p30 (red bars) are detectable. After an incubation of 48 h, p42 remains around the level seen in the sample taken at seeding in both non-treated and PMA-stimulated cells. At the same time, p30 is induced 1.9±0.5-fold in THP-1 subjected to 100 nM of PMA,
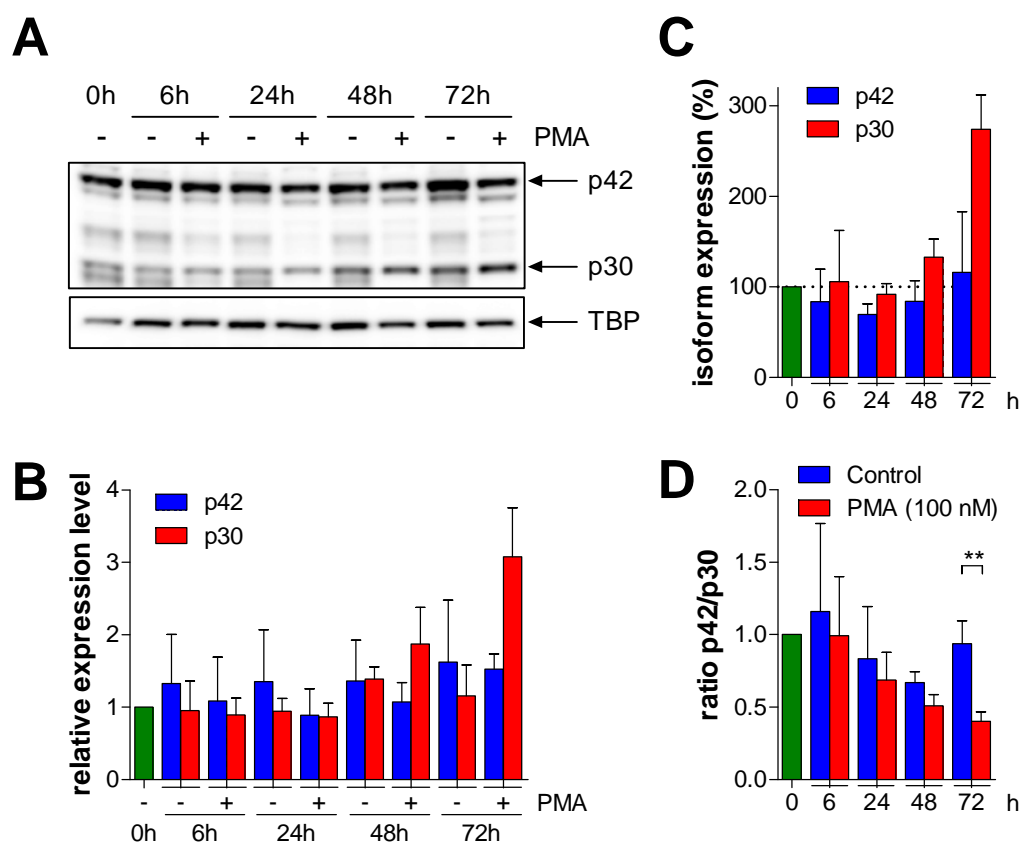

Figure 13 *C/EBPα isoform expression is differentially regulated by PMA.* (A) THP-1 were cultivated ± 100 nM PMA. At the times indicated, nuclear extracts were prepared and analyzed for C/EBPα (upper panel) expression by western blot (loading control TBP, lower panel). (B) Quantitative analysis of the time course of C/EBPα isoform expression. Western blots of extracts as shown in (A) were quantified by densitometry and normalized to loading control. Expression of p42 and p30 were calculated relative to the respective values obtained at 0 h (green bar). (C) As in (B), but isoform expression was calculated relative to the value obtained at each respective time without PMA treatment. Green bar, value at 0 h (100%). The dotted line indicates a relative expression level of 100%. (D) Ratios of p42 to p30 in the same blots as in (B) were calculated for each time point analyzed. Green bar, value at 0 h. All data are given as mean ± SD of three independent experiments. ** $p \leq 0.01$ (student's t test).

with controls slightly following that trend. In the controls, p42 is then induced higher than p30 after 72 h (1.6±0.9- *vs.* 1.2±0.4-fold, respectively). In contrast to this finding, in cells incubated with PMA for 72 h p42 remains at the same level seen in the respective controls, while p30 is markedly increased (3.1±0.7-fold).

To further illustrate the differences of C/EBPα isoform expression in differentiating THP-1, p42 and p30 expression in PMA-treated cells are shown as percentage of the levels found in the respective non-treated cells at each time point (Figure 13C, green bar). Strikingly, p42 levels (blue bars) remain relatively stable over the course of time, while p30 (red bars) is increased concomitantly during monocytic differentiation. The observed increase in p30 expression initially fluctuates during the first 2 days of differentiation before reaching 274.3±37.8% of the control level after 72 h. This indicates a definitive trend for the modulation of C/EBPα isoform expression during PMA-induced monocytic differentiation in THP-1 cells.

Since the transcription factor C/EBPα can be expressed as a full-length, transcriptionally active isoform and as a truncated, transcriptionally inactive isoform capable of binding promoter elements in a dominant-negative manner like C/EBPβ (166), its relative expression levels can be described as the p42/p30 ratio. p42 band intensities were calculated relative to the respective p30 intensities and normalized to the value obtained at 0 h (Figure 13D; green bar). In non-treated control cells (blue bars), the ratio initially recedes between 6 and 48 h of incubation but returns to the initial baseline level at 72 h (0.9±0.2-fold change). In contrast to this observation, the p42/p30 ratio is dramatically reduced in PMA-treated THP-1 (red bars). This reduction appears to be a continuous process culminating in a relative level of only 0.4±0.1-fold after 72 h, where the observed difference is highly significant ($p \leq 0.01$ by student's t test) compared to controls.

These results indicate that C/EBPα function might not be necessary or, even more dramatic, detrimental to monocytic differentiation. Expression of this protein is therefore gradually inhibited in PMA-treated THP-1. This is in good agreement with the generally accepted notion that C/EBPα is necessary for granulocytic, but not monocytic differentiation (1).

3.2.4 Comparison of cytoplasmic C/EBPα and C/EBPβ levels

As transcription factors, C/EBP proteins exert their primary function, the modulation of target gene expression, in the nuclear compartment of the cell. However, stimulus-induced translocation of C/EBPβ has been reported (73), and it is conceivable that it also exerts a cytosolic function under certain conditions (50). To determine cytoplasmic expression of

C/EBPα and β during PMA-induced monocytic differentiation, extracts were prepared and analyzed by western blotting.

As seen in Figure 14, C/EBPα p42 (top panel) is readily detected in the cytoplasmic fraction, albeit at lower levels than in the nuclear fraction (data not shown). Of note, the smaller p30 C/EBPα isoform could not be detected in the cytoplasm even at 16-fold longer exposure (data not shown). Starting at 24 h of PMA treatment, p42 expression is reduced and barely detectable after 72 h. This finding mirrors the behavior of the larger C/EBPα isoform in the nucleus (compare Fig. 13A, B).

In contrast to C/EBPα, the cytoplasmic expression of C/EBPβ is very faint and only detectable after at least 24 h of incubation with PMA (middle panel). Even after 72 h of differentiation, the bands of the large isoforms LAP* and LAP are weak. LIP could not be detected in the cytoplasm of THP-1 under any condition tested (data not shown). Since the detection of LAP* and LAP temporally coincides with the strong induction of their expression in the nucleus (compare Fig. 12A, B), it is likely that C/EBPβ is located constitutively in the nucleus in this cell type, its observed upregulation in the cytoplasm merely mirroring enhanced translation of this protein.

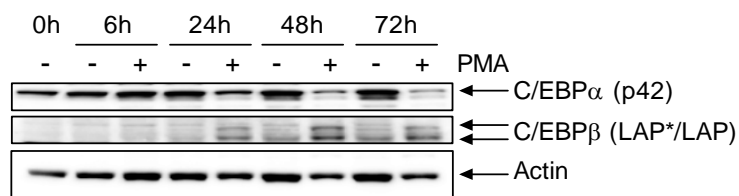In summary, the large isoform of C/EBPα can be detected in the cytoplasm of THP-1 and is reduced by PMA, reflecting its regulation in the nucleus. On the other hand, C/EBPβ is found in the cytoplasm only after PMA treatment of THP-1, and even then its cytoplasmic expression is markedly lower than that of C/EBPα.

Figure 14 *C/EBPα p42 expression is reduced while C/EBPβ LAP* and LAP are induced in the cytoplasm during monocytic differentiation.* THP-1 were cultivated ± 100 nM PMA. At the times indicated, cytoplasmic extracts were prepared and analyzed for C/EBPα (top panel) and C/EBPβ (middle panel) expression by western blot (loading control actin, bottom panel).

3.2.5 Influence of PMA on THP-1 proliferation

In order to further characterize the model used to study monocytic differentiation in the cell line THP-1, the impact of PMA on cellular proliferation was assessed. Differentiation is a process that is usually accompanied by an inhibition of cell cycle progression (1). In fact, growth inhibition has already previously been demonstrated to occur in THP-1 induced to differentiate by PMA treatment (167).

To confirm these reports, THP-1 were incubated either in normal medium or in medium supplemented with 100 nM PMA for 24, 48, or 72 h. At these time points, samples were

taken for a proliferation assay which detects cellular ATP content within a single well of the cell culture plate (Figure 15). THP-1 growing in normal medium (blue dots) are found to increase 1.7±0.03-fold every 24 h, reaching a 5 times higher RLU value after 72 h than at the time of seeding (0 h). This result confirms general observations made during the standard splitting procedure when cell counts were performed on a regular basis (data not shown). When adding PMA to the culture medium (red squares), the cells appear to grow normally within the initial 24 h. Even a slight increase of proliferation can be detected at this time, possibly indicating an initial occurrence of maturation divisions as described for differentiating HL-60 cells (168). At later time points, however, an inhibition of cellular proliferation is readily detected. Differentiating THP-1 barely increase in number between 24 and 48 h (1.9±0.09- as opposed to 2.3±0.34-fold induction, respectively), and after 72 h of PMA treatment, cells grow only 2.9±0.37-fold compared to the initial value, while those that were not incubated with this stimulus reach a value of 5±0.31-fold, which is significantly higher ($p \leq 0.01$, student's t test).

Thus, treatment of THP-1 cells with PMA potently inhibits their proliferative potential

Figure 15 *PMA treatment inhibits cellular proliferation.* THP-1 were seeded in normal growth medium or in medium containing 100 nM PMA. At the times indicated, samples were taken and analyzed by proliferation assay. Measurements were performed in triplicate. Data were normalized to the respective values at 0 h. RLU, relative light units (mean ± SD). ** $p \leq 0.01$ (student's t test).

starting after 24 h of incubation. Interestingly, this is exactly the time when C/EBPβ levels start to increase dramatically (compare Fig. 12A). It is therefore conceivable that the observed inhibition of proliferation induced by PMA may be mediated by the upregulation of C/EBPβ.

3.2.6 Forced expression of C/EBPβ potently inhibits proliferation

To test the hypothesis that expression of C/EBPβ may delay or even inhibit proliferation, HeLa epithelial cells were transfected with either an expression vector coding for full-length C/EBPβ (i.e., capable of producing all three isoforms) or with the empty control vector. After 24, 48, and 72 h, samples were taken for a proliferation assay. The RLUs measured at each time point were normalized to the values obtained at the time of transfection (0 h, Figure 16). As evident, the cells do not grow for at least 24 h after transfection, probably owing to the
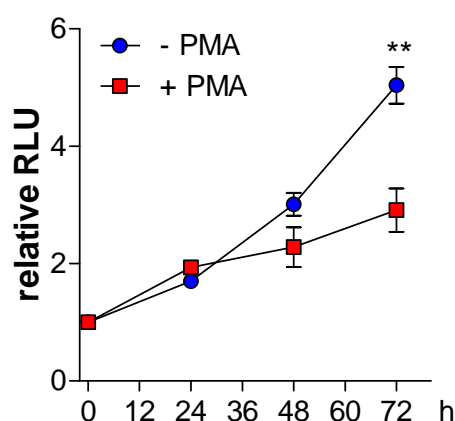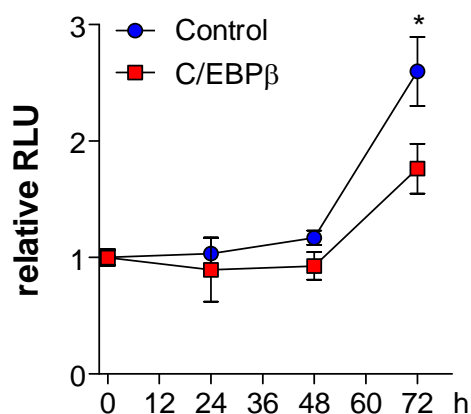
Figure 16 *Overexpression of C/EBPβ inhibits proliferation.* HeLa cells were transfected with the plasmid coding for full-length C/EBPβ (pTracer-FL) or the empty control plasmid (pTracer). Proliferation assay was performed at the times indicated. Values obtained were normalized to those measured at 0 h. RLU, relative light units (mean ± SD of one representative experiment measured in duplicate). * $p \leq 0.05$ (student's t test).

toxic effects of the reagent used. While a slight proliferation can be detected by 48 h in cells transfected with the empty control vector (blue dots), cells transfected with full-length C/EBPβ (red squares) appear to remain stagnant. A marked difference in proliferation is observed 72 h after transfection: forced expression of C/EBPβ results in a mere 1.8±0.2-fold change in RLU compared to the baseline level, while this value is induced 2.6±0.3-fold when the cells had been transfected with the control vector. The analysis by student's t test reveals that the disparity observed in this experiment is significant ($p \leq 0.05$). Overexpression of C/EBPβ in these cells was confirmed by western blot (data not shown).

Thus, expression of C/EBPβ may inhibit proliferation in various cell types including HeLa epithelial cells.

3.2.7 Morphology of macrophages derived from C/EBPβ wt and ko mice

Monocytic differentiation coincides with changes in cellular morphology (see Fig. 11). In order to address the role of C/EBPβ during this process, morphological analyses were performed with mouse macrophage-like cell lines established from C/EBPβ ko or wt mice (137). Cells from C/EBPβ ko mice that had been stably re-transfected with C/EBPβ were also used for analysis.

Macrophage-like cells were seeded at a moderate density (i.e., 300,000 cells/9.6 cm^2 in 6 well plates) and incubated in normal growth medium overnight. Cellular morphology was then assessed by light microscopy (Figure 17A). The C/EBPβ wt cell line (top panel) constitutes a heterogeneous population of round, but adherend cells and of flat, spindle-shaped, and polygonal cells, the latter revealing a morphology typical of macrophages. By contrast, C/EBPβ ko cells almost completely exhibit a round, yet adherend phenotype (bottom panel). In addition, they grow in colony-like clusters. Although these cells have been confirmed to be macrophages on the basis of antigen expression (137), hardly any cells show morphological features typical of macrophages. The cell line reconstituted with C/EBPβ exhibits a

phenotype somewhere between C/EBPβ wt and ko cells (middle panel): there are more spindle-shaped macrophage-like cells visible than in C/EBPβ ko cells, yet more cells are round than in the C/EBPβ wt line. This finding is mostly due to the known differences between C/EBPβ wt and re cells as even though C/EBPβ has been re-transfected into the C/EBPβ ko cells, protein levels in C/EBPβ re cells invariably remain much below those of C/EBPβ wt cells (137).

Based on these findings, the

Figure 17 *Loss of C/EBPβ expression dramatically alters mouse macrophage morphology.* (A) Morphological analysis of macrophage-like cell lines established from C/EBPβ wt or ko mice by light microscopy. A third line, derived from the C/EBPβ ko cells re-transfected with C/EBPβ (re), was assessed as well. Magnification, ×320. (B) Quantitative analysis of cell morphology. Cells with macrophage morphology and total cell numbers of each sample were counted in two images obtained by microscopy. Percentage of cells with macrophage morphology was calculated relative to total cell numbers (mean ± SD).

phenotype of the three cell lines was quantified by counting round as well as cells with macrophage morphology in two images obtained during examination of one single well by light microscopy. In Figure 17B the percentage of cells with macrophage morphology in each of these samples is depicted. While 53.7±2.5% of all C/EBPβ wt cells exhibit morphological features of macrophages, this is true for only 28.1±0.4% of C/EBPβ re and 5.7±1.6% of C/EBPβ ko cells.

These observations indicate that C/EBPβ has a profound impact on cellular morphology in macrophages.

3.2.8 Divergent proliferation rates in C/EBPβ wt and ko macrophages

In addition to their role in the regulation of differentiation in various tissues, the three C/EBPβ isoforms have also been implicated in modulating the cell cycle and thereby proliferation (96,101,102,106,165). The growth rates of C/EBPβ wt and ko cells were therefore compared, allowing for the detection of possible changes in proliferation induced by loss of this gene.

A total of $1.5 \cdot 10^6$ C/EBPβ wt or ko cells were seeded into a T75 cell culture flask and their numbers were assessed by standard laboratory procedures after 3 days in culture (Figure
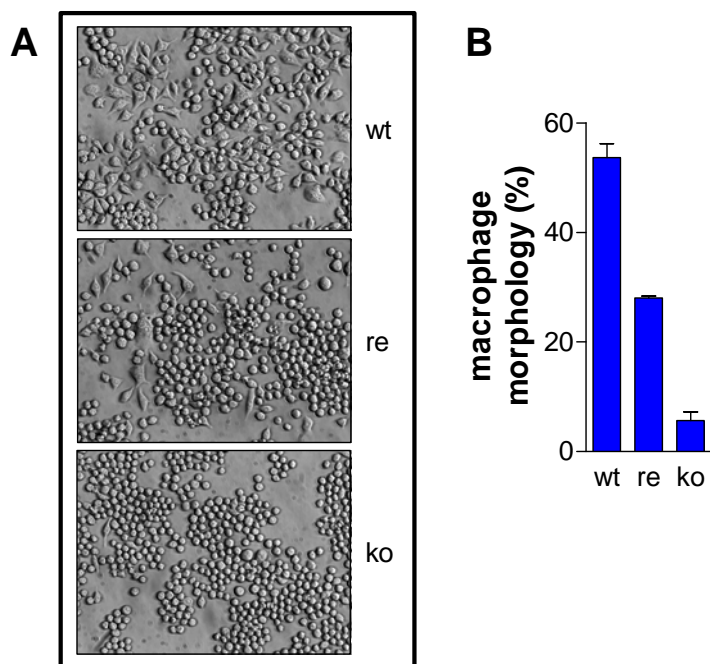
18A). On average, C/EBPβ wt cells grow to $18.7\pm6.7\cdot10^6$ cells during this time of incubation. C/EBPβ ko cells, however, grow to $32.6\pm7.0\cdot10^6$ cells during the same period of time, a cell number that is significantly higher ($p\leq0.01$, Mann-Whitney U test) than that of C/EBPβ wt cells.

These findings were confirmed by performing proliferation assays that measure cellular ATP content (Figure 18B). Over the course of 72 h, the total number of C/EBPβ wt cells increases 13.2 ± 0.6-fold (blue dots) compared to the time of seeding (0 h). During the same period of time, C/EBPβ ko cell numbers increase 35.7 ± 1.0-fold (red squares). This difference is found to be highly significant ($p\leq0.001$, student's t test). The experiments using a proliferation assay thus reflect the results obtained by manual counting of the cells.

As a next step, the amount of C/EBPβ wt and ko cells present in the different phases of the cell cycle were analyzed by propidium iodide staining. Cells were serum-starved overnight and the experiment started immediately after the addition of FCS to the flasks. After 0, 24, and 48 h, cellular DNA content was determined by flow cytometric analysis (Figure 18C). Directly after serum starvation (0 h), 69.7% of C/EBPβ wt and 73.4% of C/EBPβ ko cells are in the G_0/G_1 phases of the cell cycle, which are the resting phases (blue). 24 h after addition of FCS, 45.6% of C/EBPβ ko cells actively progress through the cell cycle, as illustrated by the red and yellow portions of the bar representing the S and G_2/M phases, respectively. At
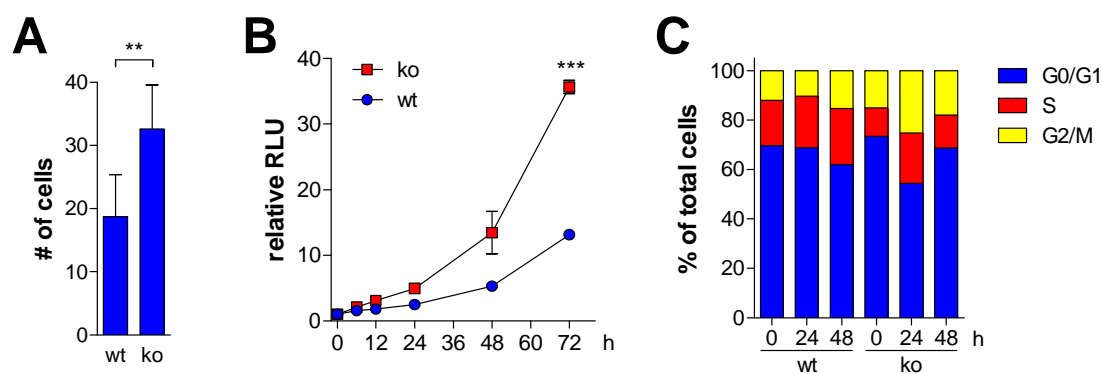

Figure 18 *C/EBPβ wt and ko macrophages exhibit divergent proliferation rates.* (A) $1.5\cdot10^6$ cells/flask (C/EBPβ wt or ko) were seeded and incubated for 3 days before trypsinization and determination of total cell numbers. The graph represents data of six independent experiments (mean $\pm$ SD). Statistical analysis (Mann-Whitney U test) was performed with these data (**, $p\leq0.01$). (B) Proliferation assay was performed with C/EBPβ wt and ko macrophage-like cells measured in triplicate. Samples were taken at the times indicated. Data were normalized to the respective values at 0 h. RLU, relative light units (mean $\pm$ SD). *** $p\leq0.001$ (student's t test). (C) Cell cycle analysis in C/EBPβ wt and ko cells. Cells were synchronized over night by serum withdrawal. Samples were taken directly or 24 and 48 h after the induction of proliferation by addition of FCS. Prior to FACS® analysis, cells were stained with propidium iodide. Normal DNA content indicates G_0/G_1 phase, duplication of DNA content reveals cells in G_2/M, and DNA content in between indicates ongoing DNA synthesis in S phase. Each bar represents 100% of the cells analyzed in each sample.

the same time, only 31.3% of all C/EBPβ wt cells undergo cell-cycle associated modifications of cellular DNA content, indicating that progression through the cell cycle at early time points is accelerated in cells devoid of C/EBPβ. This is further corroborated by the results seen at 48 h after addition of FCS, where 38.1% of C/EBPβ wt but only 31.4% of C/EBPβ ko cells are at some stage of mitosis. This possibly indicates that in comparison to C/EBPβ ko cells, C/EBPβ wt cells that had been synchronized by starvation start cell cycle progression in a delayed manner.

Combined, these results demonstrate that C/EBPβ is a negative regulator of macrophage proliferation by slowing cell cycle progression.

3.2.9 Cell cycle progression is accelerated in C/EBPβ ko macrophages

To confirm the observations made above, C/EBPβ wt and ko macrophage-like cells were subjected to further cell cycle analyses. Measurement was performed as described in Materials and Methods (see 2.15), and the cycling index was calculated for each sample. As the cell cycle analysis shown above (see Fig. 18C) did not yield synchronized cells at the beginning of the experiment (0 h), it was necessary to determine the best method to ensure synchronization of the cells first. Two approaches were tested: serum withdrawal for up to 48 h, and cell cycle arrest due to contact inhibition.

As shown in Figure 19A, serum withdrawal for 24 h leads to a dramatic reduction of the cycling index in C/EBPβ wt macrophages (red dots) but only to a slight decrease in C/EBPβ ko cells (blue squares). The trend is confirmed by serum withdrawal for up to 48 h, and it becomes evident that C/EBPβ ko cells do not seem to be affected by serum starvation, albeit their cycling index is lower than that of C/EBPβ wt macrophage-like cells already at earlier time points.

Synchronization of the cells was thus attempted by letting them grow in normal cell culture medium, allowing them to reach a high density in the well. In many cell lines, attaining confluency leads to the induction of growth inhibition due to contact inhibition (169). Cells were therefore seeded at a moderate starting density ($1 \cdot 10^6$ cells in a T25 flask) and allowed to grow in normal medium for 48 h. As evident in Figure 19B, a reduction of the cycling index can be observed at 48 h in both C/EBPβ wt and ko macrophage-like cells. Although the effect is more pronounced in C/EBPβ wt cells (red dots), both cell lines reach a comparable c_i at this time. The smaller effect on C/EBPβ ko cells (blue squares) is based on the finding that the cycling index for this cell line is already lower at 0 h.

Due to the observation that contact inhibition is more effective than serum withdrawal in the C/EBPβ ko cell line, this procedure was subsequently used for following experiments.
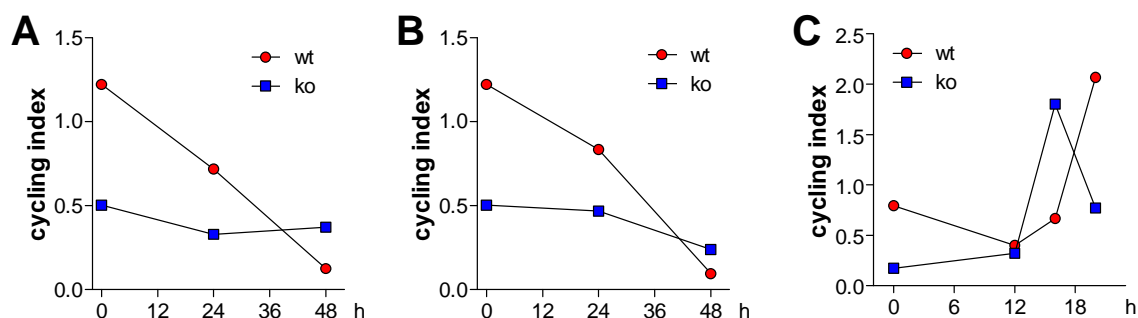
Figure 19 *Divergent cell cycle progression rates in C/EBPβ wt and ko macrophages.* (A) Cells were seeded in medium not supplemented with FCS in order to synchronize the population in G_0G_1 phase. (B) Cells were seeded in normal growth medium containing 7.5% FCS and allowed to reach high density. (C) Cells were seeded in normal growth medium containing 7.5% FCS after growing to a high density over the course of 4 days. Samples were taken at the times indicated and measured by cell cycle analysis. Cycling indices are shown [$c_i = (S+G_2M)/G_0G_1$].

C/EBPβ wt and ko cells were grown to a high cell density ($3 \cdot 10^6$ cells seeded in a T75 flask were incubated for 96 h) and subsequently seeded at a considerably lower density ($5 \cdot 10^5$ cells/T25 flask; 0 h). Starting at 12 h after seeding, samples for cell cycle analysis were taken every 4 h (Figure 19C). Interestingly, while C/EBPβ wt cells (red dots) appear to continue synchronizing within the first 12 h after seeding, the proliferation of C/EBPβ ko cells (blue squares) is already slightly induced, with the cycling index increasing from a value of 0.17 to 0.32. After another 4 h (i.e., 16 h after seeding), the cycling index of C/EBPβ ko cells reaches a value of 1.80, indicating a dramatic increase of cells actively progressing through the cell cycle. At the same time, the index of C/EBPβ wt cells is only at 0.67 which is only slightly higher than 4 h earlier, i.e., 12 h after initial seeding (0.40). 20 h after seeding, the cycling index of C/EBPβ ko cells is again dramatically lower than at 16 h, with 0.77 almost reaching the level observed 8 h earlier. In contrast, C/EBPβ wt cells dramatically start cycling at this time, reaching a value of 2.07.

These data suggest that C/EBPβ ko cells are able to initiate cell cycle progression faster than cells expressing this transcription factor. Furthermore, the conclusion of the cell cycle occurs rapidly, as 8 h after the induction and 4 h after the observed maximum of cycling, the majority of all cells has completed the cell cycle already. Thus, the observed higher proliferation rate of C/EBPβ ko cells (compare Fig. 18) most likely derives from a faster progression through the phases of the cell cycle, leading to its more rapid conclusion.

3.2.10 Regulation of Rb phosphorylation and expression by PMA and C/EBPβ

The presence of C/EBPβ seems to have a profound impact on cellular proliferation (see above). Progression through the cell cycle is a highly complex process regulated by a multitude of different proteins including Rb (157). The phosphorylation of Rb at a minimum

of four different serines enables the expression of S phase specific genes, thereby mediating cell cycle progression (170). Rb phosphorylation at the two serines Ser[608] and Ser[795] was thus analyzed in the presence or absence of C/EBPβ in PMA-treated THP-1.

In order to first confirm the efficacy of the siRNA used, THP-1 cells were transfected with siRNA specifically targeting *CEBPB* mRNA. Knock-down of C/EBPβ protein and mRNA was monitored by western blotting and RT-qPCR, respectively. The specific knock-down of all three C/EBPβ isoforms is confirmed by western blot analysis 24 h after transfection with the siRNA targeting its mRNA (Figure 20A). Transfection with the negative control siRNA (AllStars) does not alter C/EBPβ protein levels.

C/EBPβ expression levels as determined by western blot were further quantified and are presented in a graph in Figure 20B. As shown here, the magnitude of the expression of all three C/EBPβ isoforms 24 h after transfection (blue bars) is reduced by about 75% compared to the levels observed in cells transfected with AllStars negative control siRNA (the dotted line indicates an expression level of 25% relative to negative control). For the analysis, each band was normalized to actin to account for inter-lane differences in protein loading. In detail, the levels of LAP*, LAP, and LIP detected by western blot analysis reach only 24.3±7.4%, 25.9±2.3%, and 25.9±8.4%, respectively, of those observed in the relevant control samples included in each experiment. A similar inhibition is evident after 48 h (red bars), although recovery of C/EBPβ isoform expression with time seems to vary. While the LAP* level attains 30.1±4.4% of that of the controls 48 h at this time, LAP reaches 27.4±1.1% and LIP only 20.1±0.1%.

To further confirm the efficiency of C/EBPβ knock-down during differentiation of THP-1, cells were transfected with siRNA and stimulated with PMA immediately after seeding. Total RNA was extracted after 0, 12, and 24 h and analyzed by RT-qPCR (Figure 20C). Relative C/EBPβ mRNA levels normalized to GAPDH stay relatively constant over time when control-transfected THP-1 were stimulated with PMA (AllStars; blue bars). In cells transfected with C/EBPβ siRNA (red bars), however, *CEBPB* expression is markedly decreased starting at 12 h post transfection and stimulation. At this time, C/EBPβ mRNA levels are reduced more than 50% compared to control-transfected cells taken at 0 h. In comparison to the control cells taken at the same time (i.e., 12 h after transfection), *CEBPB* expression is also dramatically decreased. In detail, while in AllStars-transfected THP-1 the relative C/EBPβ mRNA level reaches 94.0±12.7%, expression after transfection with specific siRNA is only 41.8±6.4% of the 0 h control. After 48 h, *CEBPB* expression is still reduced in the cells transfected with C/EBPβ siRNA, reaching only 65.9±3.5%, while the level in cells

transfected with AllStars siRNA is 100.8±2.9%. Thus, with a knock-down by at least a third after 48 h, introduction of siRNA directed against the *CEBPB* mRNA proved to be sufficiently efficient for further experiments in which THP-1 were differentiated with PMA for 24 h, with stimulations starting 24 h post transfection to ensure low C/EBPβ levels throughout incubation.
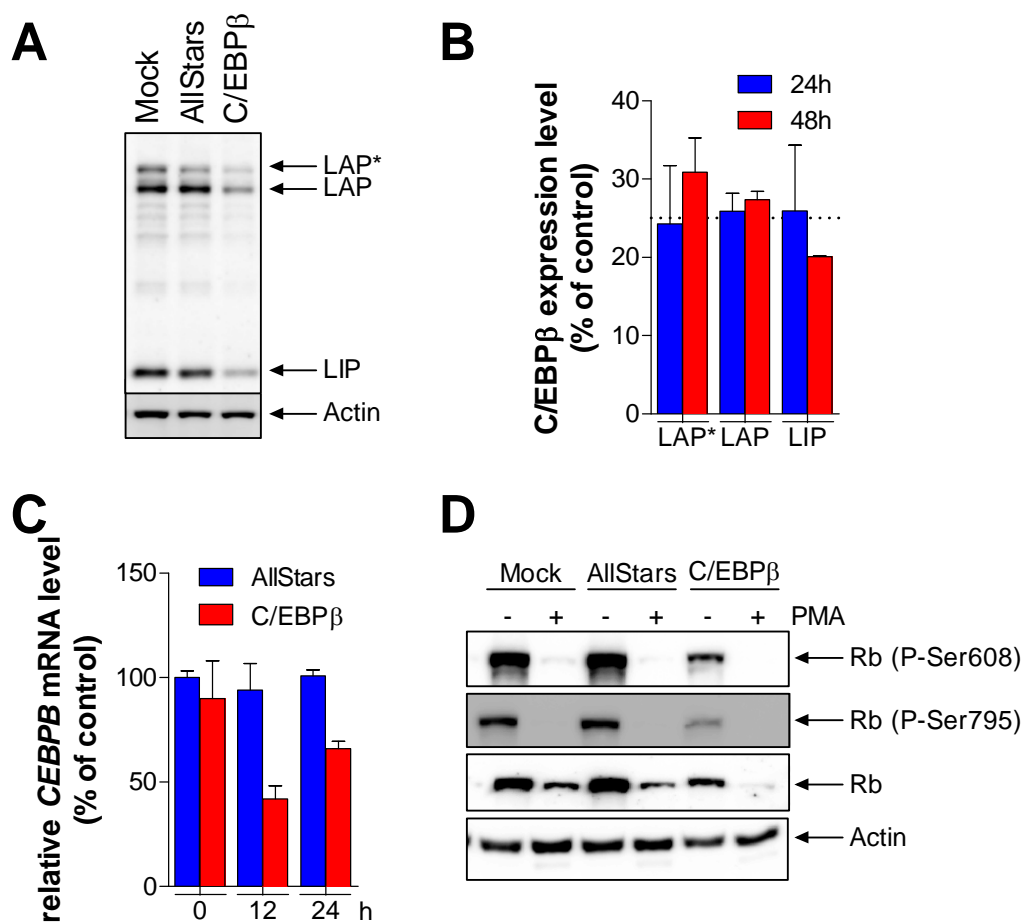

Figure 20 *Rb protein levels and phosphorylation are modulated by both PMA and C/EBPβ.* (A) THP-1 were mock-transfected or transfected with either control (AllStars) or C/EBPβ-specific siRNA (400 pmol) by nucleofection. Whole cell extracts were prepared after 24 h and analyzed by western blot for expression of C/EBPβ (upper panel). Loading control actin (lower panel). (B) Quantitative analysis of at least two independent experiments as described in (A). Extracts were prepared after 24 h or 48 h. Signal intensity of each of the three isoforms was normalized to actin and calculated relative to the values obtained with negative control siRNA at the same point of time. The dotted line indicates an inhibition level of 75% (mean ± SD). (C) THP-1 were transfected with negative control siRNA (AllStars) or siRNA targeting C/EBPβ and immediately stimulated with 100 nM PMA. RNA was extracted at the times indicated and mRNAs for C/EBPβ and GAPDH were measured by RT-qPCR. *CEBPB* mRNA levels were normalized to GAPDH levels and percentages calculated relative to the value of AllStars-transfected cells at 0 h (100%). All measurements were performed in duplicate (mean ± SD). (D) THP-1 were transfected with siRNA and, after 24 h, stimulated ± 100 nM PMA. Cells were harvested after a total of 48 h and whole cell extracts were blotted onto two separate membranes to allow for detection of Rb phosphorylated at Ser[608] and Ser[795]. Membranes were stripped and subsequently re-probed with antibodies detecting total Rb levels and actin.

Rb phosphorylation at Ser^{608} and Ser^{795} is detected in all samples not treated with PMA (Figure 20D). Phosphorylation in mock-transfected cells and the sample transfected with AllStars control siRNA is readily detectable and reaches comparable levels. The phosphorylation of Rb at both serines in the absence of PMA is markedly reduced in cells transfected with siRNA targeting *CEBPB* mRNA compared to both Mock and AllStars control samples. Efficiency of C/EBPβ knock-down in this sample was confirmed on another membrane (data not shown). As expected, Rb phosphorylation at both serines analyzed is completely abolished in all samples treated with PMA. The level of total Rb protein was subsequently analyzed by stripping and re-probing the membranes. Rb is found to be expressed at substantial levels in all untreated samples, albeit its level is lower in cells transfected with C/EBPβ siRNA. The level of Rb is attenuated in both transfected controls (Mock, AllStars) treated with PMA, but remains readily detectable. In contrast, expression of hypophosphorylated Rb in differentiating THP-1 transfected with C/EBPβ siRNA is almost completely abolished. It is quite unexpected that the absolute level of Rb expression is reduced so markedly by treatment with PMA, as other reports have indicated that its expression remains constant during monocytic differentiation (160). To ensure equal loading of all lanes, actin was detected as control. This analysis demonstrates that the dramatic changes seen in Rb phosphorylation and absolute expression levels is not due to differences in protein loading, as the actin levels appear similar in all samples analyzed.

In an attempt to elucidate the mechanism of C/EBPβ siRNA-mediated down-regulation of Rb, the human *RB1* promoter sequence was analyzed by use of the TFSEARCH software. This computational analysis revealed the existence of 4 putative C/EBPβ binding sites within this promoter at the positions between -408 to -421, -714 to -727, -1493 to -1506, and -1535 to -1548 from the transcription start site (data not shown).

C/EBPβ might thus be involved in the regulation of Rb expression, possibly explaining the observation that ablation of this transcription factor reduces the level of Rb within the cell. Further experiments will be necessary to demonstrate the potential involvement of C/EBPβ in the regulation of Rb expression in THP-1 cells. In addition, the results imply a role for C/EBPβ in retaining hypophosphorylated Rb within the differentiating cell.

3.2.11 Differential effects of C/EBPβ isoforms on cellular proliferation

The results reported above point towards an influence of C/EBPβ on proliferation of cells of the monocyte-macrophage lineage. To further assess the growth potential of THP-1 in the presence and absence of this transcription factor, cells were transfected with siRNA targeting

C/EBPβ and analyzed by proliferation assay. Mock- and AllStars-transfected cells were analyzed in parallel in these experiments.

As shown in Figure 21A, both control samples proliferate successively over a period of 100 h. The transfection procedure does not have an inhibitory effect on cell growth as both mock (blue dots) and AllStars samples (red squares) exhibit normal proliferation as early as 24 h after transfection. Surprisingly, growth of THP-1 cells that have been transfected with C/EBPβ siRNA (yellow triangles) is markedly inhibited. This effect is evident already 24 h after transfection and becomes more pronounced over time. While THP-1 transfected with C/EBPβ siRNA grow only 2.5±0.8-fold after 100 h compared to the value at 0 h, the mock and control siRNA-transfected cells grow 8.2±1.4- and 8.3±1.4-fold within the same period of time, respectively. The observed growth inhibition of C/EBPβ siRNA transfected THP-1 cells is significant ($p \leq 0.01$, student's t test) compared to both the Mock and AllStars samples.

The observation made in C/EBPβ knock-down THP-1 is in stark contrast to data obtained in C/EBPβ wt and ko macrophage-like cells. In the latter cells, the knock-out of this transcription factor
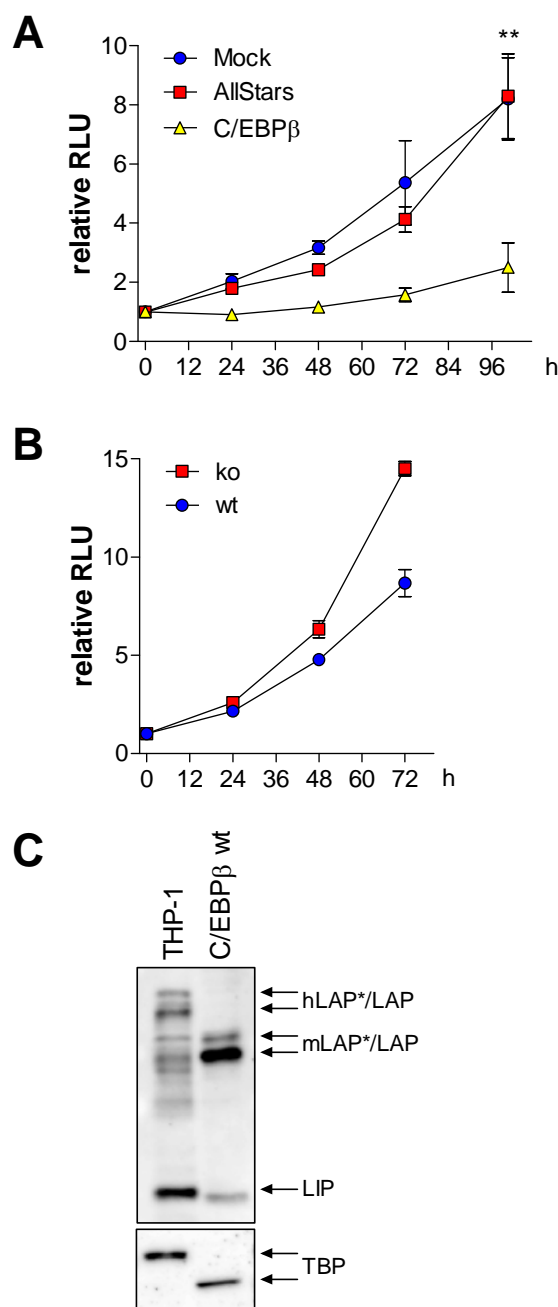

Figure 21 *C/EBPβ LAP* and LAP inhibit while LIP augments cellular proliferation.* (A) THP-1 were transfected with either control (AllStars) or C/EBPβ siRNA (400 pmol), or mock-transfected before seeding for proliferation assay. **, $p \leq 0.01$ (student's t test). (B) C/EBPβ wt and ko cells were seeded for proliferation assay. (A,B) Samples were taken at the time points indicated and measured in triplicate. Data were normalized to the respective values at 0 h. RLU, relative light units (mean ± SD). (C) Equal amounts of whole cell extract were subjected to SDS-PAGE and analyzed by western blotting. C/EBPβ expression was detected (upper panel). Loading control TBP (lower panel).

leads to a dramatic increase in cell proliferation and cell cycle progression (compare Fig. 18

and 19). To further confirm these data, a proliferation assay with these cells was performed in parallel with the transfected THP-1 cells presented above (Figure 21B). As observed before (compare Fig. 18B), C/EBPβ ko cells (red squares) proliferate faster than the C/EBPβ wt macrophages (blue dots). After 72 h of incubation, the RLU value measured in C/EBPβ ko cells is 14.5±0.4-fold higher than at the time of seeding, while growth of C/EBPβ wt macrophage-like cells is induced only 8.7±0.7-fold.

In an attempt to understand the seemingly contradictory results presented above, potential differences of C/EBPβ isoform expression in normal THP-1 and C/EBPβ wt macrophage-like cells were analyzed. To achieve this, equal amounts of nuclear extracts from both cell lines were loaded onto a gel and analyzed by western blot. As shown in Figure 21C (upper panel), all three isoforms of C/EBPβ can be readily detected in THP-1 and C/EBPβ wt cells, the large isoforms LAP* and LAP exhibiting a distinctive size difference between human (designated as hLAP*/LAP) and murine cells (designated as mLAP*/LAP), which is expected. Interestingly, the predominant C/EBPβ isoform detected in human THP-1 cells is the small isoform LIP. In contrast, murine C/EBPβ wt macrophage-like cells exhibit a strong expression of LAP dominating over both the LAP* and LIP isoforms. Although a direct comparison is difficult to achieve due to potentially varying affinities of the antibody used for the parallel detection of human and murine C/EBPβ, judging from this blot the expression levels of LIP in THP-1 and of LAP in C/EBPβ wt cells appear to be similar.

Taken together, these data suggest that the different isoforms of C/EBPβ may have differential effects on cellular proliferation. While the transient knock-down of the predominating small isoform LIP by siRNA in THP-1 leads to a reduction of cell proliferation, the knock-out of C/EBPβ in the murine macrophage-like cells mostly affects the large isoform LAP, possibly explaining why these cells can proliferate at higher rates. Thus, these data indicate that LAP may have a different effect on cellular proliferation than LIP and that these effects may be opposing. The differential expression patterns of C/EBPβ isoforms in THP-1 and C/EBPβ macrophage-like cells can most likely be explained by their different maturation status and coincides well with reports suggesting that proliferation ceases with cellular differentiation (1).

3.2.12 Proliferative capacity determines morphological appearance of C/EBPβ ko macrophages

Previous data (see Fig. 17) indicate that morphological differences observed in C/EBPβ wt and ko macrophage-like cells might be modulated by their different proliferative capacity. To test this hypothesis, these cells were cultivated in media containing varying amounts of FCS

(0.5, 2, and 5%) for up to 5 days. Morphology was examined on a regular basis by light microscopy.

C/EBPβ wt cells display a normal morphological appearance when cultured with 5% FCS (left panel), as evident by a heterogeneous population of round and polygonal cells (Figure 22A). When grown in medium supplemented with only 2% FCS, an increased number of cells exhibit a macrophage morphology (middle panel). Finally, under conditions where only 0.5% FCS is present in the medium, almost all cells are polygonal, spindle-shaped, and flattened, and the number of cells that remain round is dramatically reduced (right panel).

Interestingly, the same trend is evident in C/EBPβ ko cells (Figure 22B). When grown in medium containing 5% FCS, the cells look normal, i.e., round but adherend, growing in clusters (left panel). Upon reduction of the serum concentration in the culture medium, these cells' morphology changes, as C/EBPβ ko macrophage-like cells grown with 2% FCS start to become spindle-shaped, although most of the cells remain round (middle panel). Further reduction of the serum concentration to only 0.5% FCS leads to a strong change of morphology, as the number of round cells is reduced and a large amount of cells becomes flattened and spindle-shaped (right panel).

To further quantify the morphological changes observed in C/EBPβ ko macrophage-like cells, the cells were counted in images taken during microscopy. The number of cells exhibiting a macrophage morphology was then calculated relative to total cell numbers. As shown in Figure 22C, only 12.84±1.30% of all C/EBPβ ko cells exhibit morphological features of macrophages after incubation in medium supplemented with 5% FCS (3 days). Upon
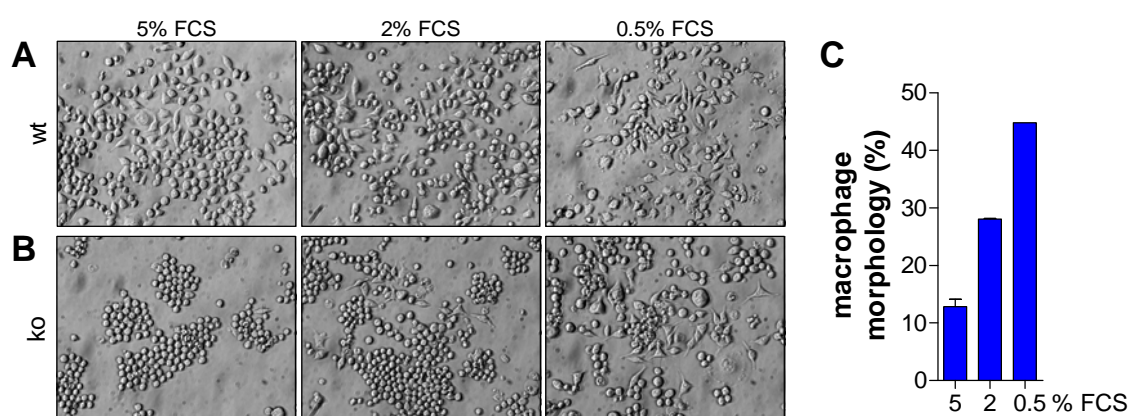

Figure 22 *Inhibition of proliferation induces morphological changes in C/EBPβ ko macrophages.* C/EBPβ wt (A) or ko (B) macrophage-like cells were incubated in cell culture medium supplemented with 0.5%, 2%, or 5% of FCS. Morphology was assessed after 3 (2% and 5% FCS) or 5 days (0.5%) by light microscopy. Magnification, ×320. (C) Quantitative analysis of C/EBPβ ko cell morphology. C/EBPβ ko cells and their total cell numbers were counted in two images obtained in one representative experiment. Percentage of cells with macrophage morphology was calculated relative to total cell numbers. Data are given as mean ± SD.

reduction of the FCS concentration to 2% for the same time, that number is increased to 28.04±0.13%. Finally, when the cells are incubated in medium containing only 0.5% of FCS, 44.81±0.06% of all cells acquire a macrophage morphology (5 days).

These observations indicate that the difference in C/EBPβ wt and ko morphology is most likely determined by their frequency of proliferation. It might be conceivable that round cells are cells actively undergoing mitosis or having just completed cell division. As C/EBPβ ko cells have a dramatically elevated rate of proliferation (see Fig. 18), they may lack the time to adjust their morphology before starting the next cell cycle.

3.2.13 Modulation of C/EBPα and ε expression in C/EBPβ ko macrophages

C/EBPβ is massively upregulated during the differentiation of monocytes towards macrophages (see Fig. 12). Despite this observation, which was also published previously (71-73), C/EBPβ ko mice contain cells of the monocytic lineage, and a macrophage cell line derived from these animals has been established (137). These macrophages have already been analyzed for potentially compensatory mechanisms by other C/EBP family members when they were first described. In this publication by Gorgoni *et al.*, an increase of both C/EBPδ and ε mRNA and protein levels in C/EBPβ ko cells was observed, while those of C/EBPα remained constant (137). However, no loading control was presented in this study and the western blots showed only one band for each C/EBPα and ε although both are known to exist as two or four different-sized isoforms, respectively. Possibly compensatory roles of C/EBPα and ε during PMA-induced differentiation were therefore examined on the basis of protein expression.

C/EBPβ wt and ko cells were stimulated with 100 nM PMA for 6 or 24 h prior to lysis and subsequent analysis by immunoblotting. Expression of C/EBPα and, in the case of C/EBPβ wt cells, C/EBPβ is confined to the nuclei, with little or no protein detectable in the cytoplasms (Figure 23A, C). This confirms the expression patterns of these C/EBP proteins observed in THP-1 cells (shown in Fig. 12-14). C/EBPα levels appear higher in unstimulated C/EBPβ ko cells compared to the respective C/EBPβ wt macrophages (Figure 23A). Interestingly, a PMA-induced down-regulation of both p42 and p30 isoforms can be observed in C/EBPβ ko cells. C/EBPα levels in C/EBPβ wt cells, on the other hand, are only slightly reduced by PMA treatment. While p42 is readily detectable, p30 expression seems to be very low as only a very weak band can be seen. Furthermore, PMA treatment appears to reduce p42 in C/EBPβ ko cells approximately to the levels seen in C/EBPβ wt macrophage-like cells. One should note, however, that overall C/EBPα expression is very faint as the exposure time
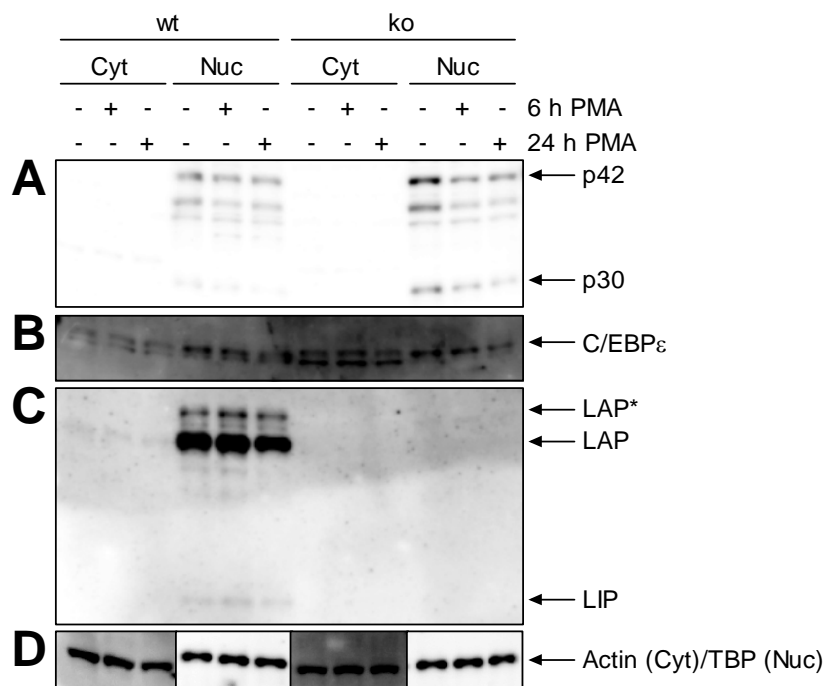
Figure 23 *C/EBPα expression is slightly increased in C/EBPβ ko macrophages.* C/EBPβ wt and ko cells were seeded and stimulated with 100 nM PMA. Stimulation occurred either directly after seeding (24 h PMA) or 18 h later (6 h PMA). All samples were harvested after 24 h of incubation. Cytoplasms and nuclei were prepared and analyzed by western blot. The antibodies used were: (A) C/EBPα; (B) C/EBPε; (C) C/EBPβ; and (D) actin and TBP (loading controls). Membrane was sequentially probed with the indicated antibodies and stripped between detections.

of the immunoblot presented in Figure 23A is several fold longer than that of all antibodies subsequently re-probed on the same membrane.

C/EBPε can be readily detected in the cytoplasm and nuclei of both C/EBPβ wt and ko cells (Figure 23B). However, only two bands, representing two isoforms, are detected in all samples except the nuclei of C/EBPβ ko macrophage-like cells. The precise identity of the two isoforms observed is not clear as they run slightly below the 28 kDa band of a molecular weight marker present on the same gel (not shown). C/EBPε is expected to produce the three large isoforms p32, p30, and p27, which in contrast to the different isoforms of C/EBPα and β are generated by splicing and different promoter usage (52,90). The same two bands seen in the western blots are also produced in the murine adipocyte NIH 3T3 cell line (positive control) confirming that these two bands represent C/EBPε (data not shown). Therefore, it is possible that either p32 and p30 or p30 and p27 isoforms are detected in this western blot. However, the expression level in C/EBPβ wt and ko cells appears to be similar and no influence of PMA treatment is observed. Apart from the absence of the smaller isoform in C/EBPβ ko nucleic extracts, the significance of which is unclear, no differential regulation of C/EBPε expression in C/EBPβ ko cells could be detected. The fourth C/EBPε isoform p14 is not observed in either lane, regardless of cellular compartment (Cyt, Nuc) or cell line (wt, ko).

C/EBPβ is expressed only in C/EBPβ wt cells as confirmed by re-probing with the appropriate antibody (Figure 23C). In contrast to the observation made in THP-1 cells (compare Fig.

12A), C/EBPβ is not upregulated by PMA treatment in this macrophage-like cell line. As shown above (Fig. 21C), LAP is the predominant isoform in these cells and its level stays relatively constant over a period during which it is induced dramatically in the premonocytic cell line. LAP* is also readily detectable, while LIP is only weakly expressed. Thus, all three C/EBPβ isoforms are neither induced nor inhibited by incubation of these C/EBPβ wt macrophage-like cells with PMA. Loading controls confirm equal amounts of protein present in all samples (Figure 23D).

In summary, only C/EBPα appears to be slightly upregulated in C/EBPβ ko macrophage-like cells. Since the C/EBPα signal intensities detected in these cells are significantly lower than those detected for C/EBPβ in C/EBPβ wt cells, it is unlikely that this slight increase of C/EBPα can compensate for the loss of the predominant C/EBPβ protein. C/EBPε, on the other hand, is found to be present at similar levels in both C/EBPβ wt and ko macrophage-like cells.

3.2.14 Influence of PMA treatment on PU.1 expression in THP-1

Even though C/EBPβ expression is massively upregulated during the PMA-induced monocytic differentiation of THP-1 (see Fig. 12), the ability of C/EBPβ ko mice to produce macrophages (137) questions the importance of this transcription factor during this process.

On the other hand, PU.1 appears to be a protein indispensable for monocytic differentiation as its deletion in mice leads to a complete lack of this lineage and early death of the affected animals (131,132). The regulation of PU.1 expression was thus assessed by western blot in THP-1 treated with 100 nM PMA for 24 h.

Figure 24 *PMA strongly induces PU.1 expression in THP-1.* THP-1 cells were cultivated ± 100 nM PMA for 24 h prior to preparation of whole cell extracts and determination of PU.1 (upper panel) and actin (lower panel) levels by western blot.

PU.1 expression is not detectable in THP-1 incubated in normal culture medium (Figure 24, upper panel). In contrast, PU.1 can be readily visualized in cells differentiated along the monocytic lineage by PMA. Actin expression is not affected by PMA treatment in this experimental setup (lower panel).

Thus, PU.1 expression is massively upregulated in PMA-stimulated THP-1. Of note, this effect appears to be more pronounced than the upregulation of C/EBPβ LAP* and LAP by the same stimulus (compare Fig. 12).
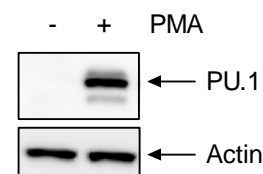
3.2.15 Comparison of PU.1 expression levels in C/EBPβ wt and ko macrophages

At least two transcription factors are found to be upregulated during monocytic differentiation in THP-1: C/EBPβ and PU.1 (see Fig. 12 and 24). C/EBPβ does not appear to be essential during this process as C/EBPβ ko mice contain monocytes and macrophages (137). To determine the role PU.1 plays in these cells, further experiments were conducted to compare the expression level of this transcription factor in C/EBPβ wt and ko macrophage-like cells.

Cells were stimulated with 100 nM PMA for the times indicated or left untreated before preparation of nuclear extracts. PU.1 expression was subsequently analyzed by western blot (Figure 25A). The level of PU.1 is not affected by incubation with PMA in either C/EBPβ wt or ko cells. However, it is obvious that PU.1 levels are lower in C/EBPβ ko macrophage-like cells compared to those observed in C/EBPβ wt cells. The only exception is the C/EBPβ ko sample taken directly after seeding (0 h) in which PU.1 expression appears to be as high as in C/EBPβ wt cells.

The membrane was subsequently probed with C/EBPβ antibody to confirm the lack of this protein in C/EBPβ ko cells (Figure 25B). Expectedly, the three C/EBPβ isoforms can be readily detected in C/EBPβ wt but not in C/EBPβ ko cells. As already demonstrated above (see Fig. 21C), LAP is the predominant isoform in this cell line.

Generally, the levels of TBP do not fluctuate dramatically between C/EBPβ wt and ko cells (Figure 25C). However, the leve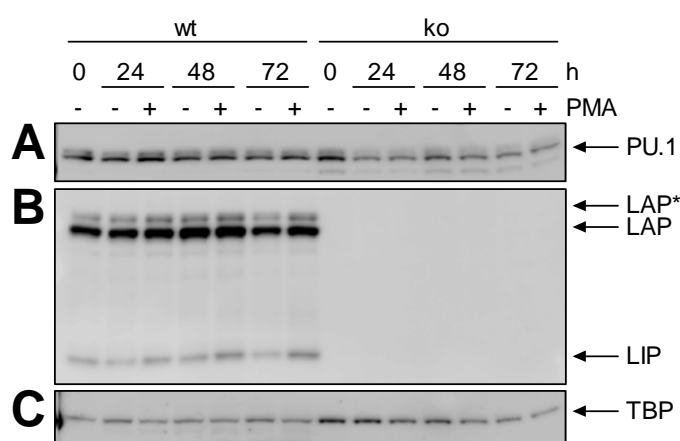l of this loading control is higher in C/EBPβ ko cells under some conditions. When taking this into account, the expression of PU.1 in C/EBPβ ko cells at 0 h does not appear to be elevated and is most likely similar to the other C/EBPβ ko samples.

These data show that PU.1 is expressed in C/EBPβ ko macrophage-like cells, most likely representing the factor enabling generation of this cell type in C/EBPβ ko mice. It is obvious, however, that the PU.1 levels are

Figure 25 *PU.1 levels are reduced in C/EBPβ ko cells.* C/EBPβ wt and ko cells were incubated ± PMA (100 nM). Cells were subsequently harvested at the times indicated. Nuclear extract was prepared and analyzed for PU.1 (A) and C/EBPβ (B) expression by western blot. Loading control TBP (C).

lower than in C/EBPβ wt macrophage-like cells, possibly pointing towards a role of C/EBPβ in PU.1 expression.

3.2.16 Overexpression of C/EBPβ augments PU.1 expression in THP-1

From the data presented above (see Fig. 25), it seems likely that C/EBPβ determines PU.1 levels as the latter are reduced in C/EBPβ ko macrophage-like cells. To test whether C/EBPβ is directly involved in PU.1 expression, monocytic THP-1 cells were transiently transfected with an expression plasmid encoding full-length C/EBPβ from a pTracer vector backbone.

THP-1 transfected with increasing amounts of plasmid were incubated for 6 h at 37°C before preparation of whole cell extracts. PU.1 expression was subsequently assessed by western blot (Figure 26, top panel). Its expression is readily detected in mock-transfected THP-1 (0 μg). Starting at about 5 μg of expression plasmid used however, a further increase of the PU.1 level can be observed. To confirm overexpression of C/EBPβ in the samples, the membrane was re-probed with an antibody detecting C/EBPβ (middle panel). As seen, C/EBPβ expression is augmented over a barely detectable level already with the use of 1 μg plasmid. The more expression plasmid was transfected, the more C/EBPβ is produced. LAP* is the isoform most prominently affected by overexpression, but LAP and LIP levels also increase concomitantly. It appears as if the first AUG is the start codon preferentially used in the context of the pTracer vector backbone, presumably due to the absence of the original 5'-UTR of the *CEBPB* mRNA in the resulting transcript. A side finding is that the non-specific bands that are frequently seen in THP-1 also increase with the plasmid concentration. This may be a hint that those "not specific" bands are in reality bands specifically detected by the antibody as they appear to be degradation products of the two large C/EBPβ isoforms. To ensure equal protein loading, actin was detected on the same membrane (bottom panel).

Figure 26 *C/EBPβ regulates PU.1 expression.* THP-1 were transfected with the indicated amount of pTracer-FL coding for full-length *CEBPB*. Cells were harvested after 6 h of incubation. Whole cell extracts were analyzed for PU.1 (top panel) and C/EBPβ (middle panel) expression by western blotting. Loading control actin (bottom panel).

In summary, these data demonstrate that C/EBPβ may induce PU.1 expression. Other factors must also play a role as C/EBPβ ko macrophage-like cells still express PU.1, albeit at a lower level than wt controls (see Fig. 25A). Although it has been noted that the PU.1 promoter
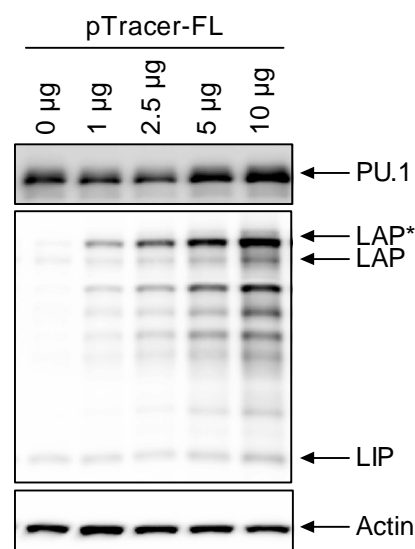
contains a C/EBP binding site (1), the induction of PU.1 protein by C/EBPβ has not yet been demonstrated. To date, only the activation of the PU.1 promoter by C/EBPβ has been suggested by two groups (124,136). These findings may help explain why C/EBPβ ko mice are nevertheless able to produce macrophages, although they exhibit a markedly different morphology (compare Fig. 17A).

3.2.17 Effects of knock-down of C/EBPβ on PMA-induced morphological changes

As shown above, C/EBPβ seems to be the only C/EBP family member of which the transcriptionally active isoform is massively upregulated during PMA-induced differentiation of THP-1. Therefore, RNA interference experiments were conducted to determine its role in the observed adoption of the macrophage morphology (see Fig. 11).

Stimulation of normal, untransfected THP-1 with PMA results in a strong change of morphology (Figure 27, left panels) as described above. Cells that are usually round and in suspension (top) undergo massive changes resulting in a flattened, adherend phenotype (bottom). In the absence of PMA, transfection of the cells with siRNA specific for C/EBPβ (middle panels) leads to the development of a morphology resembling normal THP-1, although a relatively large number of small, ruffled, and presumably apoptotic or dead cells are discernible (top). Upon treatment of these cells with PMA, they undergo the same changes in cellular morphology as normal THP-1, indicating differentiation towards a
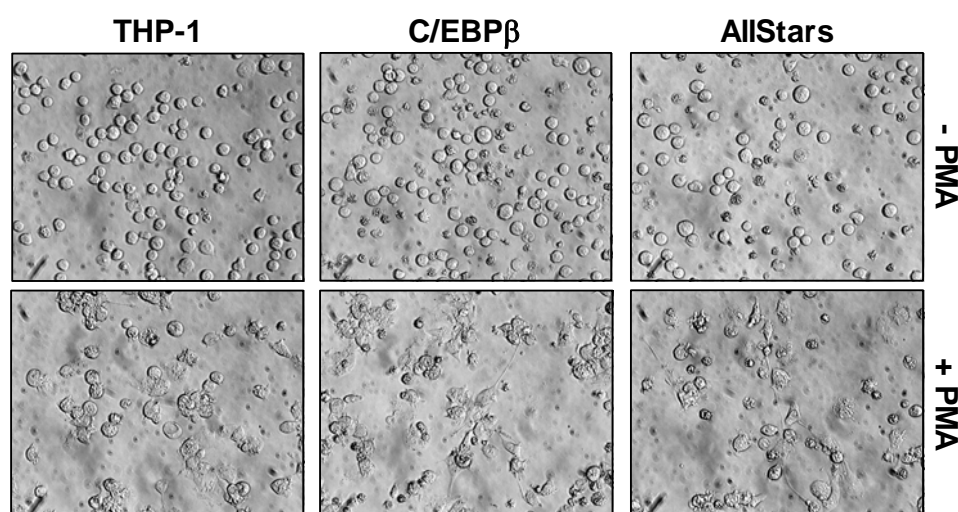

Figure 27 *Knock-down of C/EBPβ does not block PMA-induced changes of THP-1 morphology.* THP-1 were transfected with either C/EBPβ-specific or control (AllStars) siRNA (400 pmol) by nucleofection as indicated. After 24 h, cells were incubated with 100 nM PMA for additional 24 h (bottom panels) or left untreated (top panels). Magnification, ×320.

macrophage-like phenotype (bottom). The same is true for THP-1 transfected with AllStars negative control siRNA (right panels), which are non-adherend and round before incubation with PMA (top) and become flat, amoeboid, and polygonal upon exposure to this differentiating stimulus (bottom).

As demonstrated above (compare Fig. 20A-C), treatment of THP-1 cells with siRNA efficiently reduced the level of C/EBPβ within the time frames used in the experiments presented here. Thus, these results indicate that expression C/EBPβ is not essential for the PMA-induced development of a macrophage morphology in the THP-1 monocytic cell line.

3.2.18 Effects of PMA on C/EBPβ wt and ko macrophage morphology

Apart from the reported findings about the influence on cellular proliferation, the observation that C/EBPβ ko macrophage-like cells have a markedly different appearance than C/EBPβ wt macrophages prompted further experiments to determine the effect a stimulation with PMA might have on these cells. Thus, C/EBPβ wt and ko cells were stimulated with 1, 10, or 100 nM PMA for 24 h prior to morphological analysis by light microscopy.

Figure 28A shows a typical result obtained in C/EBPβ wt macrophage-like cells. Without PMA treatment (upper left panel), these cells constitute a heterogeneous population of round but adherend cells, and flat, polygonal macrophage-like cells as seen above (compare Fig. 17A). With increasing concentrations of PMA, the polygonal and flattened phenotype becomes more dominant, while the number of round cells decreases. The critical concentration of PMA lies between 1 and 10 nM, as C/EBPβ wt cells stimulated with the lower concentration (upper right panel) appear almost like non-treated cells, while those treated with 10 nM PMA are markedly different in appearance (lower left panel). Treatment of these cells with 100 nM of PMA does not seem to further shift their phenotype towards macrophages (lower right panel).

The C/EBPβ ko macrophage-like cells undergo a dramatic change of appearance following treatment with PMA and, in comparison to C/EBPβ wt cells, this effect is more pronounced (Figure 28B). In the absence of PMA, the cells compose a homologous population of almost only round but adherend cells (upper left panel), reflecting the observations described above (Fig. 17A). The cells become more and more polygonal, flattened, and spindle-shaped with the concentration of PMA used for stimulation. When treated with 1 nM PMA (upper right panel), a large proportion of the cells appear like non-treated C/EBPβ ko cells, but a few undergo a change of morphology by forming spike-like protrusions. A number of spindle-shaped and some polygonal and flattened cells are observed upon incubation with 10 nM of PMA (lower left panel). Finally, when stimulated with a PMA concentration of 100 nM, a
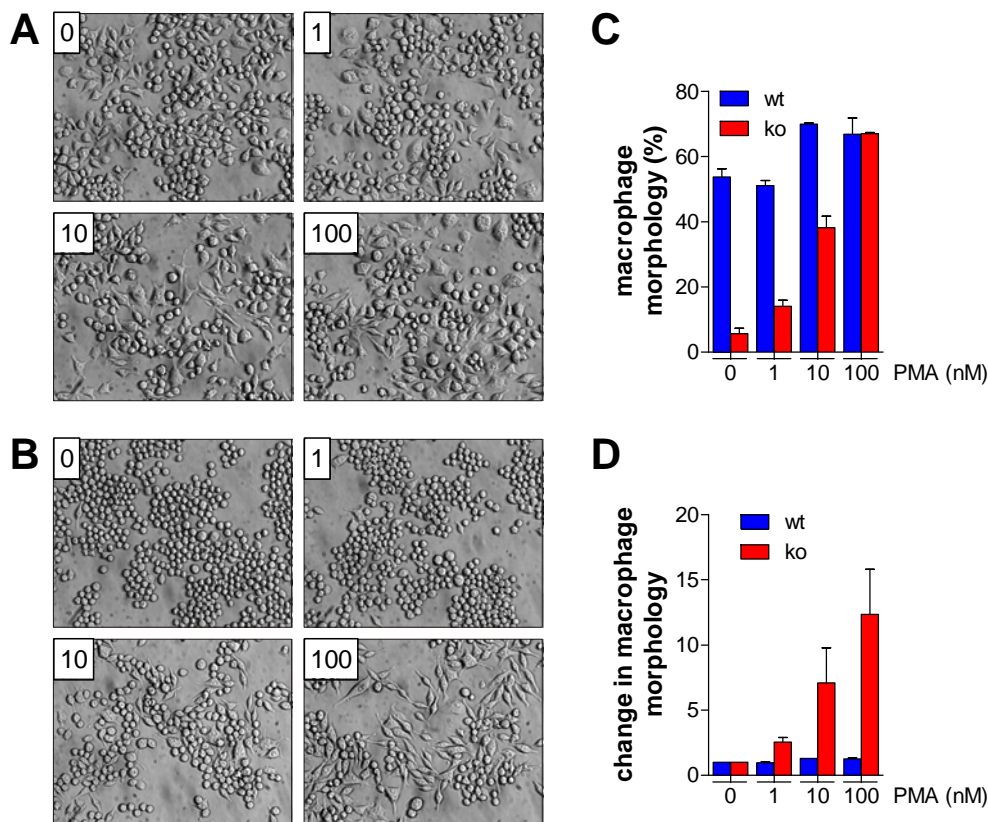
Figure 28 *PMA induces morphological changes in both C/EBPβ wt and ko macrophages.* C/EBPβ wt (A) or ko cells (B) were incubated in the presence of the indicated concentration of PMA (in nM) for 24 h and analyzed by microscopy. Magnification, ×320. (C) Quantitative analysis of cell morphology. Cells with macrophage morphology and total cell numbers were counted in each two images obtained by microscopy. Percentage of cells with macrophage morphology was calculated relative to total cell numbers (mean ± SD). (D) Further analysis of the data shown in (C). Percentage of cells with macrophage morphology was calculated relative to the value obtained without PMA stimulation (mean ± SD).

large number of cells has undergone dramatic changes in appearance, as a few polygonal and many spindle-shaped cells can be found under this condition (lower right panel). Therefore, PMA is able to induce morphological changes resembling a macrophage morphology even in the absence of C/EBPβ, and interestingly, these cells seem to be more sensitive to changes of the PMA concentration used.

As a means to get a clearer picture of the morphological changes induced by PMA in C/EBPβ wt and ko macrophages, the number of round, non-macrophage-like cells in the images obtained by microscopy was compared to the amount of flat cells with macrophage morphology present in the same sample. The number of the latter cells is given as percentage of the total number of the cells analyzed (Figure 28C). When left untreated, 53.7±2.5% of all C/EBPβ wt cells (blue bars) resemble normal macrophages in terms of morphology. This number is kept constant upon treatment with 1 nM PMA but increases to 70.0±0.4% and 66.9±5.0% when the cells are stimulated with 10 or 100 nM, respectively. In C/EBPβ ko cells

(red bars) under normal growth conditions, only 5.7±1.6% resemble macrophages. PMA is able to markedly increase the frequency of a macrophage morphology: when C/EBPβ ko cells were stimulated with 1 nM, 14.0±2.0% look like macrophages, and a dramatic increase is seen with 10 nM and 100 nM of PMA, where 38.2±3.6% and 67.1±0.4% of the cells develop morphologic changes characteristic of macrophages, respectively. Thus, when treated with high concentrations of PMA, C/EBPβ ko cells attain roughly the same level of macrophage morphology as C/EBPβ wt cells, albeit their appearance varies, as C/EBPβ wt cells tend to be polygonal and flattened, while C/EBPβ ko cells favorably become spindle-shaped.

To further analyze the morphological changes induced by PMA in C/EBPβ wt and ko cells, the percentage of cells with macrophage morphology was calculated relative to that observed in non-treated cells. As shown in Figure 28D, the amount of cells exhibiting a macrophage morphology in the C/EBPβ wt population remains relatively constant even upon treatment with PMA (blue bars): no change can be seen with 1 nM and only slight increases are observed with 10 nM (1.3±0.0-fold induction) or 100 nM (1.3±0.1-fold induction). In contrast, a pronounced macrophage morphology in C/EBPβ ko cells is induced 2.6±0.4-, 7.1±2.7-, and 12.4±3.5-fold by stimulation with 1, 10, and 100 nM of PMA, respectively (red bars).

In summary, these data show that in C/EBPβ ko cells the relative amount of cells exhibiting morphological features of macrophages can reach the level observed in PMA-treated C/EBPβ wt cells. While PMA has no dramatic effect on this ratio in C/EBPβ wt cells, a significant change is induced in C/EBPβ ko cells by this stimulus. The ability of C/EBPβ ko cells to adopt a macrophage morphology by stimulation with PMA may potentially be enabled by enhanced expression of C/EBPα, which might partially compensate for the loss of C/EBPβ (compare Fig. 23).

3.2.19 Knock-down of PU.1 inhibits PMA-induced morphological changes in THP-1

As reported above, the siRNA-based knock-down of C/EBPβ was not sufficient to inhibit the morphological changes induced by PMA in THP-1 (compare Fig. 27). Because previous data show that PU.1 is most likely responsible for the development of a macrophage phenotype in C/EBPβ ko mice [see Fig. 25A and (137)], it is feasible that knock-down of PU.1 in THP-1 might inhibit PMA-induced morphological changes. To assess this, THP-1 were transfected with siRNA targeting PU.1. PMA was added 24 h after transfection prior to incubation of the cells for another 24 h. Cellular morphology was subsequently assessed by microscopy.

As shown in Figure 29A, PMA treatment induces adherence and macrophage-typical morphological changes in control THP-1 and in cells that were transfected without siRNA (Mock) or with control siRNA (AllStars). As demonstrated before, knock-down of C/EBPβ does not inhibit PMA-induced morphological changes. However, when transfected with PU.1 siRNA, the cells remain round even in the presence of PMA. It is notable that the THP-1 cells, despite the knock-down of PU.1, still become adherend upon PMA treatment. However, acquisition of an amoeboid shape and flattening cannot be observed in these cells, while this phenomenon is detected in all other samples treated with PMA.

In order to ensure functionality of the PU.1 siRNA used for transfection, a control experiment was performed, and whole cell extracts of transfected cells were prepared after 48 h, i.e., at the time of morphological analysis by microscopy. In this case and also in the experiments presented above, C/EBPβ siRNA was transfected at a lower concentration than usual, matching the 100 pmol used in PU.1 siRNA transfections. A higher amount of PU.1 siRNA

Figure 29 *Knock-down of PU.1, but not of C/EBPβ, inhibits differentiation-induced morphological changes in THP-1.* (A) THP-1 were transfected with 100 pmol of siRNA targeting C/EBPβ, PU.1, or the negative control AllStars. Additional samples were mock-transfected or left untreated (THP-1) and incubated for 24 h at 37ºC. Where indicated, cells were subsequently stimulated with PMA (100 nM) for 24 h. Morphology was assessed 48 h after transfection by microscopy. Magnification, ×320. (B) THP-1 were transfected with siRNA as indicated (concentration given in brackets). Whole cell extract was prepared after 48 h and analyzed by western blotting for PU.1 (top panel) and C/EBPβ (middle panel) expression. Loading control actin (bottom panel).

could not be used due to volume restrictions during nucleofection. Transfection of THP-1 with PU.1 siRNA visibly reduces the level of this protein (Figure 29B, top panel) in comparison to the control-transfected samples (Mock, AllStars). Transfection with either concentration of C/EBPβ siRNA does not alter PU.1 levels in this experimental setup, probably due to the short period of incubation and the stability of PU.1 protein. Additionally, a western blot confirming C/EBPβ knock-down in the two samples treated with specific siRNA (middle panel) confirms previous observations that C/EBPβ knock-down is not complete (compare Fig. 20A, B). The blot demonstrates that C/EBPβ levels are reduced to a similar extent in cells transfected with either 100 or 400 pmol of siRNA. Interestingly, C/EBPβ expression appears to be negatively affected in the sample transfected with PU.1 siRNA, although this effect is observed only in comparison to AllStars- but not mock-transfected controls. To ensure similar loading of total protein, the membrane was subsequently probed with an actin antibody (bottom panel). The image obtained demonstrates that while actin is reduced in Mock and AllStars lanes, it remains relatively constant in all other samples. Taking the observed reduction in the control-transfected cells into account, the relative levels of PU.1 and C/EBPβ in these samples are higher than they appear in the respective western blots.

In summary, these data demonstrate that PU.1 is an essential factor driving monocytic differentiation in human premonocytic THP-1 cells. This experiment further confirms the validity of earlier experiments showing that these cells still undergo macrophage-typical morphological changes even when C/EBPβ levels are dramatically reduced by knock-down. Primary functions of C/EBPβ during monocytic differentiation thus appear to be the induction of PU.1 as well as inhibition of cellular proliferation, thereby inducing morphological changes characteristic of macrophages.

4. Discussion

4.1 Monocyte activation

Monocytes are an essential component of the vertebrate immune system, linking the activation of innate immunity to the generation of a specific adaptive immune response. Mice lacking cells of the myelomonocytic lineage die early after birth due to lethal pathogenic infections (131,132). As mononuclear phagocytes, monocytes are able to recognize pathogens and their components, e.g., LPS, *via* interactions with PRRs present on their cell surface. Ligation of these receptors leads to the activation of intracellular signaling cascades. Several transcription factors including NF-κB are the effectors of these signal transduction pathways, their activation leading to the expression of a large range of proinflammatory proteins. These include cytokines such as IL-1 and TNF as well as chemokines like IL-8. Monocytes can in turn be activated by these factors and subsequently augment crucial cellular functions such as antigen presentation and phagocytosis (15-17).

The aim of this study was to further elucidate the mechanisms involved in monocytic desensitization towards TNF in the process of TNF tolerance. As in LPS tolerance, which is much better understood, TNF tolerance leads to the loss of cellular activation after repeated stimulation with a low dose of this cytokine. Tolerance towards potentially harmful stimuli can be beneficial for the organism, for example when it helps to prevent excessive tissue damage due to inflammatory processes (5,18). When tolerance leads to a lasting inactivation of the immune system, however, the organism is at great risk of suffering a potentially lethal infection due to immunoparalysis (18,29,30). Thus, although tolerance may initially be a beneficial reaction, the mechanism of its generation is of great interest as prolonged insensitivity towards an essential cytokine like TNF can turn into a potentially harmful trait.

TNF tolerance can be induced in rodents like mice, rats, and guinea pigs by repeated injection of a low dose of TNF over the course of several days. These animals are then protected against the potentially harmful effects of a high dose of TNF, including fever, cachexia, or gastrointestinal toxicity (36,37,39). On the other hand, induction of tolerance in tumor-bearing mice leads to a reduced anti-tumor activity of TNF, making the administration of higher doses necessary to achieve the same effect (171). At the cellular level, TNF tolerance has been linked to an inhibition of NF-κB phosphorylation by enhanced interaction with C/EBPβ and reduced degradation of IκB-α (47,49,50,172).

4.1.1 Experimental conditions

This study was aimed at elucidating the mechanisms leading to the development of TNF tolerance in primary monocytes isolated from human whole blood. A first step was therefore to verify the purity of monocytes isolated by a negative selection procedure and, if necessary, to improve the protocol. Flow cytometric analysis by FACS® technology confirmed that the isolated monocyte fraction reached a purity of at least 95% by simultaneous staining with antibodies directed against HLA-DR and CD14 (Figure 4B). Both of these molecules are generally accepted to be present on the cell surface of human monocytes (3,4). The attempt to detect potentially contaminating lymphocyte fractions (Figures 5, 6) demonstrated that these cell types were barely present in the monocyte preparations obtained by the negative selection protocol. Therefore, a monocyte purity of between 95% and 99% can be assumed.

The inducibility of purified human monocytes by TNF was assessed next. IL-8 production in the cell culture supernatant was chosen as the readout parameter as its regulation during TNF tolerance in THP-1 has been demonstrated previously (49,50). As expected, TNF induced IL-8 secretion of primary human monocytes in a time- and dose-dependent manner. A slight activation of IL-8 production was observed starting at a TNF concentration of 1.25 ng/ml, and secretion of IL-8 was increased concomitantly with higher doses of TNF (Figure 7). Importantly, the activation of IL-8 production lasted for up to 72 h (Figure 8). However, the maximum IL-8 concentration was measured in the supernatants of monocytes stimulated with TNF for 24 h only. It is interesting to note that IL-8 levels start to recede one day after stimulation, as it would be expected that, unlike mRNA which has a comparably short half-life within the cell, secreted protein may accumulate in the supernatant over time. The reduction of IL-8 over time can possibly be explained by monocytic reaction to this stimulus. It is known that following ligation, signaling through the IL-8 receptor leads to internalization of the complex (173), potentially reducing the amount of IL-8 present in the cell culture well after several days. Additionally, the level of TNF is likely to be reduced by a similar mechanism in the course of the experiments. Therefore, it is important to note that TNF is able to stimulate primary human monocytes to produce IL-8 for at least 72 h, even if the maximum is reached two days earlier.

4.1.2 TNF tolerance

At the molecular level, the mechanisms underlying the TNF tolerance phenomenon have been studied almost exclusively in cell lines (45-47,49,50). The goal of this project was to identify new proteins involved in the generation of TNF tolerance in primary human monocytes. To this end, isolated human monocytes were subjected to conditions leading to the development

of TNF tolerance and analyzed by ELISA, RT-qPCR, or Affymetrix® microarray. The remarkable finding of these experiments is that some monocyte preparations exhibited IL-8 expression patterns characteristic of TNF tolerance, while others failed to do so (Figure 9). Even in the samples that were rendered TNF tolerant, the inhibition of IL-8 expression was never as complete as that observed in the premonocytic cell line THP-1 under similar conditions (49,50).

A possible explanation for this observation is that the concentration chosen for pre-stimulation of the monocytes was too low. For the gene expression analysis, monocytes were treated with 1 ng/ml of TNF for 72 h prior to re-stimulation (compare Chapter 3.1.3). While 1.25 ng/ml induced IL-8 expression in monocytes during a short-term stimulation of only 5 h, other experiments did not show activation after 72 h with a similarly low concentration. Of course the rationale for the choice of the TNF concentration used was to only slightly activate the cells during pre-stimulation. It is additionally important to note that the biological activity of the different lots of TNF changed markedly during the course of this study. The earlier experiments assessing the ability of TNF to stimulate monocyte IL-8 secretion were performed with a TNF lot exhibiting an activity of 20 U/ng. That means that the cells were initially supposed to be pre-stimulated with TNF concentrations ranging between 20 and 25 U/ml. In the experiments aimed at generating TNF tolerant samples for gene expression analysis, however, the lot of TNF had a biological activity of 66.7 U/ng according to the manufacturer. Monocytes were thus pre-treated with a TNF concentration of 66.7 U/ml in these experiments, and when generating the samples for the RT-qPCR analysis, even 100 U/ml were used. The biological activity used thus was at least three times higher than that used for pre-stimulation or other tests in earlier experiments. Still, these monocytes could not be stably rendered TNF tolerant. If the biological activity of the recombinant TNF is indeed the determining factor, the concentration used in this study must have been dramatically too low to induce tolerance in primary human monocytes. New observations appear to confirm this notion, as pre-stimulation of these cells with 400 U/ml of TNF almost always induces TNF tolerance in recent experiments (J. Günther, Institute of Clinical Chemistry, MHH; personal communication).

Another factor which may well be important for the different behavior of individual monocyte preparations under the same experimental conditions is the genotypes of the blood donors. Since blood was donated anonymously, the only certain information about the respective persons is that they were healthy and thus eligible to donate blood for medical purposes. It is therefore conceivable that the heterogeneous reactions of the different monocyte preparations

towards stimulation with a low dose of TNF may be due to genetic differences. To address this issue, it would be necessary to repeatedly perform the experiments with monocytes derived from an individual whose cells have already proven to be capable of developing a TNF tolerant phenotype. If samples from such an individual could be rendered tolerant repeatedly over time and across several monocyte preparations, then TNF tolerance would most likely be a matter of genetics. On the other hand, if repeated monocyte preparations from one individual exhibited heterogeneity in regard to their ability to attain a TNF tolerant phenotype, other, most likely experimental factors (e.g., the exact concentration and activity of TNF, rapidity of the isolation procedure, freshness of the blood, immune status of the donor) would account for this form of immunological tolerance. As mentioned above, newer experiments suggest that the TNF concentration may truly be the most important factor in the development of tolerance, and that the biological activity used herein could have been too low to exert the desired effect in primary human monocytes. Further work will be necessary to prove this observation, and it will be interesting to determine whether other factors are involved as well.

4.1.3 TNF-inducible gene families in primary monocytes

For the work presented here, the gene expression data obtained were additionally analyzed to identify novel genes or gene groups induced by stimulation with TNF in primary human monocytes (Figure 10). Although a large number of targets of TNF signaling have been described, to date no group has assessed TNF-induced gene expression patterns in human monocytes by transcriptome analysis. The data reveal that most of the genes induced belonged to the large groups of genes regulating signal transduction, the immune response, and proliferation. All of these functions of TNF are well-known and most of these genes have already been described to be induced by this cytokine (15,174). A large number of genes involved in the prevention of apoptosis was induced as well, correlating with the pro-survival role of TNF under normal cellular conditions (174). Genes encoding proteins involved in adhesion and chemotaxis, a crucial immunological function of monocytes, were also found to be induced, as were those giving rise to proteins involved in cellular metabolism and transport mechanisms. In order to draw conclusions concerning the potential functions of newly identified TNF-induced genes, further experiments will be necessary to confirm the results obtained by gene expression analysis at the protein level.

4.1.4   Conclusions

The observations discussed above lead to many open questions: Is TNF tolerance in primary monocytes, at least under the experimental conditions applied, only a transient phenomenon that is easily overcome within a short period of time? If so, would pre-stimulation with a higher dose of TNF have lead to the development of a more robust form of tolerance? Or is the notion that monocytic TNF tolerance exists an artifact generated by the use of the THP-1 cell line? With the data presented in this work, these questions are not easy to answer. Undoubtedly, some monocyte preparations exhibited IL-8 patterns resembling TNF tolerance at the protein or the mRNA level. The questions about the potentially transient nature of TNF tolerance in this context and about the influence of the dose of TNF used for pre-stimulation of the cells can only be addressed at the experimental level. Further experiments are needed to show which factor(s) was (were) responsible for the contradictory data presented in this work.

Interestingly, if the ability or resistance of monocytes to undergo the processes leading to the development of TNF tolerance really was determined by their genetic background, this may as well have important implications in the clinic. Sepsis is a severe complication frequently acquired by patients treated in intensive care units (175). The most notable characteristic of late sepsis is immunoparalysis, leading to the inability of the patient's immune system to react properly to bacterial infections (18,30,34). As a result, at least 20 – 30% of patients die as a consequence of this disease (33,34,175). The role of TNF in the development of immunoparalysis during sepsis is controversial (18,30). If TNF is indeed involved in the development of immunoparalysis during late sepsis, the factors enabling monocytes to acquire a TNF tolerant phenotype could be highly important. It may be purely coincidental that a certain proportion of sepsis patients die of this disease, and that the experiments performed in this study revealed that TNF tolerance could be induced only in a few monocyte preparations. However, it cannot be ruled out that individuals with a genetic background enabling the development of TNF tolerance may additionally be more susceptible to the detrimental effects of septic processes than others. If this conclusion proved to be valid, the role of TNF tolerance in sepsis would be distinctly different from that of endotoxin tolerance, as isolated human monocytes can be readily rendered tolerant to LPS (176), and reduced cellular reactivity towards LPS stimulation mainly serves for prognostic purposes in already septic patients (29,35). In this context it would be highly important to better understand the mechanisms of TNF tolerance and learn about the factors enabling monocytes to overcome this stimulus.

Currently, experiments are being performed to determine the percentage of monocyte preparations that can be induced to exhibit an IL-8 expression pattern resembling that seen in TNF tolerant THP-1 cells. Another study focuses on collecting monocyte material from patients suffering from severe sepsis. These samples will be analyzed by gene expression analysis and compared with the existing data presented here. Together, these experiments should shed light on the role of TNF tolerance during the development of immunoparalysis in sepsis.

4.2   Monocyte differentiation

Besides modulating the immune response to pathogenic infections by producing proinflammatory cytokines and chemokines upon activation, another important function of monocytes is their ability to give rise to tissue macrophages (1). Macrophages are the first responders to infectious processes and exhibit a high phagocytic activity following stimulation. The differentiation process giving rise to macrophages is tightly regulated by a multitude of different transcription factors (1,113). C/EBPβ, for example, has been described to be upregulated dramatically during monocytic differentiation (71-73). However, the exact role of this transcription factor remains unclear as C/EBPβ ko mice contain fully differentiated, yet functionally impaired, macrophages (137). This study was thus aimed at gaining further insight into the role of C/EBPβ during the process of monocytic differentiation.

4.2.1   Regulation of C/EBP proteins

The premonocytic cell line THP-1 was chosen for the initial experiments of this project. THP-1 cells react to stimulation with PMA by acquiring a macrophage morphology and have been widely used as an accepted model to study differentiation processes (118). As expected, PMA treatment induced differentiation of the cells even at low nanomolar concentrations. Virtually all THP-1 became polygonal, flattened, and amoeboid and formed colony-like clusters that could be easily visualized by light microscopy (Figure 11). Analysis of nuclear cell extracts from THP-1 differentiated this way revealed that C/EBPβ was massively upregulated in a time-dependent manner (Figure 12). This is in accordance with previous findings describing differentiation-induced upregulation of either C/EBPβ protein or mRNA in monocytic cells (71-73).

Conflicting data exists regarding the role of C/EBPα during monocytic differentiation (1). The experiments performed for this study show that the two isoforms of C/EBPα, p42 and its inhibitor p30, were regulated differentially when THP-1 were stimulated with PMA (Figure

13). While p42 was slightly down-regulated or remained constant compared to controls, p30 was induced concomitantly. The upregulation of C/EBPα p30, however, was markedly lower than that seen for all three isoforms of C/EBPβ under the same conditions. Maybe the opposing regulation of the two C/EBPα isoforms observed in this work is the reason why previous literature presented conflicting data regarding the role of C/EBPα during monocytic differentiation. For example, C/EBPα was reported to be induced in several cell lines by stimulation with retinoic acid (RA) (127), while its expression was reduced during the PMA-induced monocytic differentiation of 32D cells (72). The data presented here indicate that C/EBPα is differentially regulated during monocyte maturation, with an induction of the transcriptionally inactive isoform p30, potentially inhibiting C/EBPα p42 activity.

Analysis of the distribution of C/EBPα and β within the cellular compartments revealed that only the large isoforms of both transcription factors could be detected in the cytoplasm of THP-1 cells (Figure 14). Nuclear expression of these proteins, however, was much more pronounced as verified by western blot. Interestingly, neither C/EBPβ LIP nor C/EBPα p30 could be detected in the cytoplasm (data not shown). The cytoplasmic expression patterns of C/EBPα p42 and C/EBPβ LAP*/LAP resembled their regulation in the nuclei of THP-1 cells, with p42 being down-regulated and LAP*/LAP expression being induced during PMA-dependent differentiation. Especially the very weak expression of C/EBPβ in the cytoplasm might indicate that its presence there is only a side effect of its dramatic upregulation, as it could not be detected in non-stimulated control THP-1. This is in accordance with a previous report demonstrating that all C/EBP family proteins contain a nuclear localization signal in their BD, indicating that these transcription factors are constitutively nuclear (177). It is completely uncertain why neither small isoform was detectable in the cytoplasm, especially as they were found to be upregulated in the nucleus upon PMA stimulation. Maybe newly translated p30 and LIP are shuttled to the nuclei in a faster manner than the large isoforms. No literature exists to explain this unexpected finding as all isoforms contain the BD comprising the nuclear localization signal (177). The results presented here imply that the C/EBP TADs or RDs present in the large C/EBPα and β isoforms may affect nuclear translocation of the protein in some way, retaining p42 and LAP*/LAP in the cytoplasm for a certain time following translation, while p30 and LIP are shuttled to the nucleus immediately.

4.2.2 Ratio alterations

Analysis of the modulation of C/EBPα and β expression during monocytic differentiation of premonocytic THP-1 cells revealed that the large and small isoforms of both transcription factors are differentially regulated during this process. C/EBPβ LIP lacks the TAD domains

present in both LAP* and LAP and is thus a transcriptional repressor able to bind DNA and to heterodimerize with large C/EBP isoforms, thereby inhibiting their function (88). C/EBPα p30 is likewise able to inhibit the p42 isoform and thus attenuate target gene expression (178). The data presented in this work demonstrate that C/EBPβ LAP* and LAP expression was dramatically augmented during PMA-induced monocytic differentiation (Figure 12). LIP was induced as well, the magnitude of induction, however, was considerably lower than that of the two large isoforms. Further analysis of this observation led to the finding that the C/EBPβ LAP/LIP ratio increased greatly during differentiation. This effect was far more dramatic than that seen in non-stimulated control cells, in which only a slight increase of the LAP/LIP ratio over time was observed. Remarkably, the time course of ratio alterations in PMA-stimulated and control cells was markedly different. While in control THP-1 cells LAP/LIP increased progressively over the period of 72 h, a slight increase in the ratio was observed already 6 h after the addition of PMA. After 24 h, the induction of LAP* and LAP over LIP had already reached a high value that was then kept remarkably constant over the following 2 days. Even after 72 h, PMA-stimulated THP-1 cells contained a considerably higher ratio than non-stimulated control cells. Since the induction of the LAP/LIP ratio by PMA was rapid, it is conceivable that the alteration of this factor within the cell determines and stabilizes its macrophage fate. This implies that C/EBPβ is involved in the determination of the differentiation process, and that the transcriptionally active isoforms of this transcription factor are necessary. Thus, LAP* and LAP are induced to a far larger extent than the inhibitory isoform LIP.

It has been reported that in hepatocytes, LIP can inhibit LAP*/LAP function even at substoichiometric levels (88). Another report noticed, however, that a molar excess of LIP was necessary to inhibit the function of the large C/EBPβ isoforms in B cells (68). No such data are available for cells of the myeloid lineage in this regard, although it has been demonstrated that upon overexpression in the premonocytic cell line U937, LIP inhibits C/EBPβ-induced transactivation of the HIV-1 promoter in a dose-dependent manner (179). Thus, without further experiments it is difficult to estimate the effect the observed ratio alteration exerts on the transcriptional activity of C/EBPβ in differentiating THP-1. However, it is likely that this dramatic alteration of the LAP/LIP ratio serves to ensure that transcriptionally active C/EBPβ is present within the cell at a level overcoming the inhibitory effects of LIP. In this context it is important to note that in normally proliferating THP-1 cells, LIP is expressed at a notably higher level than both LAP* and LAP (Figure 21C). Thus,

in order to ensure proper C/EBPβ function, it may be necessary to dramatically raise the amount of LAP* and LAP proteins in the cell, thereby modulating the LAP/LIP ratio.

The influence of C/EBPα on monocytic differentiation is a controversial topic (1). While there are reports indicating that it is down-regulated during this process (72), others have shown that C/EBPα can reprogram cells of different lineages toward a monocyte/macrophage-like phenotype (99,146,147). New data presented in this work show that the inhibitory p30 isoform was induced during the differentiation process, while C/EBPα p42 expression remained constant or was slightly reduced (Figure 13). Calculation of the p42/p30 ratio revealed that this parameter was reduced progressively over the course of PMA stimulation, while it remained at the initial baseline level in control cells. In contrast to the C/EBPβ ratio alteration, which was induced dramatically 24 h after PMA treatment, the p42/p30 ratio decreased gradually over time. From this observation it is likely that expression of transcriptionally active C/EBPα is not detrimental to the early phase of monocytic differentiation but has to be attenuated for full development of the macrophage phenotype. Interestingly, it has been demonstrated that C/EBPα blocks PU.1 activity, thereby inhibiting differentiation towards macrophages (123). The slow regulation of C/EBPα during differentiation may possibly account for the increasing importance of PU.1 during later stages of this process.

Overall, these data demonstrate that there is a shift from transcriptionally inactive to active C/EBPβ during monocytic differentiation, while C/EBPα function is concomitantly attenuated by increasing p30 over p42 expression. Accordingly, C/EBPβ potentially plays an important role during the initial stages of the differentiation process, and the presence of C/EBPα does not appear to counteract establishment of this cell fate. It is important to note, however, that all C/EBPβ western blots presented in this work were exposed for considerably shorter times than those detecting C/EBPα in the same cell extracts. Even considering the probably different affinities of the two antibodies to their respective antigens, the expression level of C/EBPβ is almost certainly much higher than that of C/EBPα under all conditions assessed. Taking into account that the different isoforms of C/EBPα and β can form heterodimers, C/EBPα p42 is probably mostly inactive in normal THP-1 judging from the high level of LIP present within the cell. Conversely, the dramatic increase of LAP* and LAP most certainly easily exceeds the relatively weak induction of C/EBPα p30, which could potentially inhibit the large C/EBPβ isoforms as well. In summary, these observations indicate that transcriptionally active C/EBPβ is dramatically induced in differentiating THP-1 cells, while C/EBPα activity is attenuated as the cells progress towards a macrophage-like phenotype.

4.2.3 Proliferative activity during differentiation

It is generally accepted that immature progenitor cells undergo cell division, and that the proliferation rate decreases as these cells differentiate towards a more mature phenotype (1). Thus, even though continued proliferation does not necessarily inhibit monocytic differentiation, cell growth usually slows as cells mature (156). Consistently, incubation of THP-1 cells in the presence of PMA led to a dramatic reduction of cellular proliferation (Figure 15). This is in accordance with previous publications demonstrating that PMA induces cell cycle arrest in various cell lines. Growth inhibition induced by this stimulus in THP-1 is dependent on the production of reactive oxygen species (ROS) (167), and several groups suggested that the anti-proliferative effect of PMA depends on activation of p21$^{Waf1/Cip1}$ *via* MAPK signaling in differentiating cells (180-183). It is interesting to note that growth inhibition was observed starting 48 h after the addition of PMA to the cell culture medium. In contrast, after 24 h of PMA treatment, the cells had grown to the same extent as non-treated control THP-1. Even a slight increase in proliferation was visible at this point of time. As no earlier time points were analyzed in this experimental setup, it is difficult to estimate whether this weak increase in cell growth was the result of maturation divisions that might have occurred during the initial stages of differentiation. Maturation divisions have been described in the differentiating cell line HL-60 (168), while no data is available on premonocytic THP-1 cells. Further experiments analyzing earlier time points after the addition of PMA would be necessary to determine whether maturation divisions are induced in differentiating THP-1. Since the cells in the experiment presented here were not synchronized prior to the proliferation assay, it is also conceivable that no differences could be observed after 24 h because an equal amount of cells was actively cycling at the time of seeding. THP-1 have a doubling time of 35-50 h (184) and thus most likely do not immediately start into a new cell cycle after concluding the previous round of cell division. The observation that an inhibition of cellular proliferation cannot be detected until 48 h, however, points toward an involvement of the two large C/EBPβ isoforms LAP* and LAP in this process. C/EBPβ was strongly induced 24 h after the addition of PMA, which is the point of time when the LAP/LIP ratio was shifted towards the larger isoforms. Taking this into account could imply that LAP* and LAP were involved in PMA-induced growth inhibition, as the latter was observed only after the shift of the LAP/LIP ratio had occurred.

Further experiments conducted for this study revealed that overexpression of C/EBPβ indeed significantly inhibited proliferation of HeLa cells (Figure 16). The construct used for this experiment contained the complete (FL) *CEBPB* gene, potentially giving rise to all three

isoforms LAP*, LAP, and LIP. However, western blot analysis revealed that, like in THP-1 (Figure 26), transfection of this plasmid into HeLa mainly produced LAP* (data not shown). This indicates that in the context of the pTracer vector backbone lacking the normal 5'-UTR normally present in the *CEBPB* gene, C/EBPβ is preferentially translated from the first AUG start codon. Taking this observation into account, the overexpression of LAP* markedly inhibited the proliferation of HeLa cells. This further supports the notion that the PMA-induced growth inhibition seen in THP-1 is mediated by the induction of C/EBPβ LAP* and (presumably) LAP. The time course of events suggests that C/EBPβ is first induced roughly 24 h after stimulation, leading to reduced proliferation rates after 48 h. LAP has already been described to inhibit cell cycle progression in different cell types (102,106). The data presented here support these reports and show that proliferation is inhibited by C/EBPβ LAP* in the human epithelial cell line HeLa. As the inhibition of THP-1 proliferation coincides with upregulation of both large isoforms of C/EBPβ, it is likely that LAP* and LAP are responsible for this effect.

To further understand the role of C/EBPβ during myeloid proliferation, C/EBPβ ko and wt macrophage-like cells that have previously been characterized as macrophages were used for further experiments (137). Both the cell counts and proliferation assays revealed that C/EBPβ ko cells consistently had a higher growth rate than C/EBPβ wt macrophage-like cells (Figure 18). This observation is in accordance with the data obtained in C/EBPβ-transfected HeLa cells, wherein overexpression of C/EBPβ in general, and LAP* in particular, inhibited the proliferative potential of these cells (Figure 16). In addition, C/EBPβ ko cells were found to start, and conclude, cell cycle progression more rapidly than C/EBPβ wt cells. After synchronization, C/EBPβ ko macrophage-like cells attained a high proportion of actively cycling cells after only 6 h, and they had already reached the resting phase of the cell cycle (G_1G_0) when C/EBPβ wt cells massively started cycling (Figures 18, 19). It remains unclear why C/EBPβ wt cells could be synchronized more readily than C/EBPβ ko cells. As these experiments demonstrate, C/EBPβ wt macrophages were more susceptible to both contact inhibition and serum withdrawal-induced growth inhibition, while C/EBPβ ko cells barely reacted to these conditions applied to synchronize the cell population. Possibly C/EBPβ is necessary to mediate the signals necessary to inhibit cell cycle progression. On the other hand, the cycling indices of both cell lines were similar after synchronization. In summary, these experiments demonstrate that C/EBPβ exerts an anti-proliferative effect in C/EBPβ wt macrophage-like cells, thus explaining the consistently enhanced proliferative activity observed in C/EBPβ ko cells.

To confirm the proliferation data obtained in C/EBPβ wt and ko cells, THP-1 were used in a knock-down approach and subsequently monitored by proliferation assay. However, attenuation of C/EBPβ levels by siRNA in these cells led to reduced, not enhanced proliferation rates compared to controls (Figure 21). This finding was completely surprising as HeLa cells overexpressing C/EBPβ slowed cellular growth (Figure 16). The observation that knock-down of C/EBPβ in THP-1 inhibited proliferation further contrasts with the findings in C/EBPβ ko macrophage-like cells which exhibited higher proliferation rates than C/EBPβ wt cells (Figures 18 and 19). Of course the most obvious differences between C/EBPβ ko macrophages and THP-1 cells transfected with C/EBPβ siRNA is the fact that the effect induced in THP-1 is transient, while it is stable in C/EBPβ ko cells. Additionally, the knock-down of a protein is not nearly as efficient as the knock-out of a gene, wherein the latter case no residual protein expression is detectable. Direct comparison of THP-1 and C/EBPβ wt cells, however, revealed that the isoform expression patterns of C/EBPβ are markedly different in these two cell lines. While in THP-1, LIP expression dominated over the two large isoforms, C/EBPβ wt macrophage-like cells contained mainly LAP. Most likely these distinct expression profiles are a result of the different maturation statuses of these cell lines. While THP-1 represents an immature monocytic cell capable of differentiating towards a macrophage-like phenotype (118), C/EBPβ wt cells have been characterized as a cell line exhibiting many properties of mature macrophages (137). The observed difference of C/EBPβ expression patterns in these two cell lines means that in normally growing THP-1, LIP most likely inhibits the transcriptional activity of LAP* and LAP. In contrast, LAP probably dominates over the miniscule LIP expression detected in C/EBPβ wt cells. LAP itself has been implicated to inhibit cell cycle progression in various cell types (102,106). The data presented in this study further point towards this role of LAP. Judging from the different C/EBPβ isoform expression patterns in THP-1 and C/EBPβ wt cells, the contrasting effects that the knock-down and knock-out of this protein, respectively, have on these cells' proliferation rates possibly makes sense. In THP-1, applying C/EBPβ siRNA mainly leads to a reduction of the LIP protein level. Less LIP implies that the large isoforms of C/EBPβ might have an enhanced potential to exert their effects. If these effects are the inhibition of cell cycle progression, then C/EBPβ knock-down in THP-1 would lead to a reduction of proliferation rates. On the other hand, the knock-out of C/EBPβ in mice from which the C/EBPβ wt cell line has been established mainly leads to the loss of LAP expression. This in turn implies that the LAP-mediated inhibition of cell cycle progression might be eased, leading to higher proliferation rates in C/EBPβ ko macrophage-like cells. Together, these

data strongly point towards an important role of the different C/EBPβ isoforms in cellular proliferation, and they may help prove the theory that LIP is an antagonist to LAP-mediated growth inhibition as suggested in earlier studies (101,106). Further experiments knocking down LAP expression in C/EBPβ wt cells would be necessary to definitely prove this concept.

4.2.4   C/EBPβ influences and stabilizes Rb levels during differentiation

All data concerning proliferation presented herein indicate that C/EBPβ has an effect on the proliferation of cells of the myeloid lineage. In order to gain a better understanding of this phenomenon at the molecular level, Rb phosphorylation of differentiating THP-1 cells was assessed in the presence or partial absence of C/EBPβ. By binding to the transcription factor E2F1, Rb is a negative regulator of cell cycle progression that has also been implicated in monocytic differentiation (109,158,159). Phosphorylation of this protein at up to four serines releases E2F1 from the complex and thereby enables expression of genes necessary for G_1-S transition (157). For this study, phosphorylation of Rb at Ser^{608} and Ser^{795} was analyzed in PMA-stimulated THP-1 cells. Additionally, C/EBPβ was knocked down by use of a specific siRNA sufficient to reduce both C/EBPβ protein and mRNA levels. These experiments revealed that phosphorylation of Rb at the two serines analyzed was significantly reduced in differentiating THP-1 (Figure 20). Dephosphorylation of Rb was observed 24 h after the start of PMA stimulation, coinciding with the point of time at which THP-1 cells started to exhibit inhibition of cell growth (Figure 15). Attenuation of C/EBPβ levels by specific siRNA affected baseline Rb phosphorylation levels as these were markedly reduced in unstimulated THP-1. A PMA-induced decrease of Rb phosphorylation was observed in these cells as well, indicating that regulation of Rb functionality was not affected in cells with reduced levels of C/EBPβ. Surprisingly, the level of total Rb was also reduced in all samples differentiated with PMA. Previous data from primary human bone marrow progenitors differentiating towards mature monocytes indicate that Rb levels remain constant during this process and that only the phosphorylation status of this protein is modulated (160). It is important to note, however, that the publication cited assessed the maturation of progenitors towards monocytes, while in the data presented here the regulation of Rb during differentiation of premonocytic THP-1 towards a macrophage-like phenotype was investigated. Possibly the contrasting findings are due to this difference. Another striking observation made in the experiments presented here is that despite being attenuated, Rb expression in control-transfected cells stimulated with PMA was still readily detectable. In combination with the phosphorylation data this indicates that hypophosphorylated Rb remains present in these differentiating cells.

Because upon PMA treatment, total Rb was barely detectable in THP-1 transfected with C/EBPβ siRNA, C/EBPβ appears to exert a stabilizing effect on hypophosphorylated Rb within PMA-stimulated cells. Thus, C/EBPβ serves to ensure that hypophosphorylated Rb, which is a strong repressor of cell cycle progression, is retained within the cell during the differentiation process.

The experiments presented here further demonstrate that the total Rb level was reduced in cells transfected with siRNA directed against C/EBPβ regardless of PMA treatment. The implications of this observation are not clear and could indicate that Rb expression is regulated by C/EBPβ. Computational analysis by use of the software TFSEARCH confirmed the presence of several putative C/EBP binding sites in the human *RB1* promoter, indicating an involvement of C/EBPβ in Rb expression. Coincidentally, a CCAAT box motif has been identified in the promoter region of *RB1* (185) which is, however, different from those identified by bioinformatical analysis. Further experiments will be necessary to prove whether C/EBPβ is truly involved in the regulation of Rb expression in THP-1 cells. Interestingly, however, preliminary results obtained in HeLa cells indicate that overexpression of C/EBPβ indeed enhances activation of a co-transfected reporter plasmid under regulation of the *RB1* promoter (R. Huber, Institute of Clinical Chemistry, MHH; personal communication). Together, these findings may imply an important role of C/EBPβ in the regulation of Rb expression in monocytic cells.

It is important to note that reduced Rb levels, regardless of this protein's phosphorylation status, would mean that more E2F1 could be free to promote cell cycle progression. However, this contrasts to proliferation data of THP-1 cells transfected with the C/EBPβ siRNA (Figure 21). Additionally, the impact of reduced Rb levels is difficult to predict as E2F1 protein levels were not assessed in this study. It is possible that expression of this transcription factor is also reduced upon C/EBPβ knock-down as CCAAT box motifs are present within the murine *E2f1* promoter as well as its human homolog (186), and bioinformatical analysis confirmed the presence of at least 3 C/EBPβ binding sites in the human *E2F1* promoter sequence (data not shown). As in the case of the *RB1* promoter region, however, the published CCAAT box motifs published by Hsiao *et al.* do not correspond to those identified by use of the TFSEARCH software. A definite conclusion is thus hard to reach judging from the Rb data presented in this study. Further experiments will be necessary to determine the effects of the observed reduction of Rb level and phosphorylation in C/EBPβ knock-down THP-1 samples.

4.2.5 Proliferation rates determine macrophage morphology

The one striking observation when working with C/EBPβ wt and ko macrophage-like cells was their markedly distinct morphological appearance (Figure 17). As noted before, monocytic differentiation towards a mature phenotype usually coincides with morphological changes similar to those seen in PMA-stimulated THP-1 cells (Figure 11). Consistently, C/EBPβ wt cells exhibited a typical macrophage morphology, with over half of the cells being flattened, spindle-shaped, amoeboid, or polygonal. This phenotype, however, was barely observable in C/EBPβ ko macrophage-like cells as almost all of these cells were round despite being strictly adherend. The C/EBPβ ko cell line re-transfected with C/EBPβ was found to display a morphological phenotype in between the C/EBPβ wt and ko cells, i.e., a lot more cells were flattened or polygonal than in C/EBPβ ko cells, but this number was significantly lower than in C/EBPβ wt cells. Thus, these cells expectedly exhibited an intermediate phenotype. Taken together, these data provide evidence for the involvement of C/EBPβ in the determination of macrophage morphology.

In order to assess whether the different proliferation rates accounted for the differences in C/EBPβ wt and ko morphology, serum withdrawal experiments were conducted with these cell lines. The results of these experiments appear to confirm this hypothesis (Figure 22). Since serum withdrawal (which deprives cells of growth factors) induces apoptosis (187), the serum concentration was not reduced below 0.5% FCS in the course of these experiments. In the presence of a relatively normal concentration of FCS (5%), both the C/EBPβ wt and ko cells appeared as observed in previous experiments: C/EBPβ ko cells were overwhelmingly round, while C/EBPβ wt cells constituted a diverse population of flattened/polygonal cells (macrophage morphology), and of round cells like the ones observed in the C/EBPβ ko cell line. Serum withdrawal did not dramatically affect the appearance of C/EBPβ wt cells. In the case of C/EBPβ ko cells, however, a striking effect was apparent. Upon reduction of the FCS concentration to 2% or even 0.5%, a higher proportion of cells successively adopted a macrophage morphology. These observations were confirmed by counting spindle-shaped/polygonal and round cells. Together, these data imply that the morphology of these mouse macrophages is mainly defined by their proliferation rates.

Of course this effect may be due to serum withdrawal-induced differentiation of the cells as has been described for neuroblastoma cells (188). As no such effects are known in the context of monocytic differentiation, it is however much more likely that the cells appearing round in the microscope images are in the active phase of the cell cycle or have just completed a cell division. In contrast, cells that appear like macrophages, i.e., are polygonal,

flattened, or spindle-shaped, are presumably in the resting phase of the cell cycle. In order to proceed to the S phase, the data presented herein indicate that they may have to become round again. As C/EBPβ ko cells consistently have a higher proliferation rate than C/EBPβ wt macrophages, the proportion of round cells is higher in former cell line. In these C/EBPβ ko cells, the resting phase G_1G_0 might thus be too short to allow for the formation of spine-like protrusions or other morphological alterations that would make them resemble typical macrophages. C/EBPβ may therefore only have an indirect effect on cellular morphology: by inhibiting proliferation, it potentially allows the cells to adopt a macrophage-like appearance. Thus, C/EBPβ ko morphology is determined by a higher proliferation rate, which in turn is enabled by relieving the block C/EBPβ normally exerts on cell cycle progression.

4.2.6   Compensatory mechanisms of other C/EBP family members in C/EBPβ ko macrophage-like cells

The fact that macrophages are present in C/EBPβ ko mice implies that this transcription factor is not essential for the development of this cell type, although macrophage function is partially impaired in these animals (137). Already in the publication by Gorgoni *et al.* describing the generation of the C/EBPβ ko macrophage-like cell line, the question was raised whether other C/EBP family members might compensate for the loss of C/EBPβ, enabling progenitor cells to differentiate towards macrophages. They find that both the *CEBPD* and *CEBPE* mRNAs as well as the corresponding proteins C/EBPδ and ε were increased in C/EBPβ ko cells, while no change was observed in regard to the levels of C/EBPα. The data presented in their work is not complete, though. No reliable loading controls are shown, and not all of the potentially relevant C/EBPα and ε isoforms are visible in their western blots. Protein extracts of C/EBPβ wt and ko cells were thus analyzed for C/EBP α and ε expression in this work (Figure 23). From these experiments it is obvious that C/EBPα levels were slightly augmented in C/EBPβ ko macrophage-like cells, while C/EBPε was present at similar levels as in C/EBPβ wt cells. In the case of C/EBPα, the increase was observed for both the p42 and p30 isoforms, although the difference in p30 expression appeared to be higher and thus potentially more relevant. Of note, the regulation of C/EBPα upon PMA-stimulation of C/EBPβ wt and ko cells was markedly different from that observed in differentiating THP-1 (Figure 13). Although p42 was apparently slightly reduced upon stimulation with PMA as well, p30 did not increase under these conditions in either C/EBPβ wt or ko macrophage-like cells. This difference between the premonocytic cell line THP-1 on the one hand and C/EBPβ wt or ko macrophages on the other hand might be due to their maturation status. The C/EBPβ wt and ko cells can be regarded as fully differentiated cells that possibly do not further react

to stimulation with PMA at all at the C/EBP expression level, while THP-1 cells are premonocytic progenitors that can be differentiated towards macrophage-like cells (118,137). It may thus not be surprising that the regulation of C/EBPα differs in these cell lines.

Another important observation is that compared to C/EBPβ, C/EBPα protein detected in the C/EBPβ wt and ko cells was expressed at a significantly lower level. Of course it is difficult to compare expression levels of two proteins detected by two different antibodies in western blots. Different binding affinities might account for apparently divergent expression levels, and this effect cannot be fully ruled out in these experiments either. However, the exposure times of the western blot membranes detecting C/EBPα were dramatically longer than those detecting C/EBPβ (10 min as opposed to 25 sec, respectively). Therefore it is very likely that C/EBPβ is indeed expressed at much higher levels than C/EBPα in C/EBPβ wt cells. The upregulation of C/EBPα in C/EBPβ ko cells is not nearly as dramatic as the difference observed for C/EBPα and β in C/EBPβ wt cells. Even taking the possibility into account that some of that difference is due to the binding affinities of the two antibodies used, it is unlikely that the increased expression of C/EBPα in C/EBPβ ko macrophages is enough to counteract the consequences the loss of C/EBPβ in these cells exerts on their proliferation and morphology. This finding corroborates the generally accepted notion implying that C/EBPα most likely drives granulocytic differentiation at the expense of monocytic maturation, indicating that these two transcription factors have distinct functions (1,76).

Finally, as in THP-1 cells, C/EBPα expression was restricted to the nucleus in C/EBPβ wt and ko macrophage-like cells. As there were no observed differences in the level of C/EBPε, it is irrelevant that only two of the potentially four isoforms of this protein were detectable in these cells. Unfortunately from the data obtained it is impossible to tell which two isoforms were present in both C/EBPβ wt and ko cells. However, as these were not modulated in any way, it appears that this protein is most likely not involved in potential mechanisms rescuing C/EBPβ function in macrophage differentiation. In this context it is interesting to note that C/EBPε has been proposed to play a role in macrophage differentiation and function (84). The fact that this protein is expressed in C/EBPβ ko cells at similar levels as in C/EBPβ wt cells may account for their ability to adopt macrophage-like properties. In such a scenario it is unclear why C/EBPε is not upregulated in cells lacking C/EBPβ during differentiation. However, an induction of C/EBPε at an earlier time point during the development of the C/EBPβ ko cells cannot be ruled out. A similar effect was most likely seen in the C/EBPβ wt cells, where C/EBPβ expression was high and not modulated by PMA. This again indicates that, on the one hand, these cells do not react to this stimulus the same way as THP-1. On the other hand

the differential regulation of C/EBPβ in these macrophage-like cells and in THP-1 shows that modulation seen during the differentiation process may not be visible anymore in the mature cell. Thus, the role of C/EBPε during the maturation of C/EBPβ ko macrophage-like cells remains unclear.

4.2.7 Regulation of PU.1 expression in C/EBPβ macrophage-like cells

Apart from the family of C/EBP proteins, PU.1 belonging to the ETS transcription factor family has been implied to play an important role in the generation of monocytes/macrophages from immature precursor cells. Mice harboring a ko mutation in the *Sfpi1* gene are unable to produce cells of the myelomonocytic lineage and die early after birth due to their immune system's inability to cope with infections (131,132). Experiments in a cell culture setting have additionally revealed a crucial role of PU.1 in phorbol ester-induced differentiation of U937 cells (189,190). Since no data were available for the THP-1 cell line, first of all the regulation of PU.1 expression by PMA stimulation was assessed in this study. The experiments demonstrated that normally growing THP-1 cells did not express detectable amounts of this transcription factor (Figure 24). However, PMA-induced differentiation of THP-1 cells was accompanied by a strong induction of PU.1 expression. In addition, C/EBPβ expression was also dramatically elevated, and the magnitude of the effects appeared to be comparable (Figure 12). Three scenarios regarding the time course of these processes are conceivable: i) C/EBPβ and PU.1 are induced around the same time; ii) C/EBPβ is induced first and augments PU.1 expression; or iii) induction of PU.1 expression leads to the upregulation of C/EBPβ. To estimate the succession of events in PMA-stimulated THP-1, further experiments will be necessary to determine the time dependence of the upregulation of both transcription factors during monocytic differentiation in this model. Interestingly, no reports exist demonstrating an induction of PU.1 due to treatment with phorbol esters. PU.1 expression, however, has been linked to ATRA-induced differentiation only recently (130). One study further indicated that PU.1 phosphorylation is modulated during U937 differentiation, and that this phosphorylation is not accompanied by enhanced *SPI1* mRNA expression (189). As the induction of PU.1 expression has been mainly linked to the cellular differentiation status, physiological extracellular molecules that might augment PU.1 levels within the cell remain unknown (112). The data presented here are the first report of PMA-induced PU.1 expression in the human premonocytic cell line THP-1. As noted above, further experiments will be necessary to fully understand the mechanisms and time course of PU.1 induction in this system. However, both the dramatic upregulation of this transcription factor

in THP-1 presented here and data from the literature (189,190) imply that it fulfills a crucial role in the differentiation of these cells.

Several groups have demonstrated in *ex vivo* studies that hematopoietic progenitor cells isolated from PU.1 ko mice cannot be differentiated towards a monocyte/macrophage phenotype regardless of the stimulus used (133,134). The availability of macrophage-like cells from C/EBPβ ko mice indicates that a transcription factor other than C/EBPβ must be present to determine this phenotype. In their study, Gorgoni *et al.* suggested that PU.1 levels were similar in the C/EBPβ wt and ko macrophage-like cells established as a cell line (137). However, no data were presented to confirm this. Thus, the PU.1 levels were compared by western blot in protein extracts from C/EBPβ wt and ko cells. The data presented in this work demonstrate that PU.1 was indeed expressed in C/EBPβ ko macrophage-like cells (Figure 25). This implies that the reason why these C/EBPβ ko mice contain macrophages is the fact that progenitor cells are nevertheless able to express the crucial myeloid transcription factor PU.1. Interestingly, the observed PU.1 levels in C/EBPβ ko cells appeared to be lower than in C/EBPβ wt cells, especially when taking the loading control into account. However, this is not completely surprising. The *SPI1* gene contains C/EBP binding sites, and studies exist indicating that the PU.1 promoter is at least partly regulated by either C/EBPα or β (1,124,136). Loss of C/EBPβ would thus mean that one of the factors potentially regulating PU.1 expression is missing. Therefore C/EBPα, which is slightly upregulated in C/EBPβ ko cells, most likely rescues PU.1 expression in these cells. Since the slightly enhanced expression of C/EBPα in C/EBPβ ko macrophage-like cells potentially cannot completely rescue C/EBPβ functionality, PU.1 levels are lower than in C/EBPβ wt cells. These data indicate that PU.1 expression is directly regulated by C/EBPβ.

The hypothesis that C/EBPβ induces PU.1 in a direct manner was tested by overexpressing C/EBPβ in THP-1. Expectedly, PU.1 expression was induced 6 h after transfection of the cells with the C/EBPβ plasmid (Figure 26). Even though the upregulation of PU.1 was only slight compared to cells that had been mock-transfected without plasmid, the PU.1 level increased with the amount of overexpression plasmid introduced into the cells. Time course analyses had revealed that C/EBPβ was maximally expressed 6 h after transfection (data not shown). Overexpressed C/EBPβ was nevertheless able to induce PU.1 levels after such a short period of incubation. Thus, these experiments confirm a report that mentioned an observed upregulation of PU.1 in 32D cells transfected with an inducible form of C/EBPβ (124). Additionally, the regulation of the PU.1 promoter by C/EBPβ has also been demonstrated (136). In summary, these findings corroborate and extend previously published

reports linking PU.1 expression to C/EBPβ. The experiments presented here further confirm the assumption that the loss of C/EBPβ in C/EBPβ ko macrophage-like cells is most likely responsible for the reduction of PU.1 levels in the cells. Altogether, these results demonstrate that C/EBPβ is critical for full PU.1 expression.

4.2.8 Regulation of macrophage morphology in the absence of C/EBPβ or PU.1

One of the key functions C/EBPβ exerts during monocytic differentiation appears to be the inhibition of proliferation, leading to morphological adjustments. At least in C/EBPβ wt and ko macrophage-like cells, this link is evident. In order to better understand the role of C/EBPβ during differentiation-induced morphological changes, further experiments were conducted in THP-1. Surprisingly, the specific knock-down of C/EBPβ in this cell line was not sufficient to inhibit PMA-induced flattening (Figure 27). This is even more striking as both protein and mRNA data showed that transfection with siRNA efficiently inhibited C/EBPβ expression (Figure 20). Of course the knock-down of C/EBPβ in THP-1 leaves a residual protein level of about one third of the original level and is thus not nearly as effective as the stable knock-out of this gene in the mouse macrophages used in other experiments. It is therefore conceivable that the remaining C/EBPβ protein present in the cells was still able to fully exert its function regarding the differentiation-associated alteration of cellular morphology. However, if C/EBPβ was involved in the regulation of cellular appearance, one would expect that the siRNA-transfected cells would look either different than those transfected with control siRNA, or that a reduced number of cells would adopt morphological changes due to the reduced amount of C/EBPβ present within the cells. No such effect was apparent upon transfection with C/EBPβ siRNA, though. Therefore, the most likely explanation for these findings is that C/EBPβ itself is not directly involved in PMA-induced morphological changes in THP-1 cells. The involvement of this transcription factor in the morphology of mouse macrophage-like cells is possibly only evident because no PMA was used in these experiments (Figures 17, 22). As PMA is a strong inhibitor of cell cycle progression, it is conceivable that this stimulus possibly overrides C/EBPβ-mediated effects in the knock-down experiments performed in THP-1 cells.

The disparity of the results obtained in C/EBPβ wt and ko macrophages and in THP-1 cells raised the question as to what the effect of PMA would be on C/EBPβ wt and ko morphology. As shown before, C/EBPβ ko cell morphology is dependent on the cells' proliferative capacity. PMA, on the one hand, is a strong inhibitor of cell cycle progression in the THP-1 cell line (167). On the other hand, PMA treatment of C/EBPβ wt cells did not induce the

changes in C/EBP expression patterns observed in THP-1 (Figure 23). Therefore, experiments monitoring C/EBPβ wt and ko morphologies were conducted in the presence of PMA (Figure 28). C/EBPβ wt cells only slightly reacted to PMA stimulation as the percentage of cells with macrophage morphology barely increased even at high PMA concentrations. In C/EBPβ ko cells, however, a dramatic increase of flattened and spindle-shaped cells was observed upon treatment with PMA. Even a low dose of this stimulus led to visible increases in the percentage of macrophage morphology in C/EBPβ ko cells. These data demonstrate that, based on morphology, PMA is capable of exerting an effect on murine macrophage-like cells. The C/EBPβ ko cells differentiated with PMA resembled those present after serum withdrawal (Figure 22). Thus, as in THP-1 cells, PMA most likely inhibits cell cycle progression in C/EBPβ macrophage-like cells, thereby inducing morphological changes. These changes are independent of C/EBPβ expression or the regulation of either C/EBPα or ε, as those were either not or only weakly affected by PMA stimulation (Figure 23). As mentioned above, THP-1 cells and the macrophage-like cells used here can only be compared to a limited extent as the former are premonocytes, while the latter are mature macrophages based on antigen expression (118,137). The finding that C/EBPβ wt cells only slightly changed their morphology in response to PMA stimulation is possibly due to the presence of high levels of C/EBPβ already before stimulation. In contrast, these amounts of C/EBPβ in general and of LAP* and LAP in particular are only induced by PMA in THP-1 (Figure 12). As no induction of LAP* and LAP occurs in C/EBPβ wt cells treated with PMA, no further cell cycle inhibition may be induced, explaining why these cells do not significantly change their morphologies under these experimental conditions. Together, these data indicate that PMA does have an effect on mature macrophages, yet due to the results obtained in the C/EBPβ ko cell line, these effects appear to be independent of C/EBPβ expression. The experiments further demonstrate that the elevated level of C/EBPα in C/EBPβ ko cells (compare Figure 23) was not sufficient to rescue the normal function of C/EBPβ. A high expression of C/EBPβ, in turn, presumably exerts effects similar to those of PMA. In this context it would be highly interesting to determine the effects of C/EBPβ overexpression in THP-1 cells. For this study, such experiments were attempted, however the transfection efficiency of the overexpression plasmids was too low (data not shown). Due to this difficulty, no data could be generated to determine if THP-1 cells overexpressing LAP* or LAP would adopt a macrophage morphology without PMA stimulation. Further experiments are underway to establish stably transfected THP-1 cells. These analyses should then be able to determine the influence of C/EBPβ expression on THP-1 morphology.

C/EBPβ has been demonstrated to bind to and enhance PU.1 transcriptional activity at the IL-1β and MD-2 promoters (140-143). Even though no direct interaction was demonstrated, a putative cooperativity of these two transcription factors also occurs at the promoter for *CHIT1* in differentiating THP-1 cells (73). One possible reason for the upregulation of C/EBPβ might thus be the enhancement of PU.1 function. Experiments using siRNA specifically attenuating PU.1 expression confirm the critical role of this transcription factor during PMA-induced monocytic differentiation of THP-1 cells (Figure 29). On a morphological basis, only the siRNA targeting *SPI1*, but not the *CEBPB* mRNA, inhibited flattening and the acquisition of an amoeboid shape in THP-1 stimulated with PMA. The efficacy of the PU.1 siRNA was confirmed by western blot. THP-1 cells transfected with PU.1 siRNA that were incubated with PMA exhibited a morphology that was strikingly different from that of normal THP-1 treated the same way: they were perfectly round, yet adherend. Normal THP-1 became amoeboid, flattened and formed aggregates upon PMA stimulation, and so did those cells transfected with C/EBPβ siRNA. Thus, most of the characteristics of the macrophage morphology were lost upon PMA treatment of PU.1 siRNA-transfected THP-1 cells. These experiments confirm that PU.1 expression is critical for the adoption of the macrophage phenotype in THP-1. Additionally, the PU.1 level appears to be of critical importance for PMA-induced morphological changes. The western blot showed that PU.1 expression was attenuated in THP-1 transfected with the corresponding siRNA, yet the extent of the knock-down was not as dramatic as that reached in C/EBPβ knock-down samples. Thus, a noticeable amount of PU.1 protein still appeared to be present in the cells despite the knock-down. However, even in the presence of PU.1, the reduction of its level was obviously enough to inhibit the formation of a typical macrophage morphology upon PMA treatment. Therefore, PU.1 is absolutely critical for the full PMA-induced differentiation of macrophages from THP-1 premonocytes.

4.2.9 Conclusions

In summary, the data presented in this work further enhance the understanding of monocytic differentiation. The use of siRNA confirms the necessity of PU.1 for the differentiation of monocytes, as reducing the level of PU.1 inhibits the formation of a macrophage morphology in the premonocytic cell line THP-1 stimulated with PMA. These data are in accordance with publications demonstrating that not only do PU.1 ko mice lack cells of the myeloid lineage, progenitor cells isolated from these animals cannot be differentiated towards a monocyte/macrophage phenotype either (131-134). Moreover, the absence of C/EBPβ during differentiation does not inhibit PMA-induced morphological alterations in THP-1. This may

indicate that in this cellular context, C/EBPβ mainly functions by binding to and enhancing PU.1 transcriptional activity. Cooperativity between these two transcription factors has been shown to play a role at the promoters of the IL-1β and MD-2 genes (140-143). Since such a cooperativity has been demonstrated, it is likely that it is involved in the regulation of other promoters as well, and possibly these promoters drive the expression of genes involved in cellular attachment and morphology.

Apart from modulating PU.1 activity, another main function of C/EBPβ appears to be the regulation of cell cycle progression during monocytic differentiation. The data presented herein indicate that LIP indeed counteracts the growth inhibitory function of LAP* and LAP. Such a mechanism has been proposed in numerous studies and cell types (56,101-103,106). Several modes of action have been suggested for the growth inhibitory effect of the large C/EBPβ isoforms. On one hand, they inhibit expression of proteins regulating cell cycle progression such as cyclin A2, c-Myc, or PCNA (103). On the other hand, C/EBPβ is able to bind Rb and presumably retains it in its hypophosphorylated form, thereby inhibiting cell cycle progression (103,107,108). Interestingly, PU.1 has also been reported to bind Rb (161). It is conceivable that Rb plays an important role in bringing C/EBPβ and PU.1 into close proximity, enabling complex formation and thus enhancing PU.1 transcriptional activity while inhibiting cellular proliferation at the same time. Furthermore, the observation that proliferation inhibition by serum withdrawal induces morphological changes similar to those induced by PMA in C/EBPβ ko macrophage-like cells is highly interesting. It further corroborates the theory that C/EBPβ mainly functions to inhibit cellular growth during differentiation, as serum withdrawal would have the same effect on Rb as C/EBPβ: retaining it in the hypophosphorylated form, thereby inhibiting S phase entry (157).

Altogether, these assumptions provide a basis as to explain why C/EBPβ contributes to the maturation of macrophages, yet is not essential in this process. PU.1 activity may be reduced in the absence of C/EBPβ, but it may still be sufficient to drive the expression of macrophage-specific genes. Secondly, C/EBPβ may inhibit cell cycle progression, but other stimuli including PMA, which was widely used in this study, do so as well regardless of the presence of C/EBPβ. However, the findings presented here help explain why C/EBPβ is dramatically upregulated during monocyte differentiation (71,72). It augments PU.1 activity, the transcription factor absolutely critical for myeloid differentiation, while concomitantly reducing the cell's proliferative capacity.

Acknowledgements

5.   Literature

1.   Auffray, C., Sieweke, M. H. und Geissmann, F. (2009). Blood monocytes: development, heterogeneity, and relationship with dendritic cells. *Annu Rev Immunol* 27: 669-692.

2.   Janeway, C. A., Jr. und Medzhitov, R. (2002). Innate immune recognition. *Annu Rev Immunol* 20: 197-216.

3.   Gordon, S. und Taylor, P. R. (2005). Monocyte and macrophage heterogeneity. *Nat Rev Immunol* 5: 953-964.

4.   Serbina, N. V., Jia, T., Hohl, T. M. und Pamer, E. G. (2008). Monocyte-mediated defense against microbial pathogens. *Annu Rev Immunol* 26: 421-452.

5.   Dobrovolskaia, M. A. und Vogel, S. N. (2002). Toll receptors, CD14, and macrophage activation and deactivation by LPS. *Microbes Infect* 4: 903-914.

6.   Jensen, P. E. (1999). Mechanisms of antigen presentation. *Clin Chem Lab Med* 37: 179-186.

7.   Weber, C., Belge, K. U., von Hundelshausen, P., Draude, G., Steppich, B., Mack, M., Frankenberger, M., Weber, K. S. und Ziegler-Heitbrock, H. W. (2000). Differential chemokine receptor expression and function in human monocyte subpopulations. *J Leukoc Biol* 67: 699-704.

8.   Geissmann, F., Jung, S. und Littman, D. R. (2003). Blood monocytes consist of two principal subsets with distinct migratory properties. *Immunity* 19: 71-82.

9.   Fingerle, G., Pforte, A., Passlick, B., Blumenstein, M., Strobel, M. und Ziegler-Heitbrock, H. W. (1993). The novel subset of CD14+/CD16+ blood monocytes is expanded in sepsis patients. *Blood* 82: 3170-3176.

10.   Thieblemont, N., Weiss, L., Sadeghi, H. M., Estcourt, C. und Haeffner-Cavaillon, N. (1995). CD14lowCD16high: a cytokine-producing monocyte subset which expands during human immunodeficiency virus infection. *Eur J Immunol* 25: 3418-3424.

11.   Tacke, F. und Randolph, G. J. (2006). Migratory fate and differentiation of blood monocyte subsets. *Immunobiology* 211: 609-618.

12.   Baud, V. und Karin, M. (2001). Signal transduction by tumor necrosis factor and its relatives. *Trends Cell Biol* 11: 372-377.

13.   Carswell, E. A., Old, L. J., Kassel, R. L., Green, S., Fiore, N. und Williamson, B. (1975). An endotoxin-induced serum factor that causes necrosis of tumors. *Proc Natl Acad Sci U S A* 72: 3666-3670.

14.   Rot, A. und von Andrian, U. H. (2004). Chemokines in innate and adaptive host defense: basic chemokinese grammar for immune cells. *Annu Rev Immunol* 22: 891-928.

15.   Hehlgans, T. und Pfeffer, K. (2005). The intriguing biology of the tumour necrosis factor/tumour necrosis factor receptor superfamily: players, rules and the games. *Immunology* 115: 1-20.

16.   Cross, C. E., Collins, H. L. und Bancroft, G. J. (1997). CR3-dependent phagocytosis by murine macrophages: different cytokines regulate ingestion of a defined CR3 ligand and complement-opsonized Cryptococcus neoformans. *Immunology* 91: 289-296.

17.   Kowalczyk, D., Mytar, B., Jasinski, M., Pryjma, J. und Zembala, M. (1995). Modulation of monocyte antigen-presenting capacity by tumour necrosis factor-alpha (TNF): opposing effects of exogenous TNF before and after an antigen pulse and the role of TNF gene activation in monocytes. *Immunol Lett* 44: 51-57.

18.   Hotchkiss, R. S. und Karl, I. E. (2003). The pathophysiology and treatment of sepsis. *N Engl J Med* 348: 138-150.

19.   Balkwill, F. und Mantovani, A. (2001). Inflammation and cancer: back to Virchow? *Lancet* 357: 539-545.

20.   O'Shea, J. J., Ma, A. und Lipsky, P. (2002). Cytokines and autoimmunity. *Nat Rev Immunol* 2: 37-45.

21.   Wajant, H., Pfizenmaier, K. und Scheurich, P. (2003). Tumor necrosis factor signaling. *Cell Death Differ* 10: 45-65.

22.   Leonardi, A., Chariot, A., Claudio, E., Cunningham, K. und Siebenlist, U. (2000). CIKS, a connection to Ikappa B kinase and stress-activated protein kinase. *Proc Natl Acad Sci U S A* 97: 10494-10499.

23.   Yang, J., Lin, Y., Guo, Z., Cheng, J., Huang, J., Deng, L., Liao, W., Chen, Z., Liu, Z. und Su, B. (2001). The essential role of MEKK3 in TNF-induced NF-kappaB activation. *Nat Immunol* 2: 620-624.

24.   Guo, D., Dunbar, J. D., Yang, C. H., Pfeffer, L. M. und Donner, D. B. (1998). Induction of Jak/STAT signaling by activation of the type 1 TNF receptor. *J Immunol* 160: 2742-2750.

25.   Ozes, O. N., Mayo, L. D., Gustin, J. A., Pfeffer, S. R., Pfeffer, L. M. und Donner, D. B. (1999). NF-kappaB activation by tumour necrosis factor requires the Akt serine-threonine kinase. *Nature* 401: 82-85.

26.   Kronke, M. (1999). Involvement of sphingomyelinases in TNF signaling pathways. *Chem Phys Lipids* 102: 157-166.

27.   Sanz, L., Sanchez, P., Lallena, M. J., Diaz-Meco, M. T. und Moscat, J. (1999). The interaction of p62 with RIP links the atypical PKCs to NF-kappaB activation. *Embo J* 18: 3044-3053.

28.   Wachter, T., Sprick, M., Hausmann, D., Kerstan, A., McPherson, K., Stassi, G., Brocker, E. B., Walczak, H. und Leverkus, M. (2004). cFLIPL inhibits tumor necrosis factor-related apoptosis-inducing ligand-mediated NF-kappaB activation at the death-inducing signaling complex in human keratinocytes. *J Biol Chem* 279: 52824-52834.

29.   West, M. A. und Heagy, W. (2002). Endotoxin tolerance: a review. *Crit Care Med* 30: S64-73.

30.   Volk, H. D., Reinke, P. und Docke, W. D. (2000). Clinical aspects: from systemic inflammation to 'immunoparalysis'. *Chem Immunol* 74: 162-177.

31.   Laursen, J. B., Mulsch, A., Boesgaard, S., Mordvintcev, P., Trautner, S., Gruhn, N., Nielsen-Kudsk, J. E., Busse, R. und Aldershvile, J. (1996). In vivo nitrate tolerance is not associated with reduced bioconversion of nitroglycerin to nitric oxide. *Circulation* 94: 2241-2247.

32.   Zahler, S., Kupatt, C. und Becker, B. F. (2000). Endothelial preconditioning by transient oxidative stress reduces inflammatory responses of cultured endothelial cells to TNF-alpha. *Faseb J* 14: 555-564.

33.   Cohen, J. (2002). The immunopathogenesis of sepsis. *Nature* 420: 885-891.

34.   Russell, J. A. (2006). Management of sepsis. *N Engl J Med* 355: 1699-1713.

35.   Biswas, S. K. und Lopez-Collazo, E. (2009). Endotoxin tolerance: new mechanisms, molecules and clinical significance. *Trends Immunol* 30: 475-487.

36.   Goldbach, J. M., Roth, J., Storr, B. und Zeisberger, E. (1996). Repeated infusions of TNF-alpha cause attenuation of the thermal response and influence LPS fever in guinea pigs. *Am J Physiol* 270: R749-754.

37.   Patton, J. S., Peters, P. M., McCabe, J., Crase, D., Hansen, S., Chen, A. B. und Liggitt, D. (1987). Development of partial tolerance to the gastrointestinal effects of high doses of recombinant tumor necrosis factor-alpha in rodents. *J Clin Invest* 80: 1587-1596.

38. Takahashi, N., Brouckaert, P. und Fiers, W. (1991). Induction of tolerance allows separation of lethal and antitumor activities of tumor necrosis factor in mice. *Cancer Res* 51: 2366-2372.

39. Socher, S. H., Friedman, A. und Martinez, D. (1988). Recombinant human tumor necrosis factor induces acute reductions in food intake and body weight in mice. *J Exp Med* 167: 1957-1962.

40. Takahashi, N., Brouckaert, P. und Fiers, W. (1995). Mechanism of tolerance to tumor necrosis factor: receptor-specific pathway and selectivity. *Am J Physiol* 269: R398-405.

41. Takahashi, N., Brouckaert, P. und Fiers, W. (1993). Cyclooxygenase inhibitors prevent the induction of tolerance to the toxic effects of tumor necrosis factor. *J Immunother Emphasis Tumor Immunol* 14: 16-21.

42. Fraker, D. L., Stovroff, M. C., Merino, M. J. und Norton, J. A. (1988). Tolerance to tumor necrosis factor in rats and the relationship to endotoxin tolerance and toxicity. *J Exp Med* 168: 95-105.

43. Porter, M. H., Arnold, M. und Langhans, W. (1998). TNF-alpha tolerance blocks LPS-induced hypophagia but LPS tolerance fails to prevent TNF-alpha-induced hypophagia. *Am J Physiol* 274: R741-745.

44. Hahn, T., Toker, L., Budilovsky, S., Aderka, D., Eshhar, Z. und Wallach, D. (1985). Use of monoclonal antibodies to a human cytotoxin for its isolation and for examining the self-induction of resistance to this protein. *Proc Natl Acad Sci U S A* 82: 3814-3818.

45. Laegreid, A., Thommesen, L., Jahr, T. G., Sundan, A. und Espevik, T. (1995). Tumor necrosis factor induces lipopolysaccharide tolerance in a human adenocarcinoma cell line mainly through the TNF p55 receptor. *J Biol Chem* 270: 25418-25425.

46. Ferlito, M., Romanenko, O. G., Ashton, S., Squadrito, F., Halushka, P. V. und Cook, J. A. (2001). Effect of cross-tolerance between endotoxin and TNF-alpha or IL-1beta on cellular signaling and mediator production. *J Leukoc Biol* 70: 821-829.

47. Poppers, D. M., Schwenger, P. und Vilcek, J. (2000). Persistent tumor necrosis factor signaling in normal human fibroblasts prevents the complete resynthesis of I kappa B-alpha. *J Biol Chem* 275: 29587-29593.

48. Sass, G., Shembade, N. D. und Tiegs, G. (2005). Tumour necrosis factor alpha (TNF)-TNF receptor 1-inducible cytoprotective proteins in the mouse liver: relevance of suppressors of cytokine signalling. *Biochem J* 385: 537-544.

49. Weber, M., Sydlik, C., Quirling, M., Nothdurfter, C., Zwergal, A., Heiss, P., Bell, S., Neumeier, D., Ziegler-Heitbrock, H. W. und Brand, K. (2003). Transcriptional inhibition of interleukin-8 expression in tumor necrosis factor-tolerant cells: evidence for involvement of C/EBP beta. *J Biol Chem* 278: 23586-23593.

50. Zwergal, A., Quirling, M., Saugel, B., Huth, K. C., Sydlik, C., Poli, V., Neumeier, D., Ziegler-Heitbrock, H. W. und Brand, K. (2006). C/EBP beta blocks p65 phosphorylation and thereby NF-kappa B-mediated transcription in TNF-tolerant cells. *J Immunol* 177: 665-672.

51. Nerlov, C. (2007). The C/EBP family of transcription factors: a paradigm for interaction between gene expression and proliferation control. *Trends Cell Biol* 17: 318-324.

52. Ramji, D. P. und Foka, P. (2002). CCAAT/enhancer-binding proteins: structure, function and regulation. *Biochem J* 365: 561-575.

53. Stein, B., Cogswell, P. C. und Baldwin, A. S., Jr. (1993). Functional and physical associations between NF-kappa B and C/EBP family members: a Rel domain-bZIP interaction. *Mol Cell Biol* 13: 3964-3974.

54. Xia, C., Cheshire, J. K., Patel, H. und Woo, P. (1997). Cross-talk between transcription factors NF-kappa B and C/EBP in the transcriptional regulation of genes. *Int J Biochem Cell Biol* 29: 1525-1539.

55. Hsu, W., Kerppola, T. K., Chen, P. L., Curran, T. und Chen-Kiang, S. (1994). Fos and Jun repress transcription activation by NF-IL6 through association at the basic zipper region. *Mol Cell Biol* 14: 268-276.

56. Calkhoven, C. F., Muller, C. und Leutz, A. (2000). Translational control of C/EBPalpha and C/EBPbeta isoform expression. *Genes Dev* 14: 1920-1932.

57. Buck, M., Zhang, L., Halasz, N. A., Hunter, T. und Chojkier, M. (2001). Nuclear export of phosphorylated C/EBPbeta mediates the inhibition of albumin expression by TNF-alpha. *Embo J* 20: 6712-6723.

58. Roman, C., Platero, J. S., Shuman, J. und Calame, K. (1990). Ig/EBP-1: a ubiquitously expressed immunoglobulin enhancer binding protein that is similar to C/EBP and heterodimerizes with C/EBP. *Genes Dev* 4: 1404-1415.

59. Ron, D. und Habener, J. F. (1992). CHOP, a novel developmentally regulated nuclear protein that dimerizes with transcription factors C/EBP and LAP and functions as a dominant-negative inhibitor of gene transcription. *Genes Dev* 6: 439-453.

60. Antonson, P., Stellan, B., Yamanaka, R. und Xanthopoulos, K. G. (1996). A novel human CCAAT/enhancer binding protein gene, C/EBPepsilon, is expressed in cells of lymphoid and myeloid lineages and is localized on chromosome 14q11.2 close to the T-cell receptor alpha/delta locus. *Genomics* 35: 30-38.

61. Birkenmeier, E. H., Gwynn, B., Howard, S., Jerry, J., Gordon, J. I., Landschulz, W. H. und McKnight, S. L. (1989). Tissue-specific expression, developmental regulation, and genetic mapping of the gene encoding CCAAT/enhancer binding protein. *Genes Dev* 3: 1146-1156.

62. Antonson, P. und Xanthopoulos, K. G. (1995). Molecular cloning, sequence, and expression patterns of the human gene encoding CCAAT/enhancer binding protein alpha (C/EBP alpha). *Biochem Biophys Res Commun* 215: 106-113.

63. Cao, Z., Umek, R. M. und McKnight, S. L. (1991). Regulated expression of three C/EBP isoforms during adipose conversion of 3T3-L1 cells. *Genes Dev* 5: 1538-1552.

64. Kinoshita, S., Akira, S. und Kishimoto, T. (1992). A member of the C/EBP family, NF-IL6 beta, forms a heterodimer and transcriptionally synergizes with NF-IL6. *Proc Natl Acad Sci U S A* 89: 1473-1476.

65. Sterneck, E., Paylor, R., Jackson-Lewis, V., Libbey, M., Przedborski, S., Tessarollo, L., Crawley, J. N. und Johnson, P. F. (1998). Selectively enhanced contextual fear conditioning in mice lacking the transcriptional regulator CCAAT/enhancer binding protein delta. *Proc Natl Acad Sci U S A* 95: 10908-10913.

66. Williams, S. C., Cantwell, C. A. und Johnson, P. F. (1991). A family of C/EBP-related proteins capable of forming covalently linked leucine zipper dimers in vitro. *Genes Dev* 5: 1553-1567.

67. Katz, S., Kowenz-Leutz, E., Muller, C., Meese, K., Ness, S. A. und Leutz, A. (1993). The NF-M transcription factor is related to C/EBP beta and plays a role in signal transduction, differentiation and leukemogenesis of avian myelomonocytic cells. *Embo J* 12: 1321-1332.

68. Cooper, C. L., Berrier, A. L., Roman, C. und Calame, K. L. (1994). Limited expression of C/EBP family proteins during B lymphocyte development. Negative regulator Ig/EBP predominates early and activator NF-IL-6 is induced later. *J Immunol* 153: 5049-5058.

69. An, M. R., Hsieh, C. C., Reisner, P. D., Rabek, J. P., Scott, S. G., Kuninger, D. T. und Papaconstantinou, J. (1996). Evidence for posttranscriptional regulation of

C/EBPalpha and C/EBPbeta isoform expression during the lipopolysaccharide-mediated acute-phase response. *Mol Cell Biol* 16: 2295-2306.

70. Tengku-Muhammad, T. S., Hughes, T. R., Ranki, H., Cryer, A. und Ramji, D. P. (2000). Differential regulation of macrophage CCAAT-enhancer binding protein isoforms by lipopolysaccharide and cytokines. *Cytokine* 12: 1430-1436.

71. Natsuka, S., Akira, S., Nishio, Y., Hashimoto, S., Sugita, T., Isshiki, H. und Kishimoto, T. (1992). Macrophage differentiation-specific expression of NF-IL6, a transcription factor for interleukin-6. *Blood* 79: 460-466.

72. Scott, L. M., Civin, C. I., Rorth, P. und Friedman, A. D. (1992). A novel temporal expression pattern of three C/EBP family members in differentiating myelomonocytic cells. *Blood* 80: 1725-1735.

73. Pham, T. H., Langmann, S., Schwarzfischer, L., El Chartouni, C., Lichtinger, M., Klug, M., Krause, S. W. und Rehli, M. (2007). CCAAT enhancer-binding protein beta regulates constitutive gene expression during late stages of monocyte to macrophage differentiation. *J Biol Chem* 282: 21924-21933.

74. Wang, N. D., Finegold, M. J., Bradley, A., Ou, C. N., Abdelsayed, S. V., Wilde, M. D., Taylor, L. R., Wilson, D. R. und Darlington, G. J. (1995). Impaired energy homeostasis in C/EBP alpha knockout mice. *Science* 269: 1108-1112.

75. Flodby, P., Barlow, C., Kylefjord, H., Ahrlund-Richter, L. und Xanthopoulos, K. G. (1996). Increased hepatic cell proliferation and lung abnormalities in mice deficient in CCAAT/enhancer binding protein alpha. *J Biol Chem* 271: 24753-24760.

76. Zhang, D. E., Zhang, P., Wang, N. D., Hetherington, C. J., Darlington, G. J. und Tenen, D. G. (1997). Absence of granulocyte colony-stimulating factor signaling and neutrophil development in CCAAT enhancer binding protein alpha-deficient mice. *Proc Natl Acad Sci U S A* 94: 569-574.

77. Screpanti, I., Romani, L., Musiani, P., Modesti, A., Fattori, E., Lazzaro, D., Sellitto, C., Scarpa, S., Bellavia, D., Lattanzio, G. und et al. (1995). Lymphoproliferative disorder and imbalanced T-helper response in C/EBP beta-deficient mice. *Embo J* 14: 1932-1941.

78. Tanaka, T., Akira, S., Yoshida, K., Umemoto, M., Yoneda, Y., Shirafuji, N., Fujiwara, H., Suematsu, S., Yoshida, N. und Kishimoto, T. (1995). Targeted disruption of the NF-IL6 gene discloses its essential role in bacteria killing and tumor cytotoxicity by macrophages. *Cell* 80: 353-361.

79. Robinson, G. W., Johnson, P. F., Hennighausen, L. und Sterneck, E. (1998). The C/EBPbeta transcription factor regulates epithelial cell proliferation and differentiation in the mammary gland. *Genes Dev* 12: 1907-1916.

80. Seagroves, T. N., Krnacik, S., Raught, B., Gay, J., Burgess-Beusse, B., Darlington, G. J. und Rosen, J. M. (1998). C/EBPbeta, but not C/EBPalpha, is essential for ductal morphogenesis, lobuloalveolar proliferation, and functional differentiation in the mouse mammary gland. *Genes Dev* 12: 1917-1928.

81. Sterneck, E., Tessarollo, L. und Johnson, P. F. (1997). An essential role for C/EBPbeta in female reproduction. *Genes Dev* 11: 2153-2162.

82. Lekstrom-Himes, J. und Xanthopoulos, K. G. (1999). CCAAT/enhancer binding protein epsilon is critical for effective neutrophil-mediated response to inflammatory challenge. *Blood* 93: 3096-3105.

83. Yamanaka, R., Barlow, C., Lekstrom-Himes, J., Castilla, L. H., Liu, P. P., Eckhaus, M., Decker, T., Wynshaw-Boris, A. und Xanthopoulos, K. G. (1997). Impaired granulopoiesis, myelodysplasia, and early lethality in CCAAT/enhancer binding protein epsilon-deficient mice. *Proc Natl Acad Sci U S A* 94: 13187-13192.

84. Tavor, S., Vuong, P. T., Park, D. J., Gombart, A. F., Cohen, A. H. und Koeffler, H. P. (2002). Macrophage functional maturation and cytokine production are impaired in C/EBP epsilon-deficient mice. *Blood* 99: 1794-1801.

85. Gigliotti, A. P., Johnson, P. F., Sterneck, E. und DeWille, J. W. (2003). Nulliparous CCAAT/enhancer binding proteindelta (C/EBPdelta) knockout mice exhibit mammary gland ductal hyperlasia. *Exp Biol Med (Maywood)* 228: 278-285.

86. Tanaka, T., Yoshida, N., Kishimoto, T. und Akira, S. (1997). Defective adipocyte differentiation in mice lacking the C/EBPbeta and/or C/EBPdelta gene. *Embo J* 16: 7432-7443.

87. Kaisho, T., Tsutsui, H., Tanaka, T., Tsujimura, T., Takeda, K., Kawai, T., Yoshida, N., Nakanishi, K. und Akira, S. (1999). Impairment of natural killer cytotoxic activity and interferon gamma production in CCAAT/enhancer binding protein gamma-deficient mice. *J Exp Med* 190: 1573-1582.

88. Descombes, P. und Schibler, U. (1991). A liver-enriched transcriptional activator protein, LAP, and a transcriptional inhibitory protein, LIP, are translated from the same mRNA. *Cell* 67: 569-579.

89. Raught, B., Gingras, A. C., James, A., Medina, D., Sonenberg, N. und Rosen, J. M. (1996). Expression of a translationally regulated, dominant-negative CCAAT/enhancer-binding protein beta isoform and up-regulation of the eukaryotic translation initiation factor 2alpha are correlated with neoplastic transformation of mammary epithelial cells. *Cancer Res* 56: 4382-4386.

90. Yamanaka, R., Kim, G. D., Radomska, H. S., Lekstrom-Himes, J., Smith, L. T., Antonson, P., Tenen, D. G. und Xanthopoulos, K. G. (1997). CCAAT/enhancer binding protein epsilon is preferentially up-regulated during granulocytic differentiation and its functional versatility is determined by alternative use of promoters and differential splicing. *Proc Natl Acad Sci U S A* 94: 6462-6467.

91. Guerzoni, C., Bardini, M., Mariani, S. A., Ferrari-Amorotti, G., Neviani, P., Panno, M. L., Zhang, Y., Martinez, R., Perrotti, D. und Calabretta, B. (2006). Inducible activation of CEBPB, a gene negatively regulated by BCR/ABL, inhibits proliferation and promotes differentiation of BCR/ABL-expressing cells. *Blood* 107: 4080-4089.

92. Timchenko, N. A., Welm, A. L., Lu, X. und Timchenko, L. T. (1999). CUG repeat binding protein (CUGBP1) interacts with the 5' region of C/EBPbeta mRNA and regulates translation of C/EBPbeta isoforms. *Nucleic Acids Res* 27: 4517-4525.

93. Wethmar, K., Begay, V., Smink, J. J., Zaragoza, K., Wiesenthal, V., Dorken, B., Calkhoven, C. F. und Leutz, A. (2010). C/EBPbetaDeltauORF mice--a genetic model for uORF-mediated translational control in mammals. *Genes Dev* 24: 15-20.

94. Johnson, P. F. (2005). Molecular stop signs: regulation of cell-cycle arrest by C/EBP transcription factors. *J Cell Sci* 118: 2545-2555.

95. Zahnow, C. A., Younes, P., Laucirica, R. und Rosen, J. M. (1997). Overexpression of C/EBPbeta-LIP, a naturally occurring, dominant-negative transcription factor, in human breast cancer. *J Natl Cancer Inst* 89: 1887-1891.

96. Zahnow, C. A., Cardiff, R. D., Laucirica, R., Medina, D. und Rosen, J. M. (2001). A role for CCAAT/enhancer binding protein beta-liver-enriched inhibitory protein in mammary epithelial cell proliferation. *Cancer Res* 61: 261-269.

97. Lamb, J., Ramaswamy, S., Ford, H. L., Contreras, B., Martinez, R. V., Kittrell, F. S., Zahnow, C. A., Patterson, N., Golub, T. R. und Ewen, M. E. (2003). A mechanism of cyclin D1 action encoded in the patterns of gene expression in human cancer. *Cell* 114: 323-334.

98. Mo, X., Kowenz-Leutz, E., Xu, H. und Leutz, A. (2004). Ras induces mediator complex exchange on C/EBP beta. *Mol Cell* 13: 241-250.

99. Xie, H., Ye, M., Feng, R. und Graf, T. (2004). Stepwise reprogramming of B cells into macrophages. *Cell* 117: 663-676.

100. Buck, M., Poli, V., van der Geer, P., Chojkier, M. und Hunter, T. (1999). Phosphorylation of rat serine 105 or mouse threonine 217 in C/EBP beta is required for hepatocyte proliferation induced by TGF alpha. *Mol Cell* 4: 1087-1092.

101. Gagliardi, M., Maynard, S., Miyake, T., Rodrigues, N., Tjew, S. L., Cabannes, E. und Bedard, P. A. (2003). Opposing roles of C/EBPbeta and AP-1 in the control of fibroblast proliferation and growth arrest-specific gene expression. *J Biol Chem* 278: 43846-43854.

102. Gheorghiu, I., Deschenes, C., Blais, M., Boudreau, F., Rivard, N. und Asselin, C. (2001). Role of specific CCAAT/enhancer-binding protein isoforms in intestinal epithelial cells. *J Biol Chem* 276: 44331-44337.

103. Sebastian, T., Malik, R., Thomas, S., Sage, J. und Johnson, P. F. (2005). C/EBPbeta cooperates with RB:E2F to implement Ras(V12)-induced cellular senescence. *Embo J* 24: 3301-3312.

104. Eaton, E. M., Hanlon, M., Bundy, L. und Sealy, L. (2001). Characterization of C/EBPbeta isoforms in normal versus neoplastic mammary epithelial cells. *J Cell Physiol* 189: 91-105.

105. Buck, M., Poli, V., Hunter, T. und Chojkier, M. (2001). C/EBPbeta phosphorylation by RSK creates a functional XEXD caspase inhibitory box critical for cell survival. *Mol Cell* 8: 807-816.

106. Buck, M., Turler, H. und Chojkier, M. (1994). LAP (NF-IL-6), a tissue-specific transcriptional activator, is an inhibitor of hepatoma cell proliferation. *Embo J* 13: 851-860.

107. Chen, P. L., Riley, D. J., Chen, Y. und Lee, W. H. (1996). Retinoblastoma protein positively regulates terminal adipocyte differentiation through direct interaction with C/EBPs. *Genes Dev* 10: 2794-2804.

108. Chen, P. L., Riley, D. J., Chen-Kiang, S. und Lee, W. H. (1996). Retinoblastoma protein directly interacts with and activates the transcription factor NF-IL6. *Proc Natl Acad Sci U S A* 93: 465-469.

109. Ji, Y. und Studzinski, G. P. (2004). Retinoblastoma protein and CCAAT/enhancer-binding protein beta are required for 1,25-dihydroxyvitamin D3-induced monocytic differentiation of HL60 cells. *Cancer Res* 64: 370-377.

110. Wessells, J., Yakar, S. und Johnson, P. F. (2004). Critical prosurvival roles for C/EBP beta and insulin-like growth factor I in macrophage tumor cells. *Mol Cell Biol* 24: 3238-3250.

111. Zhu, S., Yoon, K., Sterneck, E., Johnson, P. F. und Smart, R. C. (2002). CCAAT/enhancer binding protein-beta is a mediator of keratinocyte survival and skin tumorigenesis involving oncogenic Ras signaling. *Proc Natl Acad Sci U S A* 99: 207-212.

112. Kastner, P. und Chan, S. (2008). PU.1: a crucial and versatile player in hematopoiesis and leukemia. *Int J Biochem Cell Biol* 40: 22-27.

113. Friedman, A. D. (2007). Transcriptional control of granulocyte and monocyte development. *Oncogene* 26: 6816-6828.

114. Dakic, A., Metcalf, D., Di Rago, L., Mifsud, S., Wu, L. und Nutt, S. L. (2005). PU.1 regulates the commitment of adult hematopoietic progenitors and restricts granulopoiesis. *J Exp Med* 201: 1487-1502.

115. Iwasaki, H., Somoza, C., Shigematsu, H., Duprez, E. A., Iwasaki-Arai, J., Mizuno, S., Arinobu, Y., Geary, K., Zhang, P., Dayaram, T., Fenyus, M. L., Elf, S., Chan, S., Kastner, P., Huettner, C. S., Murray, R., Tenen, D. G. und Akashi, K. (2005).

Distinctive and indispensable roles of PU.1 in maintenance of hematopoietic stem cells and their differentiation. *Blood* 106: 1590-1600.

116. Walsh, J. C., DeKoter, R. P., Lee, H. J., Smith, E. D., Lancki, D. W., Gurish, M. F., Friend, D. S., Stevens, R. L., Anastasi, J. und Singh, H. (2002). Cooperative and antagonistic interplay between PU.1 and GATA-2 in the specification of myeloid cell fates. *Immunity* 17: 665-676.

117. Zhang, P., Zhang, X., Iwama, A., Yu, C., Smith, K. A., Mueller, B. U., Narravula, S., Torbett, B. E., Orkin, S. H. und Tenen, D. G. (2000). PU.1 inhibits GATA-1 function and erythroid differentiation by blocking GATA-1 DNA binding. *Blood* 96: 2641-2648.

118. Auwerx, J. (1991). The human leukemia cell line, THP-1: a multifacetted model for the study of monocyte-macrophage differentiation. *Experientia* 47: 22-31.

119. Laouar, A., Collart, F. R., Chubb, C. B., Xie, B. und Huberman, E. (1999). Interaction between alpha 5 beta 1 integrin and secreted fibronectin is involved in macrophage differentiation of human HL-60 myeloid leukemia cells. *J Immunol* 162: 407-414.

120. Lehtonen, A., Ahlfors, H., Veckman, V., Miettinen, M., Lahesmaa, R. und Julkunen, I. (2007). Gene expression profiling during differentiation of human monocytes to macrophages or dendritic cells. *J Leukoc Biol* 82: 710-720.

121. Liu, H., Shi, B., Huang, C. C., Eksarko, P. und Pope, R. M. (2008). Transcriptional diversity during monocyte to macrophage differentiation. *Immunol Lett* 117: 70-80.

122. Martinez, F. O., Gordon, S., Locati, M. und Mantovani, A. (2006). Transcriptional profiling of the human monocyte-to-macrophage differentiation and polarization: new molecules and patterns of gene expression. *J Immunol* 177: 7303-7311.

123. Dahl, R., Walsh, J. C., Lancki, D., Laslo, P., Iyer, S. R., Singh, H. und Simon, M. C. (2003). Regulation of macrophage and neutrophil cell fates by the PU.1:C/EBPalpha ratio and granulocyte colony-stimulating factor. *Nat Immunol* 4: 1029-1036.

124. Wang, Q. F. und Friedman, A. D. (2002). CCAAT/enhancer-binding proteins are required for granulopoiesis independent of their induction of the granulocyte colony-stimulating factor receptor. *Blood* 99: 2776-2785.

125. Iwama, A., Osawa, M., Hirasawa, R., Uchiyama, N., Kaneko, S., Onodera, M., Shibuya, K., Shibuya, A., Vinson, C., Tenen, D. G. und Nakauchi, H. (2002). Reciprocal roles for CCAAT/enhancer binding protein (C/EBP) and PU.1 transcription factors in Langerhans cell commitment. *J Exp Med* 195: 547-558.

126. Popernack, P. M., Truong, L. T., Kamphuis, M. und Henderson, A. J. (2001). Ectopic expression of CCAAT/enhancer binding protein beta (C/EBPbeta) in long-term bone marrow cultures induces granulopoiesis and alters stromal cell function. *J Hematother Stem Cell Res* 10: 631-642.

127. Matsushita, H., Nakajima, H., Nakamura, Y., Tsukamoto, H., Tanaka, Y., Jin, G., Yabe, M., Asai, S., Ono, R., Nosaka, T., Sugita, K., Morimoto, A., Hayashi, Y., Hotta, T., Ando, K. und Miyachi, H. (2008). C/EBPalpha and C/EBPvarepsilon induce the monocytic differentiation of myelomonocytic cells with the MLL-chimeric fusion gene. *Oncogene* 27: 6749-6760.

128. Jones, L. C., Lin, M. L., Chen, S. S., Krug, U., Hofmann, W. K., Lee, S., Lee, Y. H. und Koeffler, H. P. (2002). Expression of C/EBPbeta from the C/ebpalpha gene locus is sufficient for normal hematopoiesis in vivo. *Blood* 99: 2032-2036.

129. Park, M. H., Park, S. Y. und Kim, Y. (2008). Induction of proline-rich tyrosine kinase2 (Pyk2) through C/EBPbeta is involved in PMA-induced monocyte differentiation. *FEBS Lett* 582: 415-422.

130. Chen, S., Han, Y. H., Zheng, Y., Zhao, M., Yan, H., Zhao, Q., Chen, G. Q. und Li, D. (2009). NDRG1 contributes to retinoic acid-induced differentiation of leukemic cells. *Leuk Res* 33: 1108-1113.

131. McKercher, S. R., Torbett, B. E., Anderson, K. L., Henkel, G. W., Vestal, D. J., Baribault, H., Klemsz, M., Feeney, A. J., Wu, G. E., Paige, C. J. und Maki, R. A. (1996). Targeted disruption of the PU.1 gene results in multiple hematopoietic abnormalities. *Embo J* 15: 5647-5658.

132. Scott, E. W., Simon, M. C., Anastasi, J. und Singh, H. (1994). Requirement of transcription factor PU.1 in the development of multiple hematopoietic lineages. *Science* 265: 1573-1577.

133. Anderson, K. L., Smith, K. A., Conners, K., McKercher, S. R., Maki, R. A. und Torbett, B. E. (1998). Myeloid development is selectively disrupted in PU.1 null mice. *Blood* 91: 3702-3710.

134. DeKoter, R. P., Walsh, J. C. und Singh, H. (1998). PU.1 regulates both cytokine-dependent proliferation and differentiation of granulocyte/macrophage progenitors. *Embo J* 17: 4456-4468.

135. Friedman, A. D. (2007). C/EBPalpha induces PU.1 and interacts with AP-1 and NF-kappaB to regulate myeloid development. *Blood Cells Mol Dis* 39: 340-343.

136. Mueller, B. U., Pabst, T., Fos, J., Petkovic, V., Fey, M. F., Asou, N., Buergi, U. und Tenen, D. G. (2006). ATRA resolves the differentiation block in t(15;17) acute myeloid leukemia by restoring PU.1 expression. *Blood* 107: 3330-3338.

137. Gorgoni, B., Maritano, D., Marthyn, P., Righi, M. und Poli, V. (2002). C/EBP beta gene inactivation causes both impaired and enhanced gene expression and inverse regulation of IL-12 p40 and p35 mRNAs in macrophages. *J Immunol* 168: 4055-4062.

138. Oelgeschlager, M., Nuchprayoon, I., Luscher, B. und Friedman, A. D. (1996). C/EBP, c-Myb, and PU.1 cooperate to regulate the neutrophil elastase promoter. *Mol Cell Biol* 16: 4717-4725.

139. Petrovick, M. S., Hiebert, S. W., Friedman, A. D., Hetherington, C. J., Tenen, D. G. und Zhang, D. E. (1998). Multiple functional domains of AML1: PU.1 and C/EBPalpha synergize with different regions of AML1. *Mol Cell Biol* 18: 3915-3925.

140. Grondin, B., Lefrancois, M., Tremblay, M., Saint-Denis, M., Haman, A., Waga, K., Bedard, A., Tenen, D. G. und Hoang, T. (2007). c-Jun homodimers can function as a context-specific coactivator. *Mol Cell Biol* 27: 2919-2933.

141. Listman, J. A., Wara-aswapati, N., Race, J. E., Blystone, L. W., Walker-Kopp, N., Yang, Z. und Auron, P. E. (2005). Conserved ETS domain arginines mediate DNA binding, nuclear localization, and a novel mode of bZIP interaction. *J Biol Chem* 280: 41421-41428.

142. Yang, Z., Wara-Aswapati, N., Chen, C., Tsukada, J. und Auron, P. E. (2000). NF-IL6 (C/EBPbeta) vigorously activates il1b gene expression via a Spi-1 (PU.1) protein-protein tether. *J Biol Chem* 275: 21272-21277.

143. Tissieres, P., Araud, T., Ochoda, A., Drifte, G., Dunn-Siegrist, I. und Pugin, J. (2009). Cooperation between PU.1 and CAAT/enhancer-binding protein beta is necessary to induce the expression of the MD-2 gene. *J Biol Chem* 284: 26261-26272.

144. Nagulapalli, S., Pongubala, J. M. und Atchison, M. L. (1995). Multiple proteins physically interact with PU.1. Transcriptional synergy with NF-IL6 beta (C/EBP delta, CRP3). *J Immunol* 155: 4330-4338.

145. Boles, B. K., Ritzenthaler, J., Birkenmeier, T. und Roman, J. (2000). Phorbol ester-induced U-937 differentiation: effects on integrin alpha(5) gene transcription. *Am J Physiol Lung Cell Mol Physiol* 278: L703-712.

146. Laiosa, C. V., Stadtfeld, M., Xie, H., de Andres-Aguayo, L. und Graf, T. (2006). Reprogramming of committed T cell progenitors to macrophages and dendritic cells by C/EBP alpha and PU.1 transcription factors. *Immunity* 25: 731-744.

147. Feng, R., Desbordes, S. C., Xie, H., Tillo, E. S., Pixley, F., Stanley, E. R. und Graf, T. (2008). PU.1 and C/EBPalpha/beta convert fibroblasts into macrophage-like cells. *Proc Natl Acad Sci U S A* 105: 6057-6062.

148. Hegde, S. P., Zhao, J., Ashmun, R. A. und Shapiro, L. H. (1999). c-Maf induces monocytic differentiation and apoptosis in bipotent myeloid progenitors. *Blood* 94: 1578-1589.

149. Sieweke, M. H., Tekotte, H., Frampton, J. und Graf, T. (1996). MafB is an interaction partner and repressor of Ets-1 that inhibits erythroid differentiation. *Cell* 85: 49-60.

150. Sarrazin, S., Mossadegh-Keller, N., Fukao, T., Aziz, A., Mourcin, F., Vanhille, L., Kelly Modis, L., Kastner, P., Chan, S., Duprez, E., Otto, C. und Sieweke, M. H. (2009). MafB restricts M-CSF-dependent myeloid commitment divisions of hematopoietic stem cells. *Cell* 138: 300-313.

151. Friedman, A. D. (2002). Transcriptional regulation of granulocyte and monocyte development. *Oncogene* 21: 3377-3390.

152. Krishnaraju, K., Nguyen, H. Q., Liebermann, D. A. und Hoffman, B. (1995). The zinc finger transcription factor Egr-1 potentiates macrophage differentiation of hematopoietic cells. *Mol Cell Biol* 15: 5499-5507.

153. Nguyen, H. Q., Hoffman-Liebermann, B. und Liebermann, D. A. (1993). The zinc finger transcription factor Egr-1 is essential for and restricts differentiation along the macrophage lineage. *Cell* 72: 197-209.

154. Aziz, A., Vanhille, L., Mohideen, P., Kelly, L. M., Otto, C., Bakri, Y., Mossadegh, N., Sarrazin, S. und Sieweke, M. H. (2006). Development of macrophages with altered actin organization in the absence of MafB. *Mol Cell Biol* 26: 6808-6818.

155. Carter, J. H. und Tourtellotte, W. G. (2007). Early growth response transcriptional regulators are dispensable for macrophage differentiation. *J Immunol* 178: 3038-3047.

156. Studzinski, G. P., Rathod, B., Wang, Q. M., Rao, J. und Zhang, F. (1997). Uncoupling of cell cycle arrest from the expression of monocytic differentiation markers in HL60 cell variants. *Exp Cell Res* 232: 376-387.

157. Classon, M. und Harlow, E. (2002). The retinoblastoma tumour suppressor in development and cancer. *Nat Rev Cancer* 2: 910-917.

158. Chen, P. L., Scully, P., Shew, J. Y., Wang, J. Y. und Lee, W. H. (1989). Phosphorylation of the retinoblastoma gene product is modulated during the cell cycle and cellular differentiation. *Cell* 58: 1193-1198.

159. Juan, G., Li, X. und Darzynkiewicz, Z. (1998). Phosphorylation of retinoblastoma protein assayed in individual HL-60 cells during their proliferation and differentiation. *Exp Cell Res* 244: 83-92.

160. Bergh, G., Ehinger, M., Olsson, I., Jacobsen, S. E. und Gullberg, U. (1999). Involvement of the retinoblastoma protein in monocytic and neutrophilic lineage commitment of human bone marrow progenitor cells. *Blood* 94: 1971-1978.

161. Hagemeier, C., Bannister, A. J., Cook, A. und Kouzarides, T. (1993). The activation domain of transcription factor PU.1 binds the retinoblastoma (RB) protein and the transcription factor TFIID in vitro: RB shows sequence similarity to TFIID and TFIIB. *Proc Natl Acad Sci U S A* 90: 1580-1584.

162. Klappacher, G. W., Lunyak, V. V., Sykes, D. B., Sawka-Verhelle, D., Sage, J., Brard, G., Ngo, S. D., Gangadharan, D., Jacks, T., Kamps, M. P., Rose, D. W., Rosenfeld, M. G. und Glass, C. K. (2002). An induced Ets repressor complex regulates growth arrest during terminal macrophage differentiation. *Cell* 109: 169-180.

163. Dahlke, M. H., Larsen, S. R., Rasko, J. E. und Schlitt, H. J. (2004). The biology of CD45 and its use as a therapeutic target. *Leuk Lymphoma* 45: 229-236.

164. Ziegler-Heitbrock, H. W. (2000). Definition of human blood monocytes. *J Leukoc Biol* 67: 603-606.

165. Luedde, T., Duderstadt, M., Streetz, K. L., Tacke, F., Kubicka, S., Manns, M. P. und Trautwein, C. (2004). C/EBP beta isoforms LIP and LAP modulate progression of the cell cycle in the regenerating mouse liver. *Hepatology* 40: 356-365.

166. Poli, V. (1998). The role of C/EBP isoforms in the control of inflammatory and native immunity functions. *J Biol Chem* 273: 29279-29282.

167. Traore, K., Trush, M. A., George, M., Jr., Spannhake, E. W., Anderson, W. und Asseffa, A. (2005). Signal transduction of phorbol 12-myristate 13-acetate (PMA)-induced growth inhibition of human monocytic leukemia THP-1 cells is reactive oxygen dependent. *Leuk Res* 29: 863-879.

168. Brown, G., Choudhry, M. A., Durham, J., Drayson, M. T. und Michell, R. H. (1999). Monocytically differentiating HL60 cells proliferate rapidly before they mature. *Exp Cell Res* 253: 511-518.

169. Fagotto, F. und Gumbiner, B. M. (1996). Cell contact-dependent signaling. *Dev Biol* 180: 445-454.

170. Stiegler, P., Kasten, M. und Giordano, A. (1998). The RB family of cell cycle regulatory factors. *J Cell Biochem Suppl* 30-31: 30-36.

171. Fraker, D. L., Sheppard, B. C. und Norton, J. A. (1990). Impact of tolerance on antitumor efficacy of tumor necrosis factor in mice. *Cancer Res* 50: 2261-2267.

172. Ginis, I., Jaiswal, R., Klimanis, D., Liu, J., Greenspon, J. und Hallenbeck, J. M. (2002). TNF-alpha-induced tolerance to ischemic injury involves differential control of NF-kappaB transactivation: the role of NF-kappaB association with p300 adaptor. *J Cereb Blood Flow Metab* 22: 142-152.

173. Prado, G. N., Suzuki, H., Wilkinson, N., Cousins, B. und Navarro, J. (1996). Role of the C terminus of the interleukin 8 receptor in signal transduction and internalization. *J Biol Chem* 271: 19186-19190.

174. Aggarwal, B. B. (2003). Signalling pathways of the TNF superfamily: a double-edged sword. *Nat Rev Immunol* 3: 745-756.

175. Das, U. N. (2000). Critical advances in septicemia and septic shock. *Crit Care* 4: 290-296.

176. del Fresno, C., Garcia-Rio, F., Gomez-Pina, V., Soares-Schanoski, A., Fernandez-Ruiz, I., Jurado, T., Kajiji, T., Shu, C., Marin, E., Gutierrez del Arroyo, A., Prados, C., Arnalich, F., Fuentes-Prior, P., Biswas, S. K. und Lopez-Collazo, E. (2009). Potent phagocytic activity with impaired antigen presentation identifying lipopolysaccharide-tolerant human monocytes: demonstration in isolated monocytes from cystic fibrosis patients. *J Immunol* 182: 6494-6507.

177. Williams, S. C., Angerer, N. D. und Johnson, P. F. (1997). C/EBP proteins contain nuclear localization signals imbedded in their basic regions. *Gene Expr* 6: 371-385.

178. Ossipow, V., Descombes, P. und Schibler, U. (1993). CCAAT/enhancer-binding protein mRNA is translated into multiple proteins with different transcription activation potentials. *Proc Natl Acad Sci U S A* 90: 8219-8223.

179. Henderson, A. J., Zou, X. und Calame, K. L. (1995). C/EBP proteins activate transcription from the human immunodeficiency virus type 1 long terminal repeat in macrophages/monocytes. *J Virol* 69: 5337-5344.

180. Lee, C. H., Yun, H. J., Kang, H. S. und Kim, H. D. (1999). ERK/MAPK pathway is required for changes of cyclin D1 and B1 during phorbol 12-myristate 13-acetate-induced differentiation of K562 cells. *IUBMB Life* 48: 585-591.

181. Das, D., Pintucci, G. und Stern, A. (2000). MAPK-dependent expression of p21(WAF) and p27(kip1) in PMA-induced differentiation of HL60 cells. *FEBS Lett* 472: 50-52.

182. Vrana, J. A., Saunders, A. M., Chellappan, S. P. und Grant, S. (1998). Divergent effects of bryostatin 1 and phorbol myristate acetate on cell cycle arrest and

maturation in human myelomonocytic leukemia cells (U937). *Differentiation* 63: 33-42.

183. Herrera, R., Hubbell, S., Decker, S. und Petruzzelli, L. (1998). A role for the MEK/MAPK pathway in PMA-induced cell cycle arrest: modulation of megakaryocytic differentiation of K562 cells. *Exp Cell Res* 238: 407-414.

184. http://www.dsmz.de/human_and_animal_cell_lines/info.php?dsmz_nr=16. Retrieved Apr 21, 2010.

185. Hong, F. D., Huang, H. J., To, H., Young, L. J., Oro, A., Bookstein, R., Lee, E. Y. und Lee, W. H. (1989). Structure of the human retinoblastoma gene. *Proc Natl Acad Sci U S A* 86: 5502-5506.

186. Hsiao, K. M., McMahon, S. L. und Farnham, P. J. (1994). Multiple DNA elements are required for the growth regulation of the mouse E2F1 promoter. *Genes Dev* 8: 1526-1537.

187. Strasser, A., O'Connor, L. und Dixit, V. M. (2000). Apoptosis signaling. *Annu Rev Biochem* 69: 217-245.

188. Evangelopoulos, M. E., Weis, J. und Kruttgen, A. (2005). Signalling pathways leading to neuroblastoma differentiation after serum withdrawal: HDL blocks neuroblastoma differentiation by inhibition of EGFR. *Oncogene* 24: 3309-3318.

189. Carey, J. O., Posekany, K. J., deVente, J. E., Pettit, G. R. und Ways, D. K. (1996). Phorbol ester-stimulated phosphorylation of PU.1: association with leukemic cell growth inhibition. *Blood* 87: 4316-4324.

190. Garcia, A., Serrano, A., Abril, E., Jimenez, P., Real, L. M., Canton, J., Garrido, F. und Ruiz-Cabello, F. (1999). Differential effect on U937 cell differentiation by targeting transcriptional factors implicated in tissue- or stage-specific induced integrin expression. *Exp Hematol* 27: 353-364.

Curriculum Vitae

Personal details

Name:	Judith Dorothée Kandemir, née Sattler
Birth:	August 10th, 1980 in Munich
Marital status:	married
Address:	Kreillerstraße 189, 81825 München

Education

1987 – 1991	Grundschule Neukeferloh
1991 – 1996	Ernst-Mach-Gymnasium Haar
1996 – 1997	Los Altos High School (Los Altos, CA, USA)
1997 – 2000	Ernst-Mach-Gymnasium Haar
06/2000	Abitur

University education

2000 – 2003	Study of Biochemistry at the Technische Universität München (TUM)
04/2003 – 08/2003	Bachelor's thesis "Role of the 'BH3-only' protein Bmf during phagocytosis-induced apoptosis" at the Institute of Medical Microbiology, Immunology, and Hygiene, TUM (Prof. Dr. Georg Häcker)
08/2003	Degree: Bachelor of Science
2003 – 2005	Study of Biochemistry at the TUM
	Minor subjects: Clinical chemistry; Microbiology of pathogenic organisms
02/2005 – 08/2005	Master's thesis "Extracellular Nef protein induces signaling through Toll-like receptors 2 and 4 and is able to stimulate HIV-1 long terminal repeat activity" at the Institute of Virology, TUM (Prof. Dr. Gerd Sutter)
08/2005	Degree: Master of Science
05/2006 – 04/2007	Doctoral candidate at the Institute of Clinical Chemistry and Pathobiochemistry, TUM (Prof. Dr. Korbinian Brand)
Since 05/2007	Doctoral candidate at the Institute of Clinical Chemistry, Medizinische Hochschule Hannover (Prof. Dr. Korbinian Brand)

Publications

Lehmann, M.H., Kastenmuller, W., Kandemir, J.D., Brandt, F., Suezer, Y., and Sutter, G. (2009) Modified vaccinia virus Ankara triggers chemotaxis of monocytes and early respiratory immigration of leukocytes by induction of CCL2 expression. *J. Virol.* 83(6): 2540-2552

Cappello, C., Zwergal, A., Kanclerski, S., Haas, S.C., Kandemir, J.D., Huber, R., Page, S., and Brand, K. (2009) C/EBPβ enhances NF-κB-associated signalling by reducing the level of IκB-α. *Cell. Signal.* 21(12): 1918-1924

Haas, S.C., Huber, R., Gutsch, R., Kandemir, J.D., Cappello, C., Krauter, J., Duyster, J., Ganser, A., and Brand, K. (2010) ITD- and FL-induced FLT3 signal transduction leads to increased C/EBPβ-LIP expression and LIP/LAP ratio by different signaling modules. *Br. J. Haematol.* 148(5): 777-790

Gutsch, R.*, Kandemir, J.D.*, Simanowski, K., Pietsch, D., Cappello, C., Meyer, J., Huber, R., and Brand, K. C/EBPβ inhibits proliferation in monocytic cells by affecting the Rb/E2F pathway with differential effects on morphology. *J. Biol. Chem.* (in revision)

Günther, J., Kandemir, J.D., Cappello, C., Page, S., Huber, R., Müller, B., Pietsch, D., and Brand, K. TNF tolerance in primary monocytes. Manuscript in preparation

Contributions to congresses

1a. Brand, K., Kandemir, J., Cappello, C., Haas, S., Mages, J., Lang, R., and Neumeier, D. (2007) Gene expression profiles of TNF tolerant monocytes using microarray analysis (Presentation). Joint Annual Congress of The Austrian Society for Laboratory Medicine and Clinical Chemistry (ÖGLMKC) and The German United Society of Clinical Chemistry and Laboratory Medicine (DGKL), Vienna. *Abstract Book*

1b. Brand, K., Kandemir, J., Cappello, C., Haas, S., Mages, J., Lang, R., and Neumeier, D. (2007) Gene expression profiles of TNF tolerant monocytes using microarray analysis (Presentation). Joint Annual Congress of The Austrian Society for Laboratory Medicine and Clinical Chemistry (ÖGLMKC) and The German United Society of Clinical Chemistry and Laboratory Medicine (DGKL), Vienna. *Clin. Chem. Lab. Med.* 45(8): A93

2a. Haas, S., Cappello, C., Zwergal, A., Kandemir, J.D., Wehmeier, M., Schwettmann, L., Page, S., and Brand, K. (2008) Steuerung der konstitutiven NF-κB-Aktivität durch

C/EBPβ – IκB-α als Effektormolekül (Presentation). Hj.-Staudinger-Symposium of the DGKL, Bad Staffelstein. *Abstract Book*

2b. Haas, S., Cappello, C., Zwergal, A., Kandemir, J.D., Wehmeier, M., Schwettmann, L., Page, S., and Brand, K. (2008) Steuerung der konstitutiven NF-κB-Aktivität durch C/EBPβ – IκB-α als Effektormolekül (Presentation). Hj.-Staudinger-Symposium of the DGKL, Bad Staffelstein. *Klin. Chem. Mitt.* 39(1+2): 30-31

3a. Cappello, C., Zwergal, A., Haas, S., Kandemir, J.D., Wehmeier, M., Schwettmann, L., Page, S., and Brand, K. (2008) C/EBPβ sustains constitutive NF-κB activity – evidence for involvement of IκB-α (Presentation). 5th Annual Conference of The German United Society of Clinical Chemistry and Laboratory Medicine (DGKL), Mannheim. *Abstract Book*

3b. Cappello, C., Zwergal, A., Haas, S., Kandemir, J.D., Wehmeier, M., Schwettmann, L., Page, S., and Brand, K. (2008) C/EBPβ sustains constitutive NF-κB activity – evidence for involvement of IκB-α (Presentation). 5th Annual Conference of The German United Society of Clinical Chemistry and Laboratory Medicine (DGKL), Mannheim. *Clin. Chem. Lab. Med.* 46(9): A155

4a. Huber, R., Haas, S.C., Gutsch, R., Kandemir, J.D., Cappello, C., Krauter, J., Duyster, J., Ganser, A., and Brand, K. (2009) ITD- und FL-induzierte FLT3-Rezeptor-abhängige Signalwege vermitteln eine Erhöhung der C/EBPβ-LIP-Expression und der LIP/LAP-Ratio über differentielle Signalmodule (Poster). 6th Annual Conference of The German United Society of Clinical Chemistry and Laboratory Medicine (DGKL), Leipzig. *Abstract Book*

4b. Huber, R., Haas, S.C., Gutsch, R., Kandemir, J.D., Cappello, C., Krauter, J., Duyster, J., Ganser, A., and Brand, K. (2009) ITD- und FL-induzierte FLT3-Rezeptor-abhängige Signalwege vermitteln eine Erhöhung der C/EBPβ-LIP-Expression und der LIP/LAP-Ratio über differentielle Signalmodule (Poster). 6th Annual Conference of The German United Society of Clinical Chemistry and Laboratory Medicine (DGKL), Leipzig. *Clin. Chem. Lab. Med.* 47(9): A57-58

5. Gutsch, R.*, Kandemir, J.D.*, Simanowski, K., Pietsch, D., Cappello, C., Meyer, J., Huber, R., and Brand, K. (2010) C/EBPβ inhibits proliferation in monocytic cells by affecting the Rb/E2F pathway with differential effects on morphology. 7th Annual Conference of The German United Society of Clinical Chemistry and Laboratory Medicine (DGKL), Mannheim. Abstract submitted